Realia et naturalia

DISSERTATIONES
BIOLOGICAE
UNIVERSITATIS
TARTUENSIS
240

LIINA KANGUR

High-Pressure Spectroscopy Study of Chromophore-Binding Hydrogen Bonds in Light-Harvesting Complexes of Photosynthetic Bacteria

DISSERTATIONES BIOLOGICAE UNIVERSITATIS TARTUENSIS
240

DISSERTATIONES BIOLOGICAE UNIVERSITATIS TARTUENSIS
240

LIINA KANGUR

High-Pressure Spectroscopy Study of Chromophore-Binding Hydrogen Bonds in Light-Harvesting Complexes of Photosynthetic Bacteria

UNIVERSITY OF TARTU
PRESS
1632

Institute of Molecular and Cell Biology, University of Tartu, Estonia

The dissertation was accepted for the commencement of the degree of *Doctor philosophiae* in Biochemistry at the University of Tartu on June 4, 2013, by the Scientific Council of the Institute of Molecular and Cell Biology, University of Tartu.

Supervisor: Professor Arvi Freiberg, D.Sc.
Department of Biophysics and Plant Physiology, Institute of Molecular and Cell Biology, University of Tartu, Estonia

Opponent: Professor Dr. Roland Winter
Physical Chemistry (Biophysical chemistry), Faculty of Chemistry, TU Dortmund University, Germany

Commencement: Room 105, 23B Riia Street, Tartu, on August 26, 2013 at 10.00 a.m.

ISSN ISSN 1024–6479
ISBN 978–9949–32–345–6 (Print)
ISBN 978–9949–32–346–3 (PDF)

University of Tartu Press
www.tyk.ee
Order No. 270

To the brightest white light
To the apparitions of quantum field

ABSTRACT

The light-harvesting antenna complexes from purple photosynthetic bacteria are convenient model systems to examine the poorly understood role of hydrogen-bonds as stabilizing factors in membrane protein complexes. The non-covalently bound arrays of bacteriochlorophyll chromophores within native and genetically modified variants of light-harvesting complexes were used to monitor local changes in the chromophore binding sites induced by externally applied hydrostatic pressure. A unique combination of optical spectroscopy with genetic and noninvasive physical (high-pressure) engineering applied in this work provides the first demonstration and quantification of the rupture of multiple hydrogen bonds in the bacteriochlorophyll binding pockets of the LH1 and LH2 membrane chromoproteins with the individual bond-type (α and β) selectivity. While the membrane-bound complexes demonstrated very high resilience to pressures reaching 3 GPa, characteristic discontinuous shifts and broadenings of the absorption spectra were observed around 1.1 GPa for wild type LH1 and 0.5 GPa for wild type LH2 detergent-solubilized chromoproteins. These pressure effects, mostly reversible upon decompression, allowed estimating the rupture energies of the hydrogen bonds between the chromophores and the surrounding protein in the LH1 and LH2 complexes. Quasi-independent, additive role of H-bonds in the α- and β-sub-lattices in reinforcement of the wild type LH1 complex was established. The protein stabilizing effects of glycerol, a co-solvent, of high protein concentration, as well as of the presence of native carotenoids and reaction centers are also demonstrated. This study thereby provides important insights into design principles of natural photosynthetic complexes.

TABLE OF CONTENTS

ABSTRACT 7

TABLE OF CONTENTS 8

PUBLICATIONS AND THE AUTHOR'S CONTRIBUTION 10

LIST OF ABBREVIATIONS 13

1. INTRODUCTION (REVIEW OF LITERATURE) 15
   - 1.1. Photosynthesis 15
   - 1.2. Elements of photosynthesis apparatus of purple bacteria 16
     - 1.2.1. Peripheral antennas 19
     - 1.2.2. Core antennas 21
     - 1.2.3. Reaction centers 23
   - 1.3. Excitons in cyclic bacterial light-harvesting complexes 25
   - 1.4. Pressure as a thermodynamic variable 26
   - 1.5. Proteins under pressure 27
   - 1.6. Thermodynamic approach to protein stability against pressure 28

2. AIMS AND OBJECTIVES OF THE STUDY, AND THE MAIN EXPERIMENTAL APPROACH 30

3. MATERIALS AND METHODS 31
   - 3.1. Materials 31
   - 3.2. Sample preparation 31
     - 3.2.1. Native and mutant membrane-bound complexes 33
     - 3.2.2. Detergent-isolated complexes 33
   - 3.3. High-pressure spectroscopy 34
     - 3.3.1. Diamond anvil high pressure cell 34
     - 3.3.2. Pressure detection 34
     - 3.3.3. Spectral measurements 35
   - 3.4. Data analysis and estimations of the experimental error 36

4. RESULTS AND DISCUSSION 37
   - 4.1. Overview of the optical absorption spectra of the samples under ambient conditions 37
     - 4.1.1. Peripheral antenna complexes 37
     - 4.1.2. Core complexes 39
     - 4.1.3. Full intracytoplasmic membranes 41
   - 4.2. Pressure-induced modifications of the spectra 42
     - 4.2.1. Exciton absorption band positions and widths as a function of pressure 44
     - 4.2.2. Relative band shift and broadening 46
     - 4.2.3. The reference state/sample problem 49
     - 4.2.4. Reversibility of the high-pressure effects 49
   - 4.3. Estimation of the chromophore-binding hydrogen bond energies. 51
     - 4.3.1. Peripheral complexes 52

4.3.1.1. Isolated complexes 52
4.3.1.2. Effect of detergent on the LH2 protein stability. 54
4.3.1.3. Native membrane bound complexes 56
4.3.2. Core complexes 59
4.3.3. Characterization the hidden high-energy conformational states revealed by high pressure 62

5. CONCLUSIONS AND THE MAIN RESULTS..... 65

SUMMARY IN ESTONIAN 67

REFERENCES..... 69

ACKNOWLEDGEMENTS 78

APPENDIX: DIRECTIONS OF THE FUTURE RESEARCH 79

PUBLICATIONS 81

CURRICULUM VITAE 137

PUBLICATIONS AND THE AUTHOR'S CONTRIBUTION

Original publications (with annotation):

I L. Kangur, K. Leiger, A. Freiberg (2008) "Evidence for High Pressure-Induced Rupture of Hydrogen Bonds in LH2 Photosynthetic Antenna Pigment-Protein Complexes". J. Phys.: Conf. Ser. 121: 112004.

First evidence was obtained for reversible high-pressure-induced rupture of hydrogen bonds in an integral membrane protein using the intrinsic protein chromophores as sensitive optical probes. The membrane-embedded LH2 complexes appear more resilient to damaging effects of the compression than the complexes extracted into detergent environment. This difference was tentatively explained by more compact structure of the membrane-embedded complexes.

II L. Kangur, K. Timpmann, A. Freiberg (2008) "Stability of Integral Membrane Proteins under High Hydrostatic Pressure: The LH2 and LH3 Antenna Pigment-Protein Complexes from Photosynthetic Bacteria". J. Phys. Chem. B 112 (26): 7948–55.

A systematic study was performed of the high-pressure stability of the bacteriochlorophyll *a*-containing LH2 and LH3 membrane protein complexes from photosynthetic bacteria. It was demonstrated that high pressure does induce significant alterations to the tertiary structure of the protein complexes not only in proximity of the 800 nm-absorbing bacteriochlorophyll *a* molecules known previously (Gall, A. et al. Biochemistry 2003, 42, 13019) but also of the 850 nm- and 820 nm-absorbing molecules, including breakage of the H-bond they are involved in. It was proposed that the principal reason of the pressure-induced denaturation of the proteins is penetration of the surrounding water molecules into the hydrophobic protein interior.

III A. Freiberg, L. Kangur, J. D. Olsen, C. N. Hunter. (2012) "Structural Implications of Hydrogen-Bond Energetics in Membrane Proteins Revealed by High-Pressure Spectroscopy". Biophys. J. 103 (11): 2352–60.

Local changes in the bacteriochlorophyll *a* binding sites of the core membrane complexes from wild type and hydrogen bond-mutant photosynthetic bacteria induced by hydrostatic high pressure were explored. A quasi-independent, additive role of hydrogen bonds belonging to the α- and β-sublattices in reinforcement of the wild type core complex was established, providing important insights into the design principles of natural photosynthetic complexes.

IV L. Kangur, J. D. Olsen, C. N. Hunter, A. Freiberg (2012) "Estimating Hydrogen Bond Energy in Integral Membrane Chromoproteins by High Hydrostatic Pressure Optical Spectroscopy". Protein Structure, Eshel Faraggi (Ed.), ISBN: 978-953-51-0555-8, InTech, DOI: 10.5772/37309.

A minimalistic two-state thermodynamic model of protein denaturation was developed and applied to evaluate the free energy and the partial molar volume

changes related to the high pressure-induced rupture of hydrogen bonds in wild type and carotenoids-mutant LH2 complexes. The results highlighted the important role the carotenoids play in reinforcement of the photosynthetic light harvesting protein structures.

Conference reports (oral presentations):

V L. Kangur, A. Freiberg (2007) "Evidence for High Pressure-Induced Rupture of Hydrogen Bonds in Isolated LH2 Photosynthetic Antenna Pigment-Protein Complexes". Joint 21st AIRAPT and 45th EHPRG International Conference on "High Pressure Science and Technology". 17–21 September, Catania, Italy.

VI A. Freiberg, L. Kangur (2009) "High-pressure Manipulation and Spectroscopy of Photosynthetic Pigment-protein Complexes". Zing Nanobiophysics & Chemistry with Nanomedicine & Toxicology. 21–25 January, Jolly Beach, Antigua, Book of Abstracts p. 18.

VII A. Freiberg, L. Kangur (2009) "Stability of integral membrane proteins under high hydrostatic pressure: The antenna and reaction centre pigment-protein complexes from photosynthetic purple bacteria". Light-Harvesting Processes. March 10–14, Banz Monastery, Germany, Book of Abstracts p. 67.

VIII L. Kangur, A. Freiberg (2010) "High Hydrostatic Pressure Effects on Membrane Proteins Related to Reversible Rupture of Hydrogen Bonds: Cyclic Light-harvesting Complexes From Purple Bacteria". International conference on High Pressure Research, The 48th European High Pressure Research Group (EHPRG) Conference. July 25–29, Uppsala, Sweden, Book of Abstracts p. 98.

IX A. Freiberg, L. Kangur (2011) "Membrane Proteins Under High Hydrostatic Pressure Reveal Cooperative and Reversible Rupture of Hydrogen Bonds". 3rd International Conference on Drug Discovery & Therapy. February 7–10, Dubai, UAE.

X L. Kangur, A. Freiberg (2012) "High-Pressure Optical Spectroscopy Study of Hydrogen Bond Energetics and Structural Stability of Integral Membrane Chromoproteins". 50th EHPRG Meeting. 16–21 September, Thessaloniki, Greece, Program and Book of Abstracts, Book of Abstracts p. 53.

XI L. Kangur, A. Freiberg (2012) "Dissociation of Bacterial Light-Harvesting Complex LH1 by High Hydrostatic Pressure" TÜMRI aastakonverents. Annual conference 2012. Program and Book of Abstracts p. 37.

Author's contribution:

The author participated in the study design, performed the experiments, analyzed the data, and participated in preparation of the papers.

Other publications of the author not included into the thesis:

P. Palumaa, A. Voronova, L. Kangur, R. Sillard, W. Meyer-Klaucke, T. Meyer, A. Rompel (2005) "Mammalian copper chaperone Cox17 exists in two metalloforms, linked by oxidative switch". FEBS Journal, 272(Suppl. 1): 386–387.

P. Palumaa, L. Kangur, A. Voronova, R. Sillard (2004) "Metal-binding mechanism of Cox17, a copper chaperone for cytochrome c oxidase". Biochemical Journal, 382: 307–314.

P. Palumaa, E. Eriste, K. Kruusel, L. Kangur, H. Jornvall, R. Sillard (2003) "Metal binding to brain-specific metallotifhonein-3 studied by electrospray ionization mass spectrometry". Cellular and Molecular Biology, 49(5): 763–768.

A. Nurk, J. Simisker, L. Kangur, L. Medijainen, E. Heinaru, A. Heinaru, (2002) "A novel thermophilic isolate for the production of L (+)-lactate". In: The 9th International Symposium on the Genetics of Industrial Microorganisms Abstract book. Gyeongju, Korea 1.–5.06 2002: The 9th International Symposium on the Genetics of Industrial Microorganisms; Gyeongju, Korea; 1–5 June 2002.

L. Kangur, P. Palumaa (2001) "The effects of physiologically important non-metallic ligands in the reactivity of metallothionein towards 5,5'-dithiobis (2-nitrobenzoic acid)". European Journal of Biochemistry, 268(18): 4979–4984.

V. Bonetto, L. Kangur, P. Palumaa, V. Mutt, H. Jornvall, R. Sillard (1999) "Large-scale HPLC purification of calbindin D9k from porcine intestine". Protein Expression and Purification, 17(3): 387–391.

L. Kangur, P. Toomik, P. Palumaa (1999) "Metallotioneiin-ligand seostumiskonstantide määramine – (Determination of binding constants for metallothionein-ligand interactions)". XXV Eesti keemiapäevad: teaduskonverentsi ettekannete referaadid (25th Estonian Chemistry Days: abstracts of scientific conference), Tallinn, 1999: 45–46.

LIST OF ABBREVIATIONS

Samples:

i	isolated
m	membrane
IC	intracytoplasmic
WT	wild type
Rba.	*Rhodobacter*
LH2	light-harvesting complex 2
α mutant	the LH2 mutant with broken H-bonds to the α-BChl
αβ mutant	the double mutant with broken H-bonds to both α-BChl and β-BChl
B800- + CrtC-	the B800 deficient LH2 double mutant, where the native carotenoids are replaced by neurosporene
CrtC-	the LH2 mutant, where the native carotenoids are replaced by neurosporene
LH1	light-harvesting complex 1
RC-LH1	reaction center light-harvesting complex 1
RC-LH1-Puf X	WT reaction center light-harvesting complex 1
RC	reaction center
Puf X	the *pufX* gene product encoded for dimerization of LH1-RC complex into native form
α+11	shorthand notation for the αTrp_{+11} mutation of amino acid in the α-polypeptide position +11 with respect to the BChl-coordinating His in LH1
β+9	shorthand notation for the βTrp_{+9} mutation of amino acid in the β-polypeptide position +9 with respect to the BChl-co-ordinating His in LH1
$\alpha\beta\text{-BChl}_2$	dimeric subunit of the LH1 complex

Chromophores:

BChl	bacteriochlorophyll-a
B800	BChls absorbing light at 800 nm
B820	BChls absorbing light at 820 nm
B850	BChls absorbing light at 850 nm
B875	BChls absorbing light at 875 nm
Car	carotenoid

Buffer components:

β-DDM	n-dodecyl-β-D-maltoside
DHPC	1,2-diheptanoyl-sn-glycero-3-phosphatidylcholine
EDTA	ethylenediaminetetraacetic acid
HEPES	N-(2-hydroxyethyl)piperazine-N´-(2-ethanesulfonic acid)
LDAO	lauryldimethylamine-N-oxide

TEN	buffer solution: 20 mM TRIS-HCl, pH = 8.0, 1 mM EDTA, 0,1 M NaCl
TRIS	tris(hydroxymethyl)amino methane

Varia:

CPK	a color convention for distinguishing atoms of different chemical elements in molecular models. The scheme is named after the CPK molecular models designed by chemists Robert Corey and Linus Pauling, and improved by Walter Koltun
DAC	diamond anvil cell
FWHM	full width at half maximum
H-bond	hydrogen bond
NA	not applicable
PSU	the photosynthetic unit
$P_{1/2}$	the midpoint pressure
Q_y	the lowest singlet electronic transition of BChl
Q_x	the second lowest singlet electronic transition of BChl
ΔG	the Gibbs free energy change
ΔV	the partial molar volume change

1. INTRODUCTION (REVIEW OF LITERATURE)

1.1. Photosynthesis

Photosynthesis is a fundamental process that accumulates the Sun's light energy into chemical energy. Photosynthesis can be performed by higher plants, algae, and bacteria. In plants and algae the light energy fixation is taking place in oxygenic conditions and the harvested light energy is transferred to split water molecule to produce hydrocarbons and O_2, and to reduce CO_2 into biomass. The bacterial photosynthesis is very variable because the diverse environments they adapt to live. In early condition of life on Earth, when the first living organisms appeared, the anaerobic environment was prevailing. The anoxygenic phototrophic bacteria, among them the purple anoxygenic photosynthetic bacteria, are suggested to be one of the earliest photosynthesis performing life-forms on the Earth [1,2]. The word "phototrophic" refers to a metabolic mode in which organisms convert light energy into chemical energy for growth. To grow and multiply, these organisms were expected to use light energy, and instead of splitting water like more modern plants and algae, they were consuming sulfur and nitrogen compounds as the source of electrons.

The photosynthetic purple bacteria are model organisms for research of photosynthesis. Their name is connected to their coloration demonstrated in Figure 1 – the spring bottom where among the green algae lay areas of purple phototrophic bacteria showing intensive pink color.

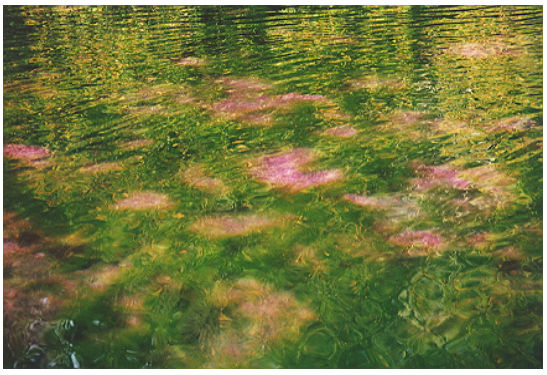

Figure 1. Purple photosynthetic bacteria mixed with green algae at the bottom of the spring [3].

Like most other photosynthetic bacteria, purple bacteria do not produce oxygen, because the reducing agent (electron donor) involved in photosynthesis is not water. In some bacteria called purple sulfur bacteria, it is either sulfide or elemental sulfur. At one point these were considered families, but RNA trees show that the purple bacteria make up a variety of separate groups, each closer related

to the non-photosynthetic proteobacteria than one another [4]. Purple bacteria belong to the phylum *Proteobacteria* that produce bacteriochlorophyll *a* or *b* under oxic or anoxic conditions. Their RC-s contain heterodimeric cores with quinines as terminal electron acceptors and membrane-intrinsic caroteno-BChl antennae; many oxidize sulfide, thiosulfate, or H_2 and fix carbon by the reductive pentose-phosphate (Calvin–Benson–Bassham) cycle. The trans-membrane light harvesting complexes investigated in this work mainly come from the purple non-sulfur bacterium *Rba. sphaeroides*, which is one of the most often exploited photosynthetic species for model studies of photosynthesis mechanisms and structures of photosynthesis apparatus.

1.2. Elements of photosynthesis apparatus of purple bacteria

In bacteria the photosynthesis apparatus is arranged into continuous system of IC membranes [2]. The bacterial IC membranes may be organized into vesicles, tubules, thylacoid – like membranes sacs or highly organized membrane stacks. Schematic structure of a vesicle-like membrane that is characteristic to *Rba. sphaeroides*, the bacterial species studied in the present work, is shown in Figure 2. The spherical membrane is mainly populated by two types of light-harvesting pigment-protein complexes, LH2 and LH1.

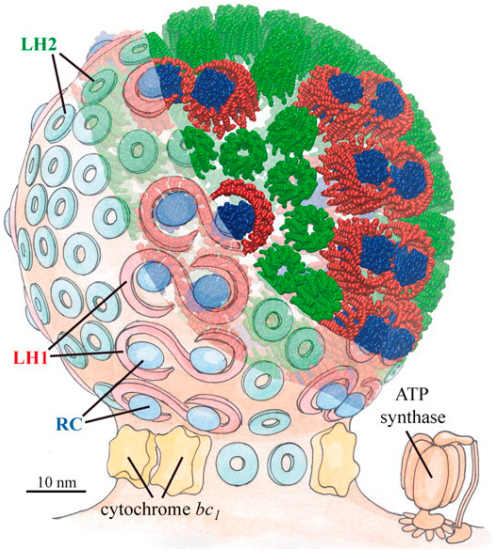

Figure 2. Schematic view of the vesicle-like cytoplasmic photosynthetic membrane from *Rba. sphaeroides* [5]. Indicated with different colors are the LH2 (green), LH1 (red), RC (blue), cytochrome bc_1 (yellow) complexes, and the ATP synthase (orange). Notice the 10-nm scale bar at the left bottom corner of the figure.

The LH1 complex is directly encircling the RC complex forming a core RC-LH1 complex, while the LH2 complexes are found in the periphery. The ratio of peripheral and core antennas are known to vary, depending on the light irradiance during the growth of the bacterium [6]. Together, the core complex and the surrounding peripheral complexes, being in functional contact with the core complex, shape a functional entity called PSU [7] (see also [8] for a review).

The sequence of processes taking place in photosynthetic apparatus of phototrophic purple bacteria is schematically shown in Figure 3. Photosynthesis is triggered by the absorption of solar energy quanta, photons (wavy black arrow), by the light collecting system comprising multiple LH2 and LH1 complexes. The absorbed energy is subsequently donated to the RC by energy transfer mechanisms briefly explained below. In RC the excitation energy is transformed into potential chemical energy by sequential electron transfer processes, whereby the primary electron donor of RC called special pair is oxidized and the electron transfer cofactors (see below) are reduced. At the last stage the quinone Q in RC is reduced to hydroquinone QH_2. The QH_2 then moves away from RC to the cytochrome bc_1 complex reducing it. The reduced cytochrome bc_1 complex pumps protons across the membrane. The cytochrome c_2 (blue) transports electrons back to the RC from the ubiquinone–cytochrome bc_1 complex (yellow). The electron flow across the membrane, shown by blue arrows, includes a simultaneous proton movement producing the proton gradient. The generated this way proton gradient drives the synthesis of ATP from ADP by ATPase, as a result of the flow of protons through ATPase.

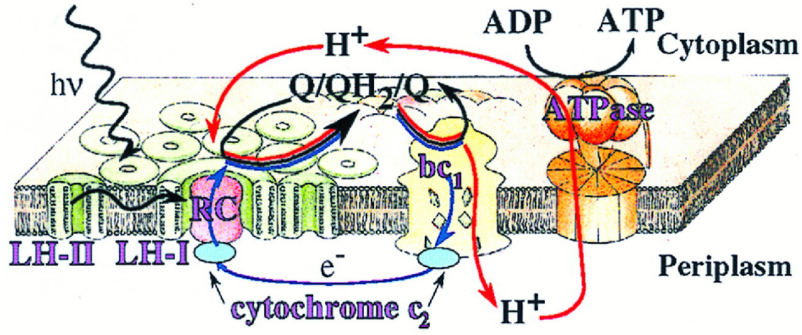

Figure 3. Schematic representation of the working stages of the photosynthetic apparatus in the intracytoplasmic membrane of purple bacteria. [9].

Energy transfer in PSU of photosynthetic bacteria is a well-studied area (see for reviews [9,10]). Figure 4 demonstrates the localization of photosynthetic chromophores (BChls and carotenoids) in photosynthetic membranes (the protein components are discarded and the specific numbers indicated may vary, depending on the literature source). The chromophores are packed inside the hydrophobic core of the proteins and are located in a way to grant the migration

of the absorbed photon energy to RCs along the energy lowering order Car>B800>B850>B875>RC, established by overlapping absorption regions. The excitation energy flow between peripheral LH2 and core LH1 antenna complexes with the closest approach of the chromophores from different complexes of 2–3 nm can be explained by the classical Fröster mechanism [11]. The neighboring BChl within the LH1 and LH2 ring structures are in much closer arrangement (see below). Strong resonant interactions between the transition dipole moments of the chromophores in these structures readily distribute the excited states over the full ring, forming so-called excitons. Excitons thus mainly transfer the solar excitation energy inside the peripheral and core antenna complexes.

It has been established by previous workers that energy transfers in *Rba. sphaeroides* membranes from Car to BChls in LH1 and LH2 complexes takes about 200 fs [12,13]. The efficiency of this transfer varies, being in LH2 between 70 % (when transferred directly to B850) and 30 % (when transferred through B800 to B850) [13–15]. The energy transfer from B800 to B850 molecules within LH2 occurs in 1–2 ps [16–19]. The energy transfer time from LH2 to LH1 is heterogeneous; it is measured to be less than 10 ps for 70% of excitations and about 50 ps for the remaining part of excitations [16,17,20]. The energy transfer from LH1 to RC takes 35–50 ps and back transfer, 8–12 ps [21–23].

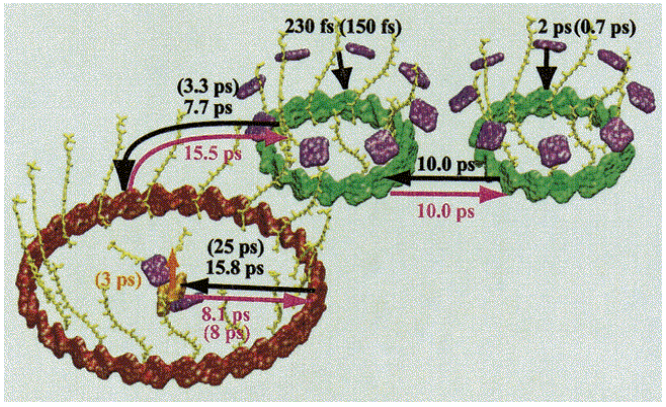

Figure 4. Schematic pathways of energy transfer in PSUs of purple bacteria. The strongly excitonically coupled BChl rings are shown in red (B875 in LH1) and green (B850 in LH2), respectively; the largely monomeric B800 BChls in LH2 and Car are correspondingly shown in violet and yellow colors. The periplasmic side is down and cytoplasmic side up. The energy flows towards RC are shown by black and backwards by red arrows. Shown also are the respective experimental and calculation (in brackets) excitation transfer times. Figure adapted from [24].

1.2.1. Peripheral antennas

The LH2 peripheral antenna pigment-protein complex of purple photosynthetic bacteria is one of the best characterized membrane proteins, apart from the RC pigment-protein complex (see below). The crystal structure of isolated LH2 from *Rps. acidophila* strain 10050 [25] and *Rhodospirillum molichianum* [26] solved at 2.0 Å and 2.4 Å, respectively, reveal highly symmetric rings of 9 or 8 dimeric pigment-protein subunits αβ-$BChl_2$, each containing two (α and β) helical membrane-spanning polypeptides, three non-covalently bound BChl molecules, and a Car pigment. The 25 residues of the α- and β-polypeptide chains form transmembrane α-helix, while the N- and C-terminus parts have a random coil structure. The α- and β-polypeptides form two concentric cylinders providing, respectively, inside and outside support to the cofactor rings between them, as shown in Figure 5.

A most striking feature of the organization of the 27 BChl molecules in LH2 from *Rps. acidophila* is their partition into two concentric rings, with the closest distance between the BChls in different rings being 18.4 Å. A ring of 18 tightly coupled (intermolecular separation <1 nm) BChl cofactors in a waterwheel-like arrangement are seen in the lumenal part of the photosynthetic membrane (bottom side of figure 5B). It is responsible for the intense near infrared exciton absorption of the LH2 complex at about 850 nm (see part 1.3 for the optical properties of the bacterial LH complexes). The position of the B850 cofactors relative to each other is determined by the H-bonds to the surrounding protein as well as by the coordinating bonds between the central magnesium ion of the BChls and the highly conserved His residues of the apoproteins [27]. As demonstrated in Figure 5C, participating in H-bonding is only the α-polypeptide, which forms a short bent α-helical structure in *C*-terminal side carrying two H-bonding amino acids, αTyr44 and αTrp45 It also supports α Tyr41, relevant for H-bonding in LH3, another bacterial antenna complex, briefly discussed below. Remarkably, the αTyr44 and αTrp45 residues from the α-polypeptide chain form H-bonds with the BChls belonging to two neighboring protomers, thus firmly tying the dimeric αβ-$BChl_2$ protomers to each other.

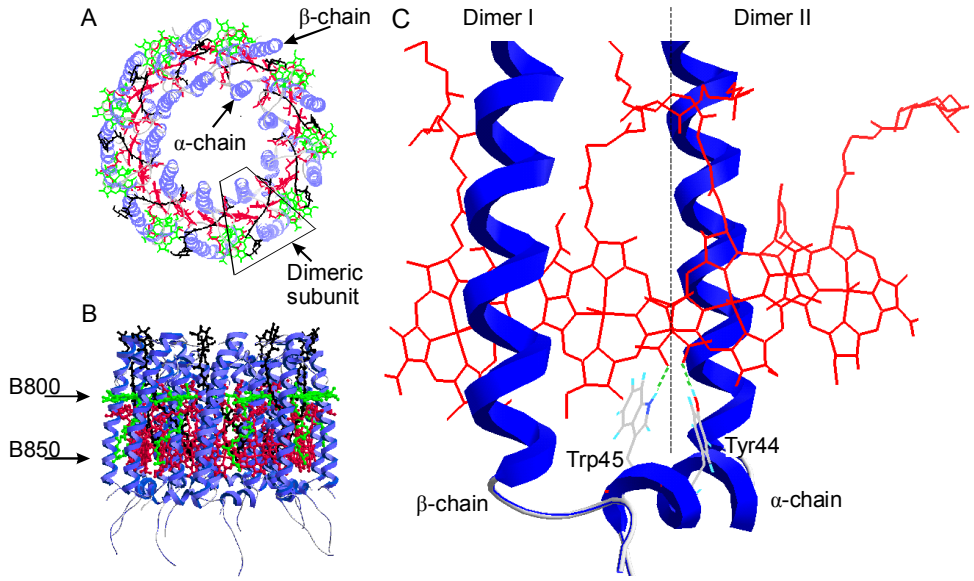

Figure 5. Structure of the LH2 complex from *Rps. acidophila*, based on the X-ray crystallographic data of [25]: top view (A), side view (B, lumenal part down, cytoplasmic part up), and the blown up view of a subunit of the B850 ring containing 4 BChls that belong to two neighboring protameric subunits of the protein ring (C). Shown in blue are the α- and β- trans-membrane polypeptides; in green, the B800 BChls; in red, the B850 BChls; in black, the carotenoids. Panel C demonstrates that H-bonds (turquoise dashed lines) to the two B850 BChls from the neighboring dimeric subunits (dimers I and II) are provided by two different amino acids of the same α-polypeptide: Tyr 44 forms the bond with the α-side BChl and Trp45, with the β-side BChl. Notice that in the amino acid sequence of *Rba. sphaeroides* instead of Trp45 stands Tyr. The structure was created using the pdb data and Swiss-PdbViewer3.7.

This might be the main reason why the multimeric LH2 protein withstands dissociation into its dimeric sub-units under even very high detergent concentration, differently from the LH1 complex (see the last part of this work). The B850 BChl molecules have their bacteriochlorin planes parallel to the symmetry axis of the complex. They are well protected from the outside medium by very tight hydrophobic parts of the α- and β-polypeptide walls. The core of the LH2 complex is highly hydrophobic; in detergent-isolated complexes, it is filled with detergent [28]. Another ring of 9 BChl molecules (intermolecular distance ≥2 nm) is located towards the polar cytoplasmic part of the membrane (top side of figure 5A); these chromophores are in charge of the absorption band peaking at 800 nm. The central Mg^{2+} ions of B800 BChls are suggested to have ligation with COO-α-Met1; its C_3-acetyl group is coordinated with βArg20 [25]. The B800 molecules have little support from outside, while there is a rigid α-poly-

peptide wall from inside (see Figure 5B). The B800 and B850 spectral bands both are related to the lowest Q_y singlet electronic transition observed in individual BChl molecules, as will be in some detail explained below. Although the atomic-resolution crystallographic data for the LH2 complexes from *Rba. sphaeroides* – the major samples of the present study – are not available, low-resolution projection data suggest their very similar organization to the complexes from *Rps. acidophila [29]*.

Variant peripheral antenna complexes called LH3 and LH4 develop under stressed (low light and/or low temperature) growth conditions of photosynthetic bacteria. Although highly homologous with the LH2 protein in terms of amino-acid sequences, the LH3 complex from *Rps. acidophila* (strain 7750) [29] appears spectrally very different. Specifically, the main exciton absorption band in the LH3 complex peaks at ~820 nm, being several tens of nanometers up-shifted relative to its position in regular LH2 (strain 10050). A couple of well-defined differences in the H-bonding patterns of the 850 nm- and 820 nm-absorbing BChls have been identified [25,29] that might be responsible for the observed spectral differences. Firstly, the H-bond coordinating the β-BChls in LH2 with the surrounding protein is missing in LH3. There are thus 18 H-bonds in LH2 and only 9 H-bonds in LH3 coordinating the 18 Bchl molecules in the B850 or B820 rings, respectively, to the surrounding protein scaffold. Secondly, the α-BChls that in LH2 are H-bonded with αTyr44 is in LH3 tied to another protein residue, αTyr41. As a result, the C_3-acetyl chain, which in LH2 complexes is almost parallel to the BChl macrocycle plane, tilts in LH3 significantly out from that plane. Based on theoretical calculations [30], it was suggested [29] that the altered torsional angle of the C_3-acetyl group dominates in the blue shifting of the B820 band in LH3. By analyses of the antenna absorption and polarized fluorescence excitation spectra measured at 5 K, significant modifications of antenna exciton properties were also revealed [31]. It was hence confirmed that in LH3 complexes almost the entire red shift of the absorption band (relative to the absorption of individual BChls) has exciton origin, whereas in regular LH2 complexes the exciton mechanism is responsible for just slightly over half of the absorption band shift.

1.2.2. Core antennas

In phototrophic bacteria such as *Rba. sphaeroides*, peripheral LH2 complexes donate energy to the LH1 complexes, which encircle the RCs, forming a core RC-LH1 complex. Low-resolution structural models of core complexes have been obtained for a number of species [32–35]. Like in LH2 complexes, the basic building block for in vivo assembly of the LH1 complex is a αβ-$BChl_2$ heterodimer of membrane-spanning α-helical α- and β-polypeptide, with each apoprotein noncovalently binding one BChl molecule [36] (see Figure 6). The organization of bacterial core complexes can vary, and consists of 15 [33], 16 [37], or 28 [34] such dimeric structural elements. In WT *Rba. sphaeroides*, open

C- or *S*-shaped antenna structures encircling one or two RCs in planar or non-planar geometry are known to coexist in photosynthetically grown cells [6] as shown in Figure 7.

Due to the multimeric nature of these complexes, where each WT αβ-$BChl_2$ subunit has two H-bonds, one to α- and another to β-polypeptide, the total number of H-bonds per LH1 complex is large: 32 in the LH1-only and RC-LH1 mutant complexes, 56 in the RC-LH1-PufX dimer complex, and 28 in the RC-LH1-PufX monomer complex. Two point mutations of the RC-LH1-PufX complexes that eliminate the H-bonds to specific BChls at positions αTrp_{+11} and βTrp_{+9} have been constructed [38]. These αTrp_{+11} or βTrp_{+9} mutants will have half the number of H-bonds of the equivalent WT complex.

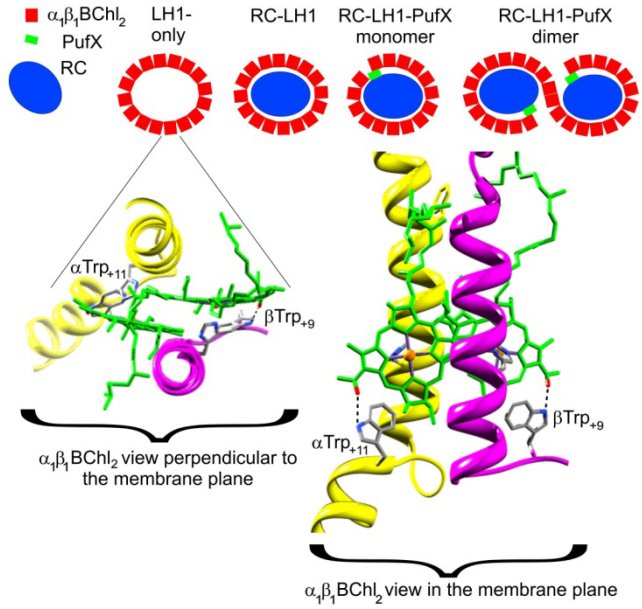

Figure 6. Diagrammatic representation of the core LH complexes. Each red square represents the αβ-$BChl_2$ heterodimer 'building block' of the LH1 complex. Below are two views of the αβ-$BChl_2$ subunit based upon the atomic structure of the LH2 complex from *Phaeospirillum molischianum*, together with mutagenesis, atomic force microscopy, and cryo-electron microscopy data [34,35,39,40]. The two residues that have been altered from Trp to Phe in the αTrp_{+11} and βTrp_{+9} mutants are in stick representation, whilst the rest of the transmembrane polypeptides are depicted as a ribbon. The BChls and the H-bond partners are also shown.

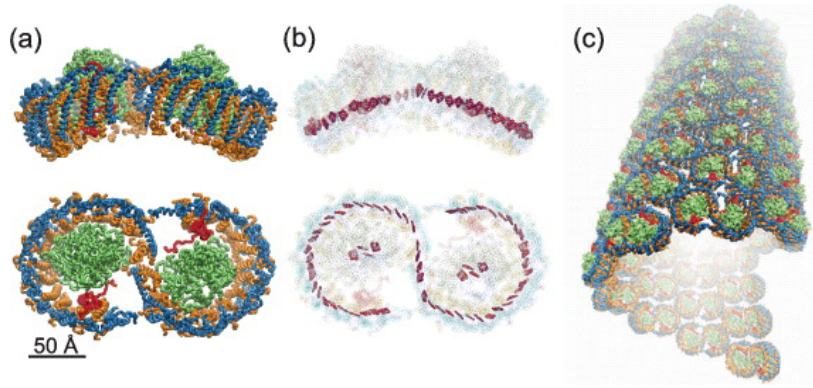

Figure 7. (a, b) Models of the *Rba. sphaeroides* RC-LH1-PufX core complexes proposed in [41–44]. The α- and β-transmembrane helixes are shown in orange and blue, respectively, RC complexes in green, PufX complexes in red, BChls in purple. Top: side view along the membrane plane; bottom: a view from above. (c) A perspective view of a segment of the tubular photosynthetic membrane composed solely from the RC-LH1-PufX core complexes.

1.2.3. Reaction centers

In the RCs, the excitation energy is transformed into potential chemical energy by a sequence of ultrafast charge separating electron transfer processes in a membrane. The best characterised RC systems are found in purple nonsulfur bacteria. The X-ray crystal structure of the bacterial RC has been determined with nearly atomic resolution [45], giving us a detailed picture of the positions and orientations of the redox active pigments as well as a structural basis for understanding the important protein-pigment interactions. In *Rba. sphaeroides* the electron transfer system consists of a dimer of BChl molecules – the primary donor of electrons (customarily denoted as *P*), two accessory BChl molecules (B_A and B_B), two molecules of bacteriopheophytin (H_A and H_B), and two quinones (Q_A and Q_B). As shown in Figure 8, these electron transfer cofactors are arranged in two approximately symmetric branches, termed *L* and *M*, that span the membrane, but only the *L* branch, involving B_A, H_A, and Q_A, is photochemically active under normal conditions.

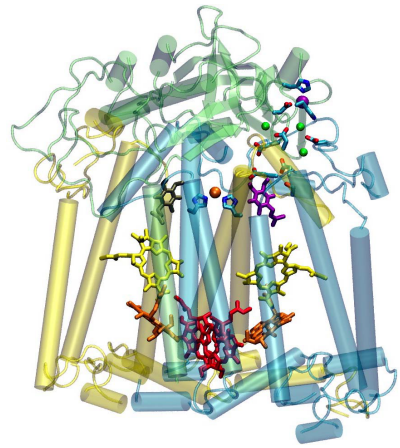

Figure 8. A side view of the RC from the photosynthetic bacterium *Rba. sphaeroides*. The quasi-two fold symmetry axis, which runs vertically and is perpendicular to the membrane plane, creates pairs of identical cofactors, yet with very different properties. *http://mcb.illinois.edu/faculty/profile/cwraight*

The overall sequence and kinetics of the electron transfer process is well known [46] (Figure 9). Photoexcitation of *P* results in the transfer of an electron from *P** (an excited state of *P*) to H_L in a few picoseconds. The recombination yield is less than 1 % and the energy stored within the relaxed charge separated state $P^+ H_A^-$, is 84 % of the excitation energy of *P**. No artificial donor-acceptor system can match these values. The subsequent stabilizing reaction, involving electron transfer from H_A to Q_A occurs in approximately 200 ps. Further electron transfer from Q_A to Q_B is already much slower and takes about 200 μs. The doubly reduced Q_B is protonated from the external medium *[46]*.

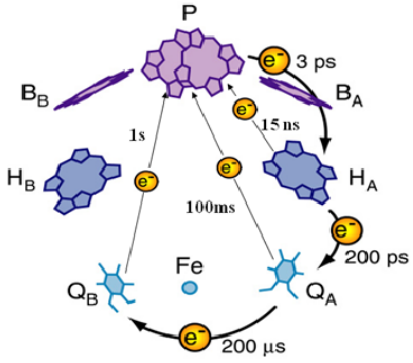

Figure 9. Schematics of light-induced electron transfer processes in bacterial RCs. Picture credit: N.Woodbury.

1.3. Excitons in cyclic bacterial light-harvesting complexes

The spectroscopic properties of LH1 and LH2 chromoproteins have been extensively studied [9,47–49]. While free in organic solvents, the lowest singlet (Q_y) electronic transition of BChl is located in the near infrared region at ~775 nm [50,51]. Significant red shifts of this transition are observed in the antenna systems. Major absorption bands in LH2 and LH1 complexes from *Rba. sphaeroides* peak at 850 and 875 nm. That is why they are called the B850 and B875 bands, respectively. The spectroscopic equivalent of the αβ-$BChl_2$ dimeric subunit of LH1 is called B820, showing a maximum at 820 nm [52]. The large shifts of the spectra of the BChl oligomers with respect to the spectra of monomeric BChl molecules in normal solvents are primarily related to unique arrangement of the BChl chromophores imposed by the surrounding protein scaffold, which promotes strong inter-pigment (exciton) interactions.

Availability of the high-resolution structural data of the LH2 complexes has made it possible to study exciton interactions within the B850 system thoroughly (see [48,53–57] for reviews). The 18 strongly coupled BChl molecules are arranged into two interspaced C_9 symmetrical rings. Interactions between the Q_y transition dipole moments of these molecules split the resulting 18 exciton states energetically into a broad exciton band schematically shown in Figure 10. The general circular geometry of the BChl aggregate determines that majority of the transition dipole moment is concentrated into the $k=\pm1$ states at the low-energy exciton band edge, which shape the characteristic B850 absorption band of LH2. The origin of the B875 spectra of the cyclic core complexes is similar. The only major difference is that the exciton band contains more states (being in the lowest order of approximation equal to the number of the BChl molecules in the specific aggregate, 56 in the RC-LH1-PufX complex, for example) and their energy density is higher [44].

The 9 BChls in the B800 ring on the cytroplasmic side of the complex are widely separated (~2 nm); therefore these chromophores are commonly considered to be monomeric. The B800 band shift from the molecular 775-nm absorption is mainly determined by interactions between the chromophores and the surrounding protein. Universal dispersion interactions aside, the factors that contribute most to the solvent/protein shifts are H-bonds to the C_3-acetyl carbonyl of the B800 BChls [58,59] and various conformational interactions [30,60].

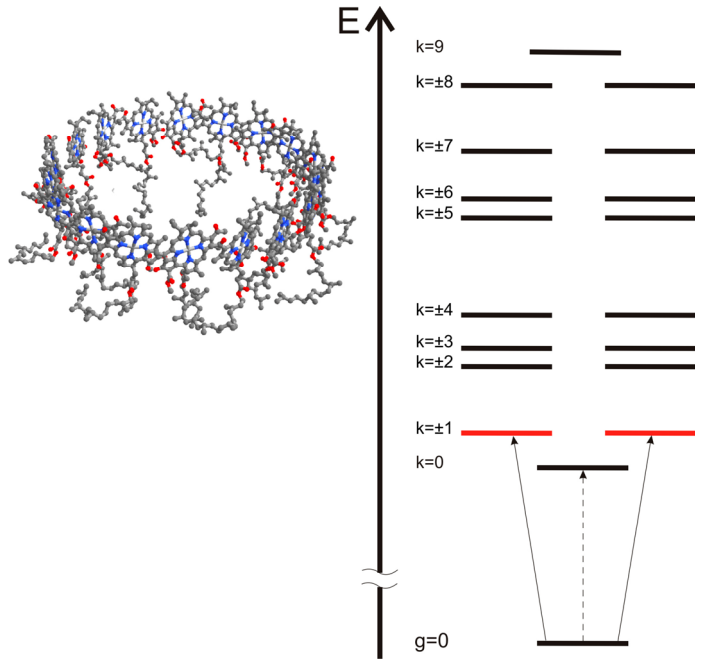

Figure 10. Idealized exciton level structure (bars) for the 18 BChls in the cyclic B850 LH complex shown on the left hand side. The two k=±1 exciton states, which possess nearly all the oscillator strength for the transitions from the ground state are highlighted with red. Dashed arrow designates weak absorption from the ground state g to the lowest-energy k=0 exciton state, which is optically (nearly) forbidden.

1.4. Pressure as a thermodynamic variable

Pressure governs the equilibrium of physicochemical processes according to the Eq. 1:

$$\frac{\partial \ln K}{\partial P} = -\frac{\Delta V}{RT}, \tag{1}$$

where K is the equilibrium constant, P is the pressure , ΔV is the partial molar volume change, R is the universal gas constant and T is the absolute (thermodynamic) temperature. Pressure shifts the equilibrium towards the state with the lowest volume – the rule called Le Chatelier principle.

The pressure also affects reaction rates. The dependence of the rate constant, k, on pressure is determined by the activation volume V_a of the reaction:

$$\frac{\partial \ln k}{\partial P} = -\frac{V_a}{RT}. \tag{2}$$

Pressure as a physical (thermodynamic) variable is different from temperature. By changing temperature one simultaneously affects both the internal energy and the volume (via thermal expansion) of the system, whereas pressure acts only to the volume of the system.

1.5. Proteins under pressure

The first report about action of high pressure on a protein was by Bridgman almost exactly a hundred years ago. He also showed that the egg white protein denatures irreversibly under the applied pressure of several 100 MPa [61]. Second half of the last century marks the advent of high-pressure studies of proteins. To date many water-soluble globular proteins have been investigated under high pressures, with the result that functional protein structures cover just a narrow region in the phase diagram around physiological temperatures [61–64]. Relatively little is still known about pressure effects on integral membrane proteins, which is the main tasks of the present study.

Apart from purely scientific curiosity, there are two practical motivations behind high pressure studies of proteins. One is the evolutionary ability of living organisms to adjust to harsh environmental conditions like high pressures [65]. The highest pressure in the biosphere is at the bottom of the Mariana Trench in the Pacific Ocean reaching about 110 MPa (1.1 kbar), and some life forms have been discovered there. The second practical motivation is pascalization, i.e., preserving and sterilizing foods through high pressure processing, where pressures in the range of 100–800 MPa are routinely used [66].

Proteins are complex assemblies of polypeptides that possess secondary, tertiary, and quaternary structure. Protein functional folds (conformations) are mainly determined by relatively weak (compared with the firm covalent bonds that govern the protein primary structure) interactions like H-bonding, hydrophobic interactions and certain ionic interactions. Proteins may also contain cofactors bonded by covalent or non-covalent bonds (H-bonds, coordination bonds, and hydrophobic interactions). All structurally important protein interactions are in principle influenced by external pressure, the pressure effects being reversible (elastic) or non-reversible (plastic). It is common practice in case of the soft protein matter, justified at not too high pressures, that pressure modifies only weak intra- and intermolecular interactions, leaving the covalent bonds (and the respective structures) mostly unchanged.

From the literature, it is known that most of the multi-chain (multi-domain) soluble proteins dissociate at room temperature already below 0.2 GPa [63], while small monomeric proteins easily survive pressures in the range of 0.4–0.8 GPa [63,65]. Following Eq. 1, the high-pressure denaturation processes are driven by a decrease in volume, which results from both the release of intramolecular voids [67] or/and the exposure of the interior of the protein to a polar solvent [68,69]. The protein structure and folding is intimately connected to hydrophobic interactions. Molecular dynamic simulations together with experi-

mental results show correlations in protein denaturation and changes in water structure [70]. The water as the main biological solvent has well-known anomalies, which are due to existence of the H-bond network. Under high pressure the structure of water changes, and so do hydrophobic effects [70].

H-bond energies in simple model compounds and small peptides, generally found to be between 4 and 20 kJ/mol, have been investigated in great detail [71,72]. This is not the case for folded globular proteins, and especially for membrane proteins, where individual H-bonds are much more difficult to characterize [73,74]. As brought out by NMR spectroscopy, the H-bond network in proteins is highly heterogeneous [75]. This is in agreement with variant H-bond strengths demonstrated in [76,77] for polypeptide chains. The previous publications have revealed that H-bonds in the secondary and tertiary structures of the proteins may be either widely insensitive to pressure [78] or promoted by it [79,80]. This seemingly contradictory information can be explained by the fact that each protein structure is unique.

Scanning calorimetry and titration with chemical denaturants such as urea are commonly used to study H-bond energies of proteins; however, since they probe the unfolding of the whole protein, they do not usually yield any bond-specific information. Moreover, scanning the temperature at constant pressure, as in calorimetry, causes simultaneous changes of the system's energy and its volume/density that are difficult to separate. Denaturants are often chemically active and may also modify the solute properties. For these reasons, the usage in the present work of pressure, rather than temperature, has significant advantages.

1.6. Thermodynamic approach to protein stability against pressure

In the simplest version of the thermodynamic modeling just two global protein states, native (*N*) and denatured (*D*), are assumed. In the present case, the *N* state corresponds to the protein at ambient pressure, while the *D* state, to its compressed state with broken H-bonds [63,64,81]. The thermodynamic stability of a protein is characterized by a change in Gibbs free energy upon the equilibrium transition from the N state to the D state. The equilibrium constant of this two-state reaction is given by Eq. 3, where [*N*] and [*D*] indicate the concentrations of native and denatured protein, respectively, *R* is the universal gas constant, *T* is the thermodynamic temperature, and *P* is the pressure

$$K(P) = [D]/[N] = \exp\left[-\Delta G(P)/RT\right]. \tag{3}$$

In the linear approximation, the pressure dependence of the free energy change associated with the protein denaturation can be represented as

$\Delta G(P) = \Delta G^0 + \Delta V^0 P$, where $\Delta G^0 = G_D^0 - G_N^0$ is the standard Gibbs free energy difference between the denatured and the native states, and $\Delta V^0 = V_D - V_N$ is the standard partial molar volume change between the states. ΔG^0, has to be positive in order for the protein to be stable. If the volume of the denatured state is smaller than the volume of the native state, i.e., ΔV^0 is negative, the free energy change decreases with increasing pressure. Past the transition midpoint pressure, $P_{1/2}$, the denatured state has lower free energy and is thus stabilized against the native state.

A connection of this minimalistic model with the spectroscopic experiment is established by calculating the pressure-dependent equilibrium constant as

$$K(P) = \left[\Delta\nu(P) - \Delta\nu_i\right] / \left[\Delta\nu_f - \Delta\nu(P)\right], \tag{4}$$

where $\Delta\nu(P)$ is the relative peak shift at pressure P (as plotted in Fig.18A), and $\Delta\nu_i$ and $\Delta\nu_f$ are the shifts measured at initial (i) and saturating final (f) pressures, respectively. Taking logarithm from both sides of Eq. 3 results in linear equation with respect to pressure

$$-RT \ln K(P) = \Delta G^0 + \Delta V^0 P. \tag{5}$$

Solution of Eq. 5 with Eq. 4 in place of $K(P)$ provides the prime model parameters, ΔV^0 and ΔG^0, as the slope and initial (P=0) value, respectively; additionally, $P_{1/2}$ can be found from the phase boundary condition: $\Delta G^0 + \Delta V^0 P_{1/2} = 0$. This way the valuable thermodynamic parameters characterizing protein stability against high pressure are evaluated from spectroscopic data. Graphical presentation of of Eq. 5 is shown in Figure 11.

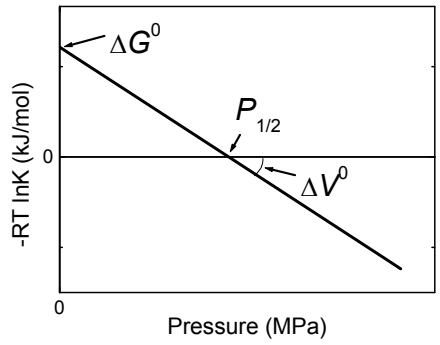

Figure 11. Graphical presentation of Eq. 5 to find the model parameters ΔG^0, ΔV^0, and $P_{1/2}$.

2. AIMS AND OBJECTIVES OF THE STUDY, AND THE MAIN EXPERIMENTAL APPROACH

As it was noted in previous paragraphs, there is a lack of general understanding of the mechanisms, which contribute into structural and functional stability of proteins, especially of integral membrane proteins. The current work is a step forward toward this goal, concentrating on H-bonds, the major stabilizing factor in any protein. The challenge is that there are generally too many different H-bonds in proteins as well as too little atomic-level structural data available about the proteins to obtain meaningful information about particular H-bonds. Therefore, for the present study, we were looking for the membrane proteins for which high- or at least medium-resolution structural data existed. The cyclic LH1, LH2, and LH3 LH pigment-protein complexes found in photosynthetic membranes of purple bacteria meet this requirement. It has been shown [25,82–84] that in bacterial pigment-protein complexes the intrinsic BChl chromophores participate in the well-defined H-bonds to the surrounding protein. It has also been established [85] that integrity of the protein complexes can be monitored with sub-nanometer spatial resolution by the so-called molecular probe method, using absorption (or fluorescence) spectra of the chromophores as spatially local and sensitive optical probes. This is the experimental approach used in the present work to study, identify, and quantify the energetics of individual H-bonds that undergo major changes under externally applied hydrostatic high pressure.

The objectives of this work are:

(i) To develop the non-invasive high-pressure methodology for studying the energetics of the H-bonds in membrane chromoproteins.

(ii) To apply this method for investigation of the stability of native and genetically engineered variants of LH membrane chromoproteins from *Rb. sphaeroides* and other species against hydrostatic high pressures reaching 3 GPa.

(iii) To compare high-pressure stability of detergent-isolated and the native membrane-embedded LH complexes.

(iv) To quantify H-bond energies, which structurally stabilize the BChl chromophores in bacterial LH complexes.

(v) To examine the roles of RC, carotenoids, protein/detergent ratio, and co-solvents such as glycerol in stabilizing the LH chromoproteins against pressure.

3. MATERIALS AND METHODS

3.1. Materials

The samples studied in this work are membrane chromoproteins from the photosynthetic purple bacterium *Rba. sphaeroides*. They were kindly provided to us through collaborations with the biochemists from the Sheffield University (group lead by Prof. N. Hunter).

The *Rba. sphaeroides* DD13 deletion strain [86], manipulated to remove the genes encoding the LH2, LH1 and RC complexes, was complemented with plasmid-borne copies of the *puf BALMX* genes to produce photosystems containing only the LH2, LH1, monomeric RC-LH1, or dimeric RC-LH1-PufX complexes.

The same strain was used to produce different H-bond mutants and carotenoid mutants of LH2 and LH1 complexes. The point mutations were introduced into either the *pufA* or *pufB* gene encoding α- and β-apoproteins, respectively, in LH1 or LH2. In the LH1 complex, one of these mutations ($\alpha Trp_{+11}Phe$) alters the tryptophan that H-bonds to the C_3-acetyl carbonyl group (IUPAC numbering) of one of the BChls in the αβ-$BChl_2$ structural unit [38,40], the other, $\beta Trp_{+9}Phe$, disrupts the H-bond to the C_3-acetyl carbonyl group of the other BChl [38]. The LH2 α-mutant has a mutation in the αTyr44 site to Phe that disconnects the H-bond to the BChl close to the α-apoprotein chain. In the αβ-mutant of LH2 both BChl molecules in the αβ-$BChl_2$ unit have lost their H-bonds to the protein due to the mutations of αTyr44 to Phe and αTyr45 to Leu [25,87,88] (see Figures 5 and 6).

The carotenoid mutant strain DD13/G1, further indicated as CrtC-, has mutation in the *crtC* gene, which changes the native mixture of spheroidene and spheroidenone (those carotenoids determine the purple color of the WT sample) to neurosporene and its derivatives. This results in green coloration of the mutant sample [86]. The B800-deficient mutant of the same strain with destabilized B800 binding site (B800- for short) was produced as described in [56].

Unfortunately, not all kinds of mutants are available to from a "full set", mostly because they proved not to be sufficiently stable even under normal conditions. For this reason, for instance, our list of samples misses isolated αβ-mutant LH2 complexes or the $\alpha Trp_{+11}Phe$ + $\beta Trp_{+9}Phe$ double mutant.

3.2. Sample preparation

As follows we will describe procedure of preparation protein samples for high-pressure spectroscopy measurements. Since the technology is different for native membrane-bound complexes and detergent-isolated complexes, they will be evaluated separately. Common to all samples, is that they are stored at liquid nitrogen temperature and thawed prior the experiments. The samples are diluted with TEN or HEPES buffer to obtain a reasonable optical density of about 0.3–0.4 at the B850 or B875 absorption band maximum in the assembled sample

cell (about 10 per 1 cm optical path). Buffering ability of the TEN and HEPES buffers is preserved over a broad pressure and temperature range [89,90].

For overview, the buffers and detergents used for preparing the studied samples are gathered into Table 1.

Table 1. Buffers and detergents used for preparing the samples from *Rba. sphaeroides*.

Sample	Buffer	Detergent
WT IC membrane vesicles	TEN	NA
CrtC- IC membrane vesicles	20 mM HEPES pH 7.5, 1mM EDTA	NA
iLH2	TEN	44 mM LDAO
mLH2	TEN	NA
iLH2 (CrtC-)	20 mM HEPES pH 7.8	3–131 mM LDAO
mLH2 (CrtC-)	20 mM HEPES pH 7.8	NA
iLH2 (B800-)	20 mM HEPES pH 7.8	44 mM LDAO
mLH2 (B800-)	20 mM HEPES pH 7.8	NA
iLH2 (B800- + CrtC-)	20 mM HEPES pH 7.8	44 mM LDAO
mLH2 (B800- + CrtC-)	20 mM HEPES pH 7.8	NA
mLH2 (α-mutant)	10 mM TRIS-HCl, pH 7.9, 1mM EDTA	NA
mLH2 (αβ-mutant)	10 mM TRIS-HCl, pH 7.9, 1mM EDTA	NA
iLH1	10 mM TRIS-HCl, pH 7.9, 1mM EDTA	3 mM DHPC
mLH1	10 mM TRIS-HCl, pH 7.9, 1mM EDTA	NA
iRC-LH1	10 mM TRIS-HCl, pH 7.9, 1mM EDTA	3 mM DHPC
mRC-LH1	10 mM TRIS-HCl, pH 7.9, 1mM EDTA	NA
iRC-LH1-PufX	20 mM HEPES pH 7.8	6 mM β-DDM
mRC-LH1-PufX	20 mM HEPES pH 7.8	NA
iRC-LH1-PufX ($\beta Trp_{+9}Phe$)	20 mM HEPES pH 7.8	6 mM β-DDM
mRC-LH1-PufX ($\beta Trp_{+9}Phe$)	20 mM HEPES pH 7.8	NA
iRC-LH1-PufX ($\alpha Trp_{+11}Phe$)	20 mM HEPES pH 7.8	6 mM β-DDM
mRC-LH1-PufX ($\alpha Trp_{+11}Phe$)	20 mM HEPES pH 7.8	NA

3.2.1. Native and mutant membrane-bound complexes

WT and CrtC- mutant chromatophores were diluted with buffers containing 20 mM TRIS-HCl (pH 8.0), 1 mM EDTA, 0.1 M NaCl and 20 mM HEPES (pH 7.5), 1 mM EDTA, respectively.
The LH2-only membranes were diluted with a buffer of 20 mM TRIS-HCl (pH 8.0), 0.1 M NaCl, 1mM EDTA or 20 mM HEPES (pH 7.8).
The LH2 H-bond mutant membranes were diluted in 10 mM TRIS-HCl (pH 7.9), 1 mM EDTA.
The 20 mM HEPES (pH 7.8) buffer was used for dilution the B800 deficient LH2 membranes.
The LH1 samples of membrane origin were diluted with 20 mM HEPES (pH 7.8) buffer or with 10 mM TRIS-HCl (pH 7.9), 1 mM EDTA.

3.2.2. Detergent-isolated complexes

It is widely believed that detergents above the critical micelle concentration closely mimic the embedding of the proteins in native membranes [91]. The critical micelle concentration for the detergents used in this work is as follows: 0.17 mM for β-DDM [92], 1.2 mM for LDAO [93], and 1.4–1.8 mM for DHPC [94,95].

The isolated LH2 complexes from *Rba. sphaeroides* were diluted with a 20 mM HEPES pH 7.5 buffer containing varying concentration of LDAO in order to tune the LH2 protein concentration in sample cell. The protein concentration was estimated based on the optical density of the sample and the known molar extinction coefficient of the LH2 chromoproteins (170 $mM^{-1}BChl^{-1}$ cm^{-1} [96]). The LH2 protein concentrations in different samples between 2 and 7 μM were this way determined. According to [96], to ensure well-isolated LH2 complexes in detergent micelles, the ratio of LDAO and protein molecules (D/P for short) should be in the order of 10^3 or more. This conclusion is supported by the measurements in this work (see paragraph 4.3.1.1). Commonly, LDAO concentrations exceeding 44 mM (or 1% in w/w units) were used in our measurements.

The 20 mM HEPES, pH 7.8 buffer for isolated core (LH1, RC-LH1, RC-LH1-PufX and RC-LH1-PufX mutants) complexes additionally contained detergent DHPC or β-DDM. The concentrations of used detergents (3 mM DHPC and 6 mM β-DDM) maintained the integrity of the core complexes at ambient pressure; the DHPC-solubilized complexes remained stable under elevated pressures for at least 20 hours at ambient temperature, which was more than sufficient for our present trials.

3.3. High-pressure spectroscopy

3.3.1. Diamond anvil high pressure cell

A commercial diamond anvil cell (DAC, D-02, Diacell Products Ltd.) shown in Figures 12 and 13 was used to create high pressures. The sample solution is injected into a 0.3 mm-diameter hole in about 0.35-mm thick stainless steel gasket, preindented between the anvils under small pressure. The gasket loaded with probe is squeezed between two diamonds. Pressure is achieved by tightening screws one by one to push the diamond, which is glued to the moving piston.

3.3.2. Pressure detection

A ruby-microbead pressure sensor (RSA Le Rubis SA) mounted directly into the sample volume was used to determine the pressure inside DAC. The sensor luminescence at 694.2 nm (R_2 line) was excited with a Nd:YAG laser at 532 nm and was recorded in transmitted light mode by means of a 1.5 m focal length Jobin-Yvon TH150 spectrograph equipped with a CCD (charge coupled device) camera. The accuracy of the pressure measurements (defined as the pressure needed to shift the emission line at the output of the spectrograph by one CCD camera pixel) with this apparatus is 20 MPa. In some measurements a Sm^{2+}-doped SrFCl micro-crystalline pressure sensor emitting at 690.3 nm was used. The pressure sensitivity equal to –23.05 cm^{-1}/GPa [97] of the Sm^{2+}-sensor is much greater than it is for the ruby sensor: –0.77 cm^{-1}/GPa [98,99]. Pressure dependencies for both sensors are perfectly linear over a broad pressure range.

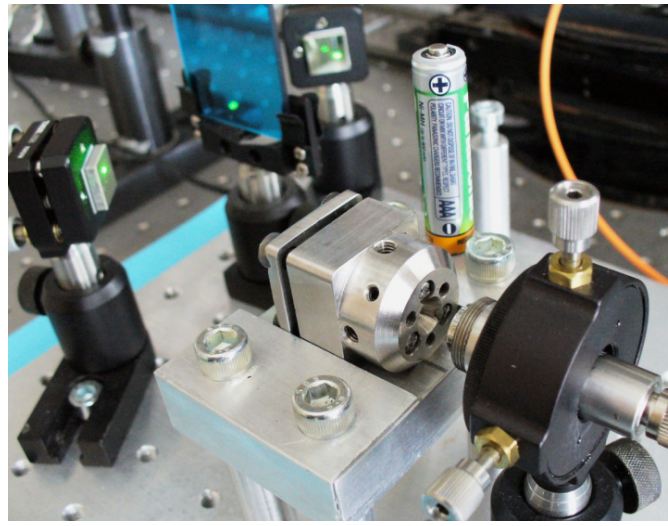

Figure 12. The diamond anvil cell (DAC D-02) on the stand in the pressure measurement setup. The cell is in the middle, aside a AAA battery for size comparison.

We have verified on two samples (isolated WT LH1 complexes and isolated CrtC- mutant LH2 complexes) that there is very little alteration in the spectra when temperature was deliberately varied between 15 and 25ºC. However, owing to high sensitivity of the *R*-lines of ruby on temperature (1 degree in temperature converts to ~19 MPa change in pressure [98,99]), stabilization of temperature when conducting DAC experiments is critical. In our trials DAC was tightened to the thermoelectrically stabilized base, thereby securing the sample temperature within 22 ± 0.5ºC, consequently the pressure uncertainty within ± 10 MPa.

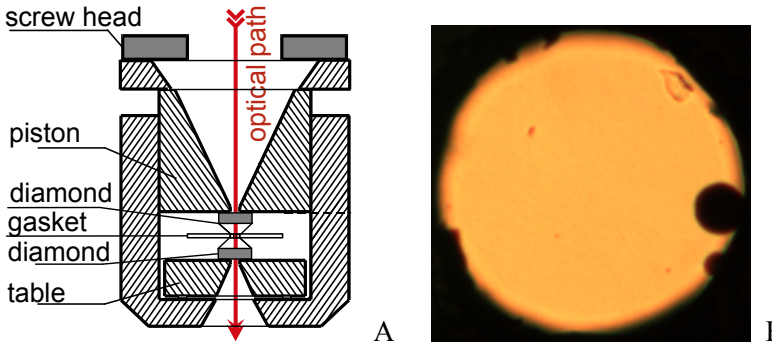

Figure 13. (A) Schematic cross-section of the DAC and (B) a photo of the gasket hole area filled with a probe and the ruby micro-bead pressure sensors (two shades on the right).

3.3.3. Spectral measurements

Mostly absorption spectra have been measured in this work. Fluorescence spectra were measured only occasionally to check integrity of the samples. By falling apart the proteins BChl molecules in the solvent phase give rise to a characteristic fluorescence emission at 780–790 nm. The absorption/transmission spectra of the samples (consisting of isolated LH complexes, membrane bound LH complexes and chromatophores at ambient pressure and temperature) were recorded using a 0.3 m spectrograph (Shamrock SR-303i, Andor Technology), equipped with a 150 lines/mm grating (blaze at 800 nm) and a thermoelectrically cooled CCD camera (iDUS DV420A-OE, Andor Technology). The light of an optical feedback-controlled 5 V tungsten incandescent lamp was passed through the sample in DAC and focused by a set of lenses on the entrance slit of the spectrograph. Spectral resolution of this apparatus with the 25 μm wide input slit is 0.56 nm/pixel. The pressure was changed stepwise with an average rate of 25–30 MPa per minute. The spectra, recorded with ~1 min acquisition time, were measured with increasing as well as with decreasing pressure. Slow residual red shift of the absorption band up to several nanometers was observed in the pressure region of protein denaturation, which

kinetics changed with pressure and temperature. We evaluated this potential source of experimental error on a control sample by prolongation of the data acquisition time up to 100 min. The variations of the so-deduced energetic parameters remained within the uncertainty limits determined by other experimental factors. Therefore, to avoid long-time protein deterioration, we stayed with the 1-min acquisition time. The same setup was used for fluorescence measurements, with the exception that fluorescence was excited at 594 nm. Occasionally, absorption spectra were also taken using a commercial V-570 spectrophotometer (Jasco) with a spectral resolution of 0.2 nm.

3.4. Data analysis and estimations of the experimental error

The sample spectra at each pressure were first corrected by subtracting a reference spectrum that was measured in DAC filled with a pure buffer (or buffer-detergent) solvent. This procedure, commonly adequate for simple solutions, gives setbacks in case of strongly scattering colloidal solutions and solidified solutions. Therefore, in most cases the background was formally approximated with a power function of wavelength, λ, in the form of $A + B\lambda^{-1} + C\lambda^{-2} + D\lambda^{-3}$, where A, B, C, and D were adjustable parameters.

The thus corrected optical spectra were then analyzed in terms of the spectral band positions and widths using curve fitting programs available in Origin 6.0 (Microcal Software, Inc.). In most measurements the estimated accuracy (standard deviation within 95% confidence level) of band positions and widths was 4–5 cm^{-1} (0.3–0.4 nm). 2 to 5 repeat measurements have been usually carried out to check reproducibility of the measurements. Reasonable reproducibility of the data in the lower pressure region below ~1000 MPa was observed. In contrast, the data obtained at pressures above 1000 MPa usually demonstrate rather poor reproducibility. This is mostly because of non-hydrostatic pressure distribution in highly viscous (such as the buffer-glycerol mixture) or solid protein solutions. In these cases the given errors of the parameters represent standard deviations of the mean that is associated with regression analysis of the data points for individual measurements.

If not indicated otherwise, experimental uncertainties (standard deviation of the mean) for the midpoint pressures ($P_{1/2}$) are ± 10 MPa, ± 5 kJ/mol for the free energy changes (ΔG), and ± 5 ml/mol for the partial molar volume effects (ΔV). Those estimated errors count possible uncertainties due to sample preparation (uncontrolled variations in the sample properties, in protein detergent ratio, and sample handling during DAC loading etc.) as well as due to temperature variations as explained above.

4. RESULTS AND DISCUSSION

4.1. Overview of the optical absorption spectra of the samples under ambient conditions

4.1.1. Peripheral antenna complexes

Figure 14 presents the overview optical absorption spectra of a representative set of the studied LH2 complexes from *Rba. sphaeroides*. The spectra recorded at ambient temperature and pressure of the detergent-isolated and native membrane-bound complexes are very similar. As can be seen in Table 2, the relative shifts of the key absorption bands for the membrane-embedded (m) and LDAO-isolated (i) LH2 complexes remain within the experimental uncertainty. A comparison with the spectrum of BChl in diethyl ether implies that the bands of the BChl chromophores in protein surrounding peaking around 800 and 850 nm are related to the Q_y molecular electronic transition, while those peaking around 590 nm are associated with the Q_x transition. The broad absorbance toward shorter wavelengths from Q_x is due to Car cofactors within the LH2 protein closely associated with the BChl cofactors (see Figure 14). The Car content in WT LH2 is a still ill-defined mixture of spheroidene and spheroidenone [100].

Origin of the absorption spectra of LH complexes was discussed in Introduction. The B850 band is strongly red-shifted (toward longer wavelengths) compared with the B800 band of loosely packed BChls in the B800 ring (as well as the Q_y band in monomeric BChl) because of strong exciton coupling [101]. The stronger B850 exciton coupling compared with B800 clarifies not only the splitting between these bands but also the larger width of the B850 band. The Q_x transitions of the BChl molecules belonging to the B800 and B850 arrangements apparently overlap. This can be interpreted as arising from the relatively weak oscillator strength of the Q_x transitions, leaving the transitions in all participating molecules almost localized. More details about exciton spectra of LH2 complexes and their temperature dependencies can be found in [57].

Mutations introduced into the WT LH2 complexes generally lead to modifications of their optical spectra. In the CrtC- mutant LH2 complexes the native carotenoids are replaced by neurosporene. Compared with the structure-less spectrum of the native mixture, the neurosporene spectrum is clear-cut as well as blue shifted, showing three sharp peaks between 430 and 490 nm (see Figure 14 below). Replacement of the WT carotenoids with neurosporene does not significantly influence the electronic transitions of the BChl cofactors. Yet it essentially compromises the structural integrity of the LH complexes, as will be shown subsequently.

A slight red shift of the B850 band in the B850-only (B800-) mutant as compared with the WT complex has been noted [102]. It was explained by somewhat enhanced exciton coupling in this complex, presumably because the missing B800 molecules allow tighter packing of the protein around the B850 array of chromophores. A weak shoulder around 795 nm in the spectrum of the B800 deficient mutant is most probably due to overlapping transitions of the B850

excitons, residual B800 molecules, and trace amounts of the "free" BChl molecules [103].

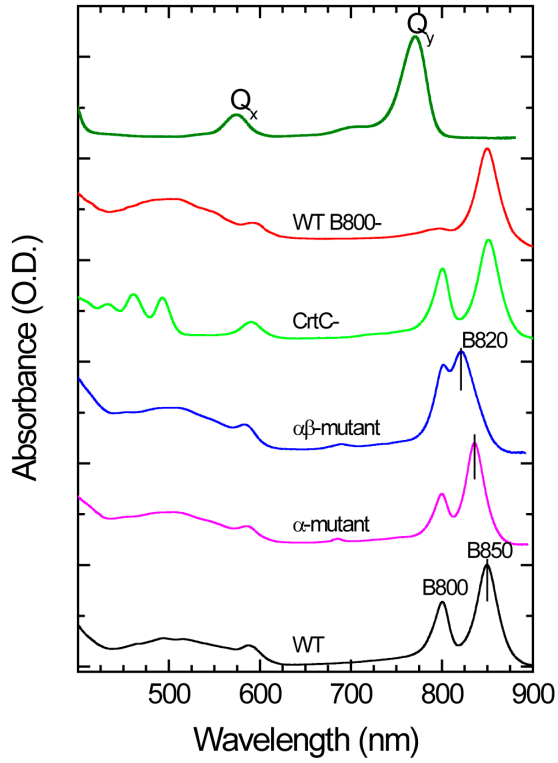

Figure 14. Absorption spectra of WT and mutant LH2 complexes from *Rba. sphaeroides*. The spectra recorded at ambient temperature and pressure are normalized with respect to the strongest absorption band peak. B800- designates the mutant peripheral antenna complex with missing B800 molecules. B800 and B850 designate the absorption bands related to B800 and B850/B820 BChl molecules in the structure of LH2/αβ-mutant complexes (see Figure 5 for structural details); Car shows the absorption range of carotenoid cofactors. Vertical lines in the bottom three spectra highlight the shift of the B850 exciton band due to rupture of single (α-mutant) or double (αβ-mutant) H-bonds in the dimeric sub-unit. The reference spectrum of BChl in diethyl ether is drawn in olive. It indicates that the B800 and B850 spectra are associated with the Q_y transition in isolated BChl chromophores.

Genetic manipulations leading to breakage of H-bonds to the B850 chromophores understandably result in the greatest spectral effects. As demonstrated in Figure 14, the B850 absorption band is observed at 849.4, at 835.9, and at 823.8 nm, respectively, in the WT, α-mutant, and αβ-mutant membrane bound complexes. The spectral shift between the WT and the single H-bond mutant thus amounts 13.5 nm (or 190 cm^{-1}), and almost twice that much (25.6 nm or

366 cm^{-1}) between the WT and the double H-bond mutant complex. Notably, the B800 and Q_x bands are almost immune to the mutations. For example, the Q_x band positions in the three samples are 587.5, 585.3, and 585.5 nm, respectively. The is understandable because the specific site directed mutations have been constructed to target just the selected BChl rings (B850 in this case) as well as because of different physical essence of the studied spectral bands (largely localized Q_x bands, in contrast to delocalized Q_y bands) explained above.

Table 2. Peak positions in nanometers (± 0.5 nm) in the absorption spectra of the membrane-bound and LDAO-isolated LH2 complexes from *Rba. sphaeroides* recorded at ambient conditions. The bands are classified according to the related BChl transitions.

Sample		Q_y		Q_x
		B850	B800	
BChl		770.8		574.3
WT	m	849.4	800.8	587.5
	i	847.8	800.8	588.4
CrtC -	m	851.1	801.1	591.3
	i	849.4	800.7	590.7
B800-	m	850.2	–	590.9
	i	849.6	–	591.8
B800- + CrtC-	m	852.4	–	594.7
	i	852.0	–	594.0
α-mutant	m	835.9	800.0	585.3
αβ-mutant	m	823.8	804.4	585.5

4.1.2. Core complexes

Absorption spectra of the studied core complexes from *Rba. sphaeroides* are shown in Figure 15. The spectra reveal multiple bands in the wavelength range from 400 to 950 nm. The broad band between 400 and 600 nm is primarily due to the carotenoids (spheroidene and spheroidenone) bound to the LH1 complex. The peaks at 590 and 875 nm are related to the Q_x and Q_y electronic transitions, respectively, in the BChl chromophores belonging to the B875 molecular arrays as shown in Figures 6 and 7. The weak spectral features seen around 760–770 nm and 800 nm in the samples containing RC complexes belong, respectively,

to the bacteriopheophytin and monomeric BChl pigments in the RC complex (see Figures 8 and 9).

Concentrating on the B875 absorption band, which peaks around 875 nm (see Table 3), one could once again notice that the spectral maxima of the membrane-bound and isolated complexes almost coincide. Notable is also that the spectral positions of the three membrane samples (LH1, RC-LH1, and RC-LH1-PufX) overlap within less than 2 nm, despite their considerable structural differences. The mutation of the Trp residues in the RC-LH1-PufX complex to the Phe residues in positions β+9 or α+11 results in a blue shift (and broadening) of the absorption band by 7.1/5.9 nm (93/78 cm^{-1}) or 23.5/22.8 nm (317/307 cm^{-1}). The data separated by slash relate to the membrane bound/detergent-isolated complexes. All these numbers are in reasonable agreement with the earlier published data [31,38–40,104].

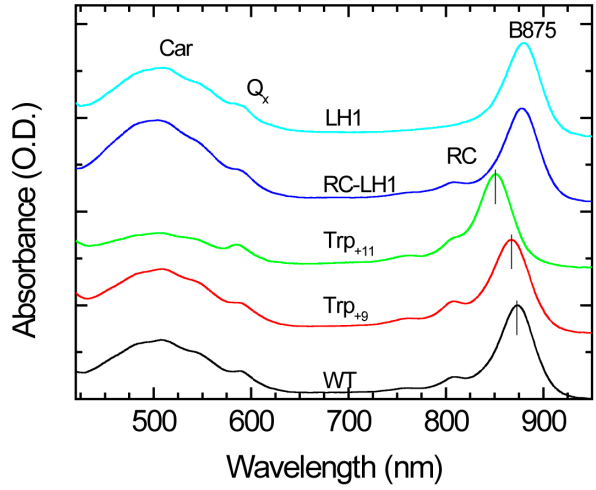

Figure 15. Absorption spectra of WT and mutant LH1 complexes recorded at ambient temperature and pressure. The spectra of detergent-isolated complexes are normalized relative to the B875 absorption band peak. WT designates the dimeric RC-LH1-PufX complex containing native mixture of spheroidene and spheroidenone, Trp_{+9} and Trp_{+11} indicate the same complexes with mutations in the amino-acid sequence at respective sites, RC-LH1 is the core complex mutant with missing PufX complex, and LH1 is the double mutant with missing RC and PufX complexes. Vertical lines in the bottom three spectra highlight the shift of the B875 exciton band due to rupture of H-bonds in the dimeric sub-unit. The band indicated by RC belongs to the RC protein.

Table 3. Peak positions in nanometers (± 0.5 nm) of the B875 band in the absorption spectra of the membrane-bound and detergent-isolated LH1 complexes at ambient conditions.

Sample		Q_y	Q_x
LH1	m	876.3	586.0
	i	876.7	ND[a]
LH1-RC	m	874.6	586.9
	i	874.6	ND[a]
LH1-RC-PufX	m	874.9	583.7
	i	873.2	588.0
LH1-RC-PufX (βTrp_{+9})	m	867.8	ND[a]
	i	867.3	585.4
LH1-RC-PufX (αTrp_{+11})	m	851.3	584.4
	i	850.4	585.1

[a]ND – not determined due to significant overlap with the Car band.

Noteworthy is the large asymmetry of spectral shifts accompanying the breakage of H-bonds in the α- and β-chromophore rings of LH1, suggesting widely different H-bond strengths to respective chromophores. In LH2 the shifts are rather evenly distributed.

4.1.3. Full intracytoplasmic membranes

Absorption spectra of full IC membranes of *Rba. sphaeroides* complete with peripheral LH2 and core antenna (LH1) complexes are shown on Figure 16. In general, the spectra can be very well represented by a sum of the component LH1, LH2, and RC spectra, allowing only the stoichiometric ratio of the core and peripheral complexes to vary. In the present work, we mainly focus on the B850 and B875 absorption bands, which are the lowest-energy optical absorption bands in the LH2 and LH1 antenna complexes, respectively. The particular interest toward these spectral features is explained by the central role the respective electronic transitions play in native photosynthesis by mediating the excitation energy funneling into the RC (see Introduction).

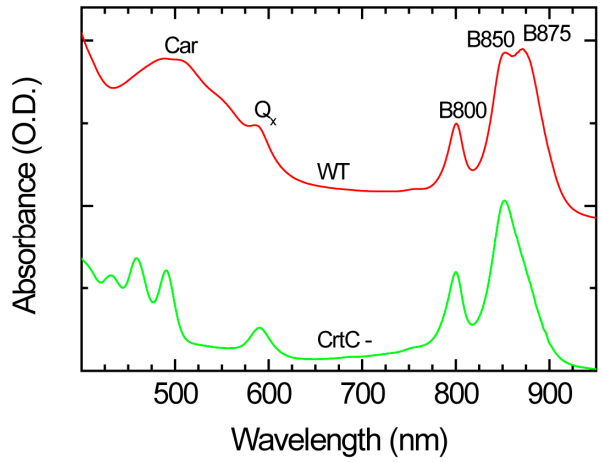

Figure 16. Absorption spectra of WT and mutant chromatophores recorded at ambient temperature and pressure. The spectra are normalized relative to the strongest absorption band peak.

4.2. Pressure-induced modifications of the spectra

Overview optical absorption spectra of the samples from *Rba. sphaeroides*, measured at different externally applied pressures between the ambient pressure of ~1 bar and 3 GPa, are shown in Figure 17. Represented in left column (panels A, B, C) of Figure 17 are the exciton spectra of the native membrane bound complexes, while in right column (panels D and E), the exciton spectra of detergent-isolated complexes. Panel F shows the data for the Car mutant IC membrane vesicles. We will shortly justify the positioning of this membrane sample in the right column of isolated complexes.

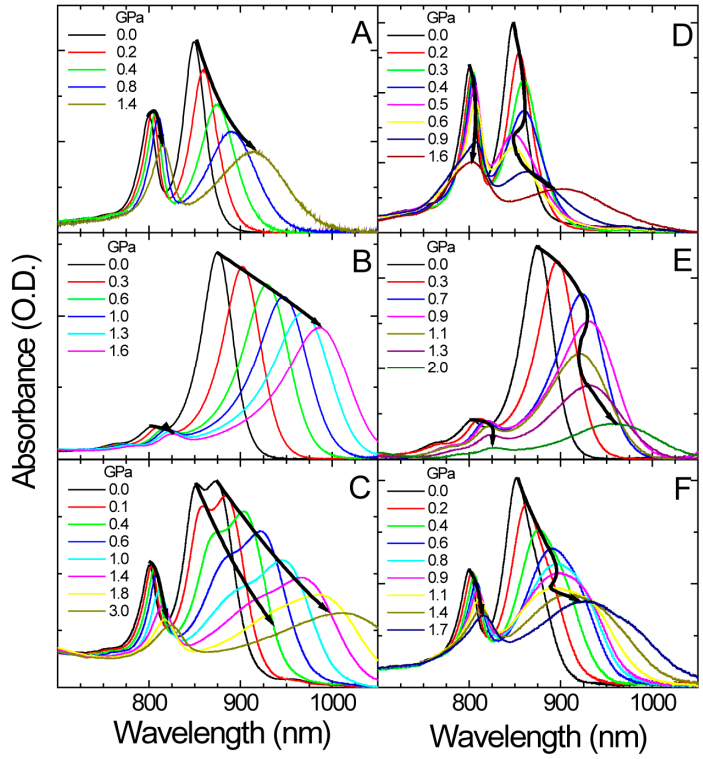

Figure 17. Area-normalized absorption spectra for different LH complexes from *Rba. sphaeroides* in the Q_y transition region, measured at different externally applied pressures indicated: (A) membrane-bound LH2; (B) membrane bound RC-LH1; (C) IC membrane vesicles; (D) detergent-solubilized CrtC- mutant LH2; (E) detergent-solubilized RC-LH1 complex; (F) CrtC- mutant IC membrane vesicles. The arrowed bold lines follow successive absorption maxima.

A few general trends of the spectra in Figure 17 are immediately evident: (i) The shift in spectral position is accompanied by spectral broadening; (ii) The B850 and B875 bands in membrane spectra behave differently from them in the spectra of detergent-isolated complexes. While the membrane spectra gradually red shift and broaden with pressure all the way from low pressures to high pressures, the spectra of isolated complexes show a back-turn at intermediate pressures, where the spectra move to the blue instead of red with increasing pressure. This positional back-turn is followed with accelerated broadening of the spectra; (iii) The spectral shift rate of excitons in core complexes is greater than it is in peripheral complexes, best seen in Figure 17C. As follows, a detailed analysis of these spectral behaviors is provided.

4.2.1. Exciton absorption band positions and widths as a function of pressure

Figure 18 displays typical responses to externally applied high pressures of the B850 (in LH2 complexes) and B875 (LH1) exciton absorption band positions (A) and widths (B). The width is defined as the full width at half maximum (FWHM). The detergent-isolated complexes were dissolved in buffer-detergent mixture, while the membrane-embedded samples were kept in neat buffer (see Table 1).

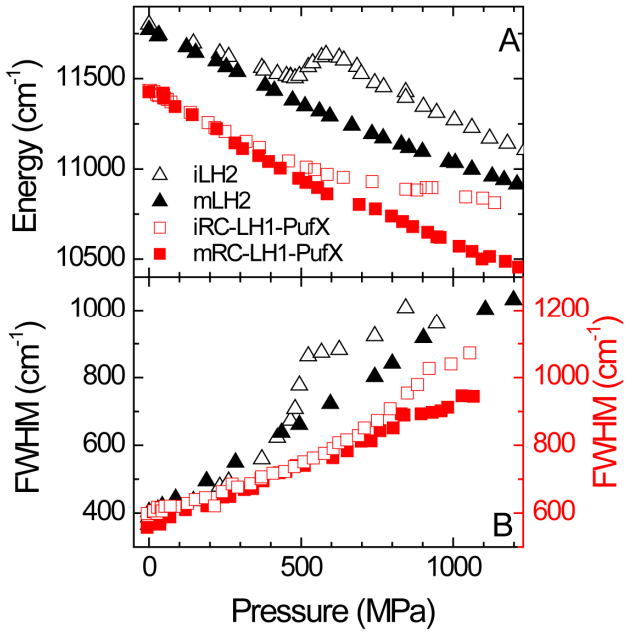

Figure 18. Pressure dependence of the B850 (triangles) or B875 (squares) absorption band position (A) and width (B) for detergent-isolated (open symbols) and membrane-embedded (filled symbols) iLH2 (black symbols) and iRC-LH1-PufX (red symbols) complexes from *Rba. sphaeroides*. The FWHM scale for LH1 complexes is on right hand side. The data for the LH2 membranes are taken in glycerol-buffer mixture, while those for the LH1 membranes, in neat buffer. The prefixes i and m denote the data for isolated and membrane complexes, respectively.

For the membrane-embedded complexes the main pressure effect seems to be a continuous red shift and similarly continuous broadening of the spectra. Similar effects have also be seen in case of free BChls in solution [105]. However, it should be stressed that the shift and broadening rates observed for the B850/ B875 exciton bands are very large compared with those for the free solubilized BChl. The initial band shift rate for LH2 is –0.60 ± 0.04 cm^{-1}/MPa (minus designates the shift to lower energies) and –1.04 ± 0.05 cm^{-1}/MPa for LH1. The

shift rate gradually diminishes with increasing pressure in all membrane samples. The rate of the band broadening (0.51 ± 0.05 cm^{-1}/MPa in LH2 and 0.24 ± 0.01 cm^{-1}/MPa in LH1) is similarly great. Those large numbers can be conveniently explained by the BChl excited states in antenna complexes having an exciton origin [106–108] (see also Introduction). The shift rate in LH1 complexes, being still larger than in LH2 complexes, is in agreement with the stronger exciton coupling found for the core complexes [43,102,109,110].

As for the detergent-isolated complexes, they behave at low pressures in much the same way as the membrane-protected complexes. Toward higher pressures, however, striking differences appear. Initially the red shift begins to decrease in magnitude and then, between 0.5 and 0.6 GPa in case of the B850 band and between 0.7 and 1.2 GPa in case of the B875 band, it is reversed with a blue shift. Past these ranges the red shift is restored, albeit generally with a different rate (Figure 18A). In bulk samples such abrupt change in the properties of the system would correspond to phase transition.

The widths of the spectra of probe molecules are sensitive to local static and dynamic disorders of the sample. Absorption bands of the isolated LH1 and LH2 complexes recorded at low pressures have almost the same width as the respective bands of membrane complexes. Toward higher pressures, however, the spectrum of isolated complexes grows significantly broader than the spectrum of membrane complexes. This difference remains up to the highest pressures (see Figure 18B). The accelerated broadening occurs in the same pressure range where essential changes of spectral shift are observed, implying their common physical origin. We shall return to this issue in the following paragraph.

Native biological membranes as well as detergent phases are known to suffer phase transitions in the >0.1 GPa pressure range [111]. Such phase transitions can usually be readily spotted by abrupt changes in the resonant (Raleigh) light scattering efficiency as a function of pressure. To verify that the irregularities observed in Figure 18 are not induced by modifications in the surrounding buffer-detergent phase, the scattered light intensity should be presented along with the absorption data on proteins. Such parallel records are demonstrated in Figure 19 in the case of the LH2 CrtC- (A) and RC-LH1 (B) complexes using different detergents (LDAO and DHPC, respectively). The scattering was measured at 680 nm, where the sample absorption is minimal, see Figures 14 and 15.

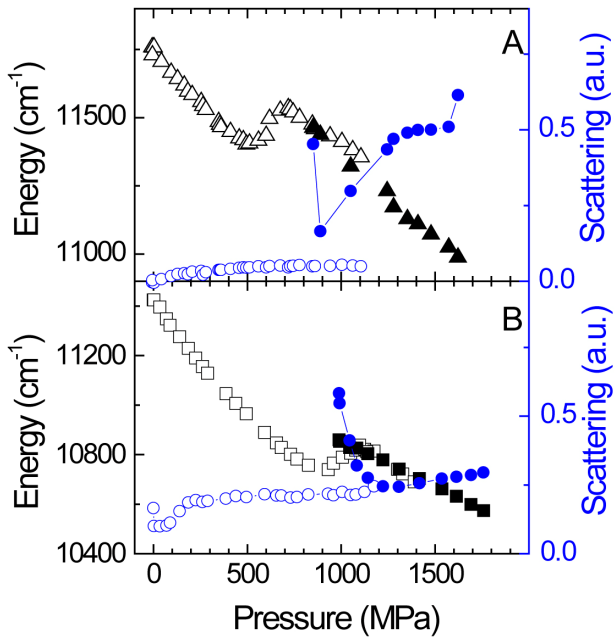

Figure 19. Pressure dependences of the B850 (A) and B875 (B) absorption band positions in CrtC- complexes and RC-LH1 complexes (detergent DHPC) together with the scattered background light recorded at 680 nm. Empty and filled symbols correspond to data in liquid and solid phase, respectively.

As seen, in the case of the LH2-buffer-LDAO system, there is no light scattering abnormality in the solvent phase. A strong scattering is observed only past ~1.1 GPa, far away from the irregularity startup in absorption, which is apparently related to solidification of the sample. Upon solidification the pressure abruptly drops to ~0.8 GPa. Similar feature due to liquid-solid phase transition is observed in the RC-LH1-buffer-DHPC mixture (Figure 19B). Observed in the latter sample, though, is another scattering rise occurring at lower pressures, around 0.2 GPa. Both these scattering features are clearly separated from the pressures where blue shifts (and accompanying broadenings) in the present samples set in. Other studied complexes expose similar results. Therefore, it is safe to propose that the irregularities observed in the detergent-isolated samples have fundamentally intramolecular cause, rather than being caused/slaved by phase transitions in the protein surroundings.

4.2.2. Relative band shift and broadening

Shown in Figure 18 were typical responses to externally applied high pressures of the exciton absorption band positions and widths both in the LH2 and LH1

complexes. Significant differences between the data for isolated and membrane-embedded complexes were noted. To enhance the variations between isolated and membrane complexes, it is worthwhile to redraw the data in relative scale, treating the data of membrane complexes as a reference.

As an example, plotted in Figure 20 are the relative peak shifts $\delta\nu$ and band broadenings $\delta\Gamma$ for the B850 and B875 absorption bands in CrtC- LH2 and RC-LH1 complexes, respectively. The former measure was calculated as $\delta\nu = \nu_i - \nu_m$, where $\nu_{i/m}$ are the experimental peak positions in isolated (i) and membrane-bound (m) samples. A blue shift of the spectrum of isolated complexes thus results in a positive-valued $\delta\nu$ and a red-shift, a negative-valued $\delta\nu$. The latter measure in Gaussian approximation of the lineshapes was evaluated as $\delta\Gamma = \left(\Gamma_i^2 - \Gamma_m^2\right)^{1/2}$, where $\Gamma_{i/m}$ are the corresponding FWHM of the B850/B875 absorption bands.

As seen in Figure 20, the relative peak shifts and band broadenings reveal characteristic step-like pressure dependencies resembling titration curves. The step heights of the relative shifts (Figure 20A) in LH1 complexes are generally greater that they are in LH2 complexes. Moreover, the step heights for WT and different mutant complexes of the same sort vary quite a bit. Specifically, the variation in case of the three isolated LH2 complexes (WT, CrtC- mutant, and B800- mutant) is from 292 cm^{-1} to 410 cm^{-1} [112]. In case of LH1 complexes the biggest variations were observed between the so-called closed-ring (LH1 and RC-LH1) and open-ring (all core forms that include PufX) structures. Thus, the height of the peak shift in the open-ring complexes generally reaches just ~2/3 that in the closed-ring samples.

Under normal pressure, the blue shifts and broadenings similar in magnitude to those in Figure 20 were previously observed for H-bond mutants of *Rba. sphaeroides* when compared with their WT counterparts. As was described in Introduction, in the B850 ring of LH2 complexes [87,88] the αTyr44 and αTyr45 residues normally form H-bonds to the C_3-acetyl carbonyls of the BChls belonging to the inner (α) and outer (β) rings of chromophores, respectively (see Figure 5). The removal of H-bonds to the αTyr45 residues (9 in total) by replacing Tyr by the non-H-boding Phe residues correlates with the blue shift of the B850 absorption band by 190 cm^{-1}. The total blue shift when all 18 H-bonds related to the αTyr44 and αTyr45 residues are crashed equals to 366 cm^{-1}. The latter shift of the double H-bond mutant almost coincides with the relative shift observed by us for the WT samples, which strongly implies the high-pressure induced breakage of each and every C_3-acetyl carbonyl H-bond in the B850 ring.

It was explained in Introduction that in LH1 complexes, the αTrp_{+11} and βTrp_{+9} protein residues normally bind BChls by forming H-bonds to the C_3-acetyl carbonyls of the α-and β-BChls, respectively [38–40,104]. The replacement in WT RC-LH1-PufX the Trp residues by Phe residues, which cannot form H-bonds, results in a blue shift of the B875 absorption band of detergent-

isolated complexes by 78 cm^{-1} (when all the H-bonds in the β half are broken and the bonds in the α half are all intact) or by 307 cm^{-1} (when the bonds in the α ring of chromophores are detached and in the β ring intact). Total sum of these shifts (385 cm^{-1}) corresponding to rupture of all the B875 chromophore-binding H-bonds once again remarkably well agrees with the height of the step for the relative shift in WT LH1 complexes, suggesting that high pressure brakes the H-bonds in both the α and β compartments also in core complexes.

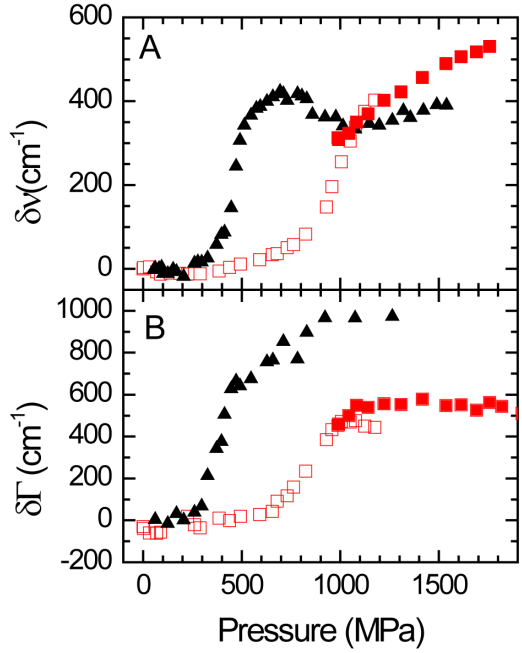

Figure 20. Relative peak shifts $\delta\nu$ (A) and band broadenings $\delta\Gamma$ (B) for the B850 and B875 absorption bands in CrtC- LH2 (black symbols) and RC-LH1 (red symbols) complexes from Rba. sphaeroides. Filled red symbols relate to the data in solid phase.

The accompanying relative broadening of the spectra, as for example revealed in Figure 20B, validates this explanation. The abrupt spectral broadening in the pressure range where irregularities of the B850/B875 band shifts start is an indication of enhanced dynamics (increased freedom of movements) of the B850/B875 BChl probe molecules in their binding sites, compared with the equivalent situation within the membrane. Because the pressure-induced denaturation of proteins is driven by a decrease in volume and possible penetration of the buffer (essentially of polar water molecules) into the protein interior [67,69,113,114], rather than swelling, the extra freedom of intra-protein movements can only be caused by breakage of the bonds that hold BChl molecules in their protein pocket. Given that axial ligation has minimal effect on the

BChl Q_y absorption band position [105], the loss of H-bonds in isolated complexes is the most likely explanation for the observed abrupt changes of the B850/B875 absorption spectra with pressure. This interpretation in the context of WT LH2 complexes was first proposed in [115].

4.2.3. The reference state/sample problem

Proper reference state/sample is crucial for the present data analyses method. Implicitly assumed by this approach is that no structural changes, which might modify absorption spectra of the particular LH complex, occur over the entire pressure range in the reference sample; most importantly, all the relevant H-bonds should remain intact in this sample. The smooth pressure-induced shifts and broadenings of absorption bands in reference samples, as observed in Figure 18, are due to physical mechanisms that may largely be considered separate from the H-bonding. Amongst these mechanisms is the change of dielectric constant of the local environment of the probe molecules as well as of intermolecular exciton couplings upon material compression.

There is no general way other than empirical to find the proper, the steadiest against high pressure, reference sample. In the resent work we choose to take merely spectroscopic measure of the protein stability. It is based on the position of the B850/B875 absorption band at high pressures: all other conditions equal, the redder shifted is absorption at particular high pressure value, the steadier the system. Following this criterion, we found that the conditions to produce reference LH1 and LH2 samples are different. In the former case, the satisfactory choice is membrane-embedded complexes in neat buffer. In the same environment the membrane bound LH2 complexes at high pressures tend to partially lose their H-bonds to B850 chromophores (see below). Yet they can be enhanced (stabilized) by adding glycerol. LH2 membranes in buffer-glycerol (1:2 v/v) mixture thus form the reference sample in case of the LH2 complexes.

The additional enhancement required in case of the LH2 membrane complexes as compared to the LH1 complexes may be related to the extra B800 pigment ring present in LH2 and not in LH1. The B800 pigments in the cytoplasmic side of the membrane directly face solvent phase. This may allow leakage of water molecules into the protein interior at high pressures.

4.2.4. Reversibility of the high-pressure effects

The above pressure effects are fast; following changes in applied pressure without noticeable delay in time scale of several minutes (see Materials and Methods). In this paragraph we report about the spectral effects that are observed upon pressure release after the full cycle of experiments at elevated pressures, which typically take about 2 hours to complete. The respective data are shown in Figure 21. The left hand side of this figure concerns absorption spectra of membrane (A) and isolated (B) peripheral (LH2) antenna complexes,

while the right hand, the absorption spectra of membrane (C) and isolated (D) core (RC-LH1) antenna complexes.

Beginning with LH2, as can be seen from the final-minus-initial difference spectrum, the main effect of the pressure treatment in the LH2 membranes is relative decrease of the B800 band. The loss of B800 chromophores (i.e., the pigments organized into the B800 ring) is known to cause a red shift (as well as some broadening) of the B850 absorption band [116]. This is exactly what is happening here, as evidenced by the dispersion-type shape of the difference spectrum around 860 nm. Figure 21B demonstrates much reduced robustness against pressure of the purified complexes when compared with the membrane samples. The absorption spectrum after pressure release shows strong decrease of both the B800 and B850 bands, accompanied by growing intensity around 770–780 nm where solubilized BChls absorb. Similar band is not apparent in the membrane spectra of Figure 21A. The spectrum in Figure 21B thus appears to be a simple sum of two sub-spectra, one belonging to the LH2 complexes that have released most or all of their BChl content and the second, representing fully intact complexes. This conclusion relies on almost perfect recovery of the B850 band shape (without accounting for the contribution of solubilized BChls). One can estimate (using a simplifying assumption that the absorbance of BChls, either solubilized or organized into the LH2 complex, is the same) that majority (over 60%) of the LH2 complexes survived the present pressure treatment. This is indeed remarkable, given the harsh conditions applied.

Similar studies on core complexes (Figures 21C and D) show that the RC-LH1 complexes are generally still more robust against high pressures, as compared with the LH2 complexes. The lost intensity from the main band after pressure treatment can be found to be rather evenly spread over a broad spectral area toward shorter wavelengths (especially well followed in case of isolated RC-LH1 complexes in Figure 21D). We have generally observed that the variant LH1 complexes, either membrane-bound or isolated are stable under pressures between 0.1 and 1 GPa for at least 20 hours under the condition that not too high concentration of detergents is used.

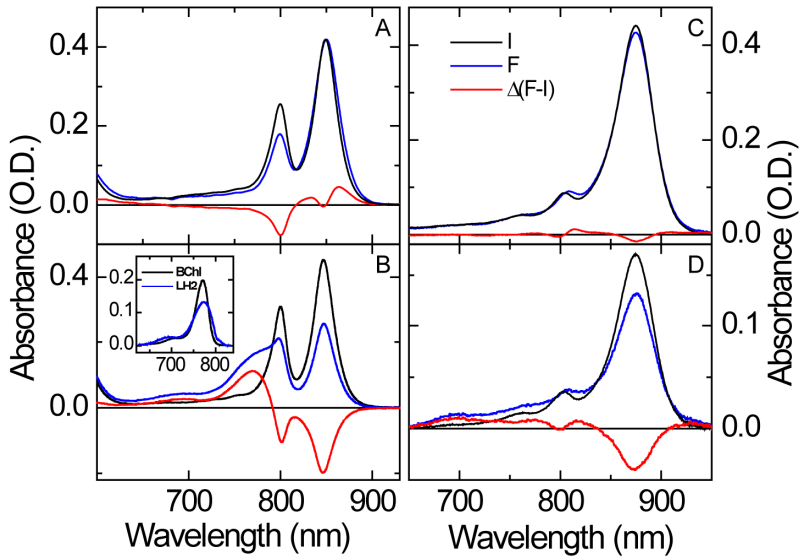

Figure 21. Recovery of the area-normalized absorption spectra for the membrane-protected (A, C) and detergent-isolated (B, D) LH2 (A, B) and RC-LH1 (C, D) complexes from *Rba. sphaeroides*. 44 mM LDAO and 3 mM DHPC was used in case of detergent-isolated LH2 and LH1 complexes, respectively. I is the initial spectrum, F is the final spectrum after pressure cycle and Δ(F–I) is the difference between the final and initial spectra. Insert shows the area-normalized absorption spectra of BChl in ether (black line) and in detergent environment (blue line).

These examples tell that both the LH1 and LH2 integral membrane chromoproteins, either isolated into detergent micelles or protected by native membranes, are rather robust against external high pressure. The full spectral recovery of the majority of isolated complexes implies that the pressure-induced H-bond breakage is reversible, allowing application of the equilibrium thermodynamic analysis to this process. Devoted to the latter issue is the subsequent part 4.3.

4.3. Estimation of the chromophore-binding hydrogen bond energies

According to the model described in paragraph 1.6 (note specifically Eq. 5), the logarithm of the equilibrium constant K for the H-bond rupture should show linear dependence on the applied pressure, from which the prime model parameters: ΔV^0, ΔG^0 and $P_{1/2}$ can be evaluated as the slope, the free energy value at zero pressure, and the pressure corresponding to zero free energy, respectively. The correspondence between K and directly measured spectroscopic band positions is provided by Eq. 4.

4.3.1. Peripheral complexes

4.3.1.1. Isolated complexes

The plots of $-RT \ln K$ as a function of pressure for the B850 absorption band in three isolated LH2 complexes are shown in Figure 22. As seen, the experimental data follow fairly linear dependences in the pressure regions where H-bonds in respective samples predominantly break, thus justifying the applied linear approximation model. The lines in all cases are descending, although with different slopes in different samples, meaning that the partial molar volume effects are negative. In other words, at elevated pressures the protein states with shattered H-bonds are stabilized against their respective native states. Numerical values of the parameters evaluated from the dependences in Figure 22 are presented in Table 4.

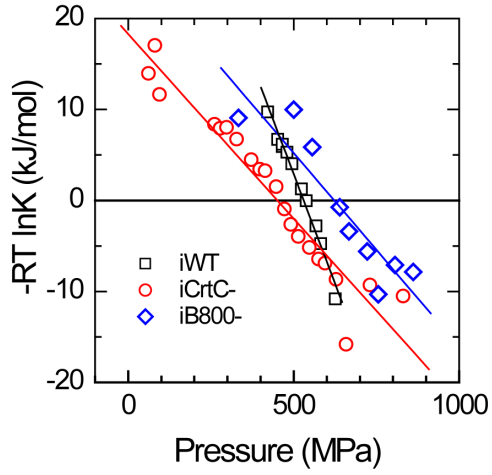

Figure 22. Pressure dependences of –RT lnK(P) for the isolated LH2 complexes indicated. Lines represent linear fits of the scattered experimental data. The plotted data points are calculated relative to glycerol-enhanced WT LH2-only membranes.

The free energy change corresponding to breaking the H-bonds (the rupture energy) in isolated WT LH2 complexes is close to 40 kJ/mol. Mutations (removal of the B800 ring and replacement of the native content of carotenoids (the CrtC- sample) has strong destabilizing effect on the LH2 complex, reducing the H-bond energy in the B850 ring almost twice. The isolated double mutant (CrtC- +B800-) complex is unstable with respect to pressure falling apart completely. Still, all the obtained ΔG^0 values are relatively large, if compared with the earlier reported single H-bond energies in globular proteins that span from 2 to 25 kJ/mol [71,72], depending on the H-bond donor and acceptor as well as their environment.

Table 4. Thermodynamic parameters characterizing breakage of H-bonds in membrane-bound and detergent-isolated LH2 complexes.[a]

Sample		ΔG^0 kJ/mol	ΔV^0 ml/mol	$P_{1/2}$ MPa
B850				
WT	m	19 ± 3	–23 ± 10	811 ± 15
	i	39 ± 2	–71 ± 10	519 ± 10
B800-	m	12 ± 5	–16 ± 10	785 ± 10
	i	26 ± 4	–43 ± 10	622 ± 10
CrtC-	m	28 ± 5	–39 ± 10	700 ± 10
	mg[b]	16 ± 2	–14 ± 10	1010 ± 15
	i	24 ± 5	–51 ± 10	445 ± 10
B800- + CrtC-	m	23 ± 7	–30 ± 10	989 ± 10
	i	N/A[c]	N/A[c]	N/A[c]
B800				
CrtC-	i	18 ± 4	–17 ± 5	1020 ± 10

[a]The data are calculated relative to the glycerol-enhanced WT LH2-only membranes.
[b]mg – CrtC- membranes in glycerol-buffer mixture
[c]N/A – the sample is not available

The replacement of Car in LH2 complexes not only undermines the B850 ring environment; it also strongly influences pigments in the B800 ring. As can be seen in Figure 23 the B800 band position in the iCrtC- mutant LH2 complex abruptly bends to the left (i.e. toward blue/shorter wavelengths) just below 1 GPa. The amplitude of the relative shift reaches 185 cm^{-1}, being comparable with the spectral shift observed when H-bonds between the C_3-acetyl carbonyls of the B800 BChls and the βArg20 protein residues have been removed by genetic engineering techniques [58] Analogy with the B850 molecules, the observed blue shift of the B800 band is related to the pressure-induced breakage of the H-bonds in the binding pocket of the B800 molecules.

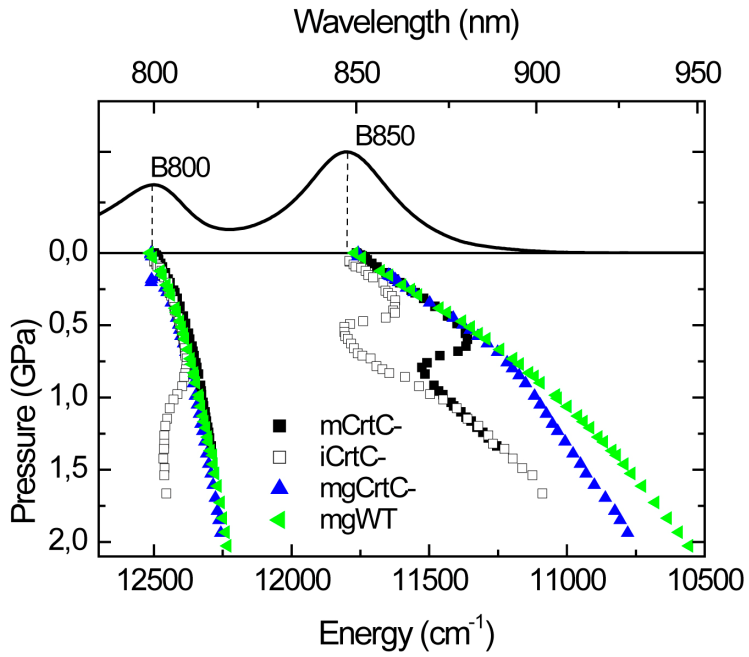

Figure 23. Pressure dependences of the B800 and B850 absorption band positions for the detergent-isolated and membrane-bound CrtC- mutant LH2 complexes along with the glycerol-enhanced WT membrane complex (mgWT). Upper part shows absorption spectrum of the WT complex.

Since the start of the blue bending in the B850 and B800 systems appears at widely different pressures (at ~0.3 GPa for B850 vs. ~0.6 GPa for B800), one might assume that these processes take place independent from each other. It is, therefore, possible to estimate the strength of H-bonds stabilizing the B800 molecules in their binding pockets. The respective energy is as large as 18±4 kJ/mol (see Table 4).

4.3.1.2. Effect of detergent on the LH2 protein stability

Detergents are known to destabilize and, at excess concentrations, irreversibly denature membrane proteins [117]. To be sure that the thermodynamic parameters in Table 4 that characterize the breakage of H-bonds in the LH2 complex are not determined by the selected "standard" detergent concentration (see Table 1), the dependence of the parameters on the ratio of detergent and protein molecules (the D/P ratio for short) was studied in case of the WT and CrtC- mutant species. See Materials and Methods section for estimating the protein concentration.

Presented in Figure 24 are pressure dependences for the B850 band peak shift in isolated complexes with different D/P ratios between $1*10^3$ and $48*10^3$. They can be compared with the data for the CrtC- mutant membranes as a limiting case of no detergent. All the data are recorded relative to the spectra of WT LH2-only membranes enhanced by adding glycerol into the buffer. The respective thermodynamic analyses data are displayed in Table 5.

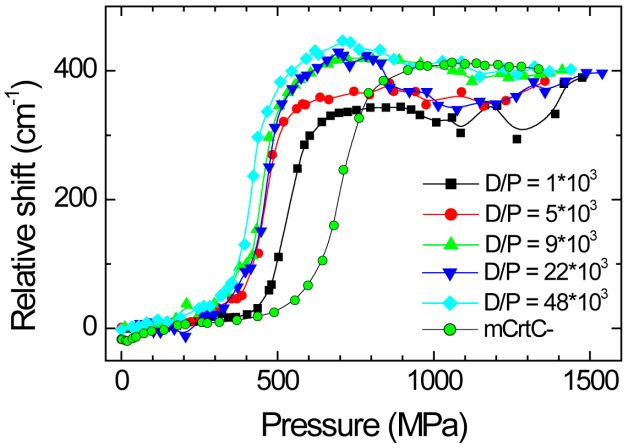

Figure 24. Relative peak shifts of the B850 band in the spectra of isolated and membrane CrtC- mutant LH2 complexes in dependence on the LDAO-protein ratio. The data are recorded relative to the spectra of glycerol-enhanced WT LH2-only membranes. Solid lines are for guiding the eye.

As can be seen in Figure 24, there is a systematic shift of the dependences toward lower pressures with increasing number of LDAO molecules per LH2 protein. The midpoint pressure ($P_{1/2}$) decreases from ~700 MPa in case of intact membrane with no detergent all the way to ~425 MPa for the complexes with D/P = $48*10^3$. In parallel the partial molar volume effect (ΔV^0) increases from –39 ml/mol to –56 ml/mol. Both these observations are in agreement with common perception of detergents as the protein destabilizing factor. Most importantly from the point of view of the present work, yet somewhat surprisingly, the value of the free energy change (ΔG^0) that characterizes the breakage of H-bonds remains well conserved over the whole range of the used detergent concentration (see Table 5).

Formally, given that $\Delta G^0 = -\Delta V^0 P_{1/2}$ (see part 1.6), this insensitivity is derived from the compensating effect of volume and pressure. However, its deeper physical meaning remains to be understood. Further studies are required to prove generality of this conjecture in case of other detergents as well as for broader classes of membrane proteins. For time being, we just assume that the H-bond energies in integral membrane proteins as determined by high-pressure

spectroscopy do not significantly depend on the used detergent concentration over a broad D/P range beyond critical micelle concentration.

It should be noticed that majority of the measurements on isolated complexes reported in the present work are performed on the samples with the D/P ratio between $9*10^3$ and $22*10^3$. This is done for consistency as well as for comparability of the data obtained on different samples. Also, in this detergent concentration range the retrieved experimental parameters appeared to be most stable.

The number of detergent molecules directly attached to the hydrophobic parts of membrane proteins depends on the nature of both detergent and protein. According to [118], at 6 μM protein concentration and using LDAO as a detergent, the LH2 complexes are well isolated from each other at D/P = $>1.6*10^3$. The existing data about the area of hydrophobic parts in case of the LH2 complex [28,119] allow estimating that only 200–500 detergent molecules form the detergent micelle around the LH2 protein. The rest of the detergent molecules remain in the solvent phase [118].

Table 5.Thermodynamic parameters characterizing rupture of H-bonds in the B850 ring of isolated neurosporene mutant LH2 complexes as a function of the LDAO-protein ratio.[a]

D/P	ΔG^0 kJ/mol	ΔV^0 ml/mol	$P_{1/2}$ MPa
mCrtC-	28 ± 5	–39 ± 10	700 ± 10
$1*10^3$	34 ± 6	–65 ± 10	528 ± 10
$5*10^3$	35 ± 11	–75 ± 25	461 ± 10
$9*10^3$	24 ± 4	–54 ± 10	445 ± 10
$22*10^3$	24 ± 5	–51 ± 10	445 ± 10
$48*10^3$	24 ± 4	–56 ± 10	425 ± 10

[a]The data are calculated relative to the glycerol-enhanced WT LH2-only membranes.

4.3.1.3. Native membrane bound complexes

It was noted earlier that the WT membrane-protected LH2 complexes are rather resilient to damage by high-pressure compression compared with isolated complexes. It was also remarked that the WT complexes can be further stabilized by adding co-solvents such as glycerol. Figure 25 shows obvious stabilizing effects of glycerol on all the studied LH2 membranes. Very clear demonstration of the same phenomenon in case of mutant complexes with exchanged carotenoids is seen also in Figure 25. To the best of our knowledge, such reinforcement of native membrane-embedded protein complexes by glycerol has not been revealed before. Possible origin of this result was discussed at the end of part 4.2.3.

Assuming that in glycerol-buffer environment all the H-bonds coordinating BChls in WT LH2 complexes remain intact, and that in neat buffer and/or in mutant membranes they may be partially shattered, even in glycerol-enhanced environment, we set to study energetic effects related to these situations. Like previously in case of isolated complexes, the membrane data were plotted against the data of glycerol-enhanced WT LH2-only membranes. The concluding results that reveal significant differences between isolated and membrane complexes are shown in Figure 26 and in Table 4 (rows marked by m).

The points of immediate notice are:

(i) The midpoint pressures, $P_{1/2}$, obtained at crossing points of the linear fitting curves with the y-axis zero, are generally larger for the membrane bound complexes (where they reach almost 1 GPa in case of the mgCrtC- mutant) than in isolated complexes (with pressure as low as ~0.45 GPa in case of the iCrtC- mutant);

(ii) The ΔV^0 values, which broadly follow the published volume changes of protein unfolding [64] are generally greater for isolated complexes (reaching –71 ml/mol in case of iWT complex) than for membrane samples (where it may be as low as –14 ml/mol in case of the glycerol-enhanced mgCrtC- mutant);

(iii) ΔG^0 values for isolated complexes are about twice greater than they are for membrane complexes.

These findings quite naturally point to better (denser and/or more orderly) packing in membrane environment compared with the more random surrounding of artificial surfactant. Due to the revealed correlation between the H-bond rupture energies in isolated and membrane complexes and since there are two H-bonds per every dimeric αβ-$BChl_2$ structural unit in the LH2 complex (see Introduction), it is only natural to think that in isolated complexes all the H-bonds in the B850 ring can be broken down by high pressure, while in the complexes protected by native membranes only half of the bonds appear to be broken. If so, the two H-bonds in the αβ-$BChl_2$ unit play additive role in reinforcement of the whole LH complex. This assumption also suggests cooperative ("all-or-nothing" type) rather than sequential H-bond breakage mechanism of H-bonds. This given, the single H-bond energies in the B850 ring of WT LH2 complexes can be estimated to be equal to ~20 kJ/mol. In agreement with data on isolated complexes, these single-bond energies in mutant complexes are much less, ~12 kJ/mol in B800- and ~14 kJ/mol in CrtC- membrane complexes.

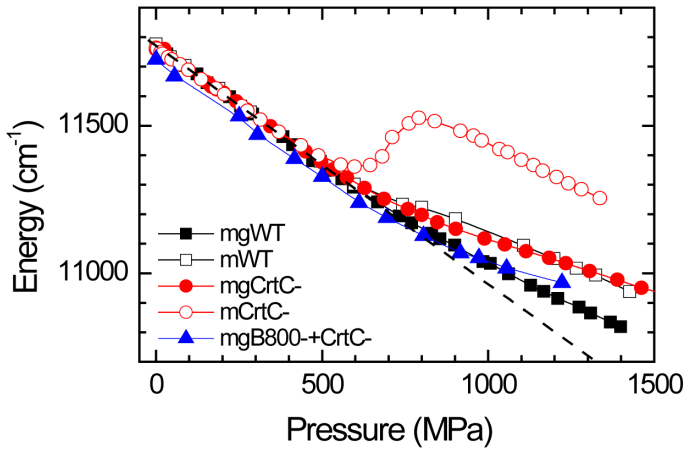

Figure 25. Pressure dependence of the B850 absorption peak energy for the membrane-bound LH2 complexes. Solid lines are for guiding the eye; dashed line represents linear extrapolation of the low-pressure data to higher pressures.

The behavior of neurosporene mutant (CrtC-) LH2 complexes under hydrostatic pressure is rather unique (see Figures 21, 23, and 24, and Table 4). Only in this case the energetic (as well as the volume) effects that characterize phase transitions in isolated and membrane complexes dissolved in neat buffer solution closely match each other. However, when the membrane complexes are stabilized by glycerol (the mgCrtC- sample), their behavior becomes similar to other membrane samples, i.e., the midpoint pressure increases, the volume effect decreases, and the energetic effect becomes approximately equal to half of that for isolated complexes (see Table 4). Since the stability of proteins against externally applied pressure correlates with the extent of water molecules penetrating into the hydrophobic interior [69,113,114], it appears plausible that the change of the native contents of carotenoids by neurosporene leads to less compact protein conformation, which is more accessible to water than the native fold.

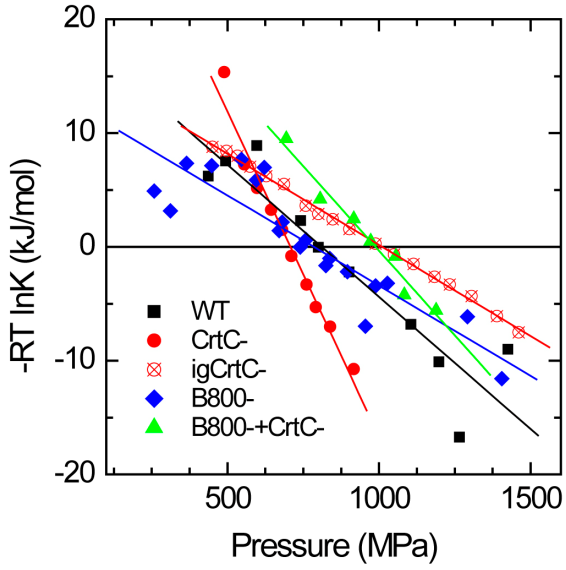

Figure 26. Pressure dependences of –RT lnK(P) for the membrane bound LH2 samples indicated. The plotted data points are calculated relative to glycerol-enhanced WT LH2-only membranes. Lines represent linear fits of the scattered experimental data.

The similar (or rather coinciding within the experimental error margins) free energy changes characterizing breakage of H-bonds in detergent-isolated (24 ± 5 kJ/mol) and membrane-bound (28 ± 5 kJ/mol) CrtC- LH2 complexes is of fundamental significance. This is the proof that data obtained on isolated membrane proteins have relevance to the state of matter in the native membrane.

4.3.2. Core complexes

The experimental pressure dependencies of $-RT\ln K$ for the isolated core complexes are shown in Figure 27. To validate the proposed pressure-induced H-bond breakage mechanism, here we studied, apart from the LH1, RC-LH1, and RC-LH1-PufX (WT) core complex, the two WT mutant complexes that have H-bond Trp to Phe mutations in either the α+11 or β+9 positions. Notice once again that the data for all core complexes have been evaluated relative to the WT membrane sample in neat buffer. In the $\alpha Trp_{+11}Phe$ mutant, the H-bonds between the α-polypeptides and its BChls are removed, thus it has half the intact H-bonds found in the WT. In the $\beta Trp_{+9}Phe$ mutant, the situation is exactly reversed: the H-bonds to β-polypeptides are broken and the other H-bonds to polypeptides are intact. The ambient-pressure spectra of these mutant samples shown in Figure 15 are blue-shifted and broader than the reference spectra of WT complexes.

The plots in Figure 27, which were built around the respective phase transition regions, are linear like in case of LH2 complexes. With respect to the transition midpoint pressure, $P_{1/2}$, the complexes clearly divide into two groups with either one or two intact H-bonds in the basic unit. The three members of the latter group (LH1, RC-LH1, and WT) with midpoint pressures ≥1000 MPa expectedly demonstrate much greater pressure resistance than the two H-bond mutants with the midpoint pressures around 700 MPa. The slopes representing ΔV^0 do not separate that clearly.

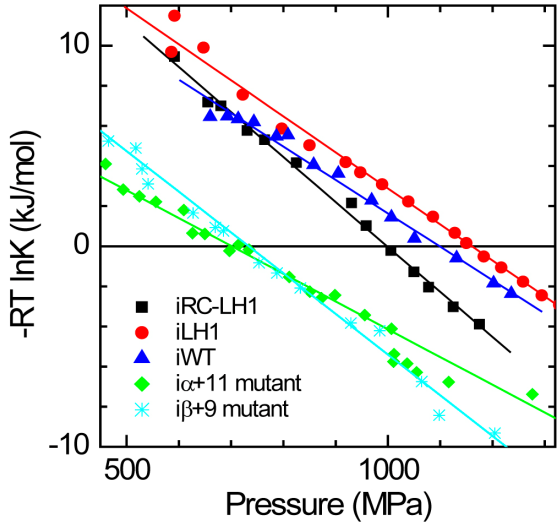

Figure 27. Pressure dependences of –RT lnK(P) for the LH1 samples indicated. The plotted data points are calculated relative to WT LH1-only membranes in neat buffer. Lines represent linear fits of the scattered experimental data.

The obtained parameters that characterize the pressure-induced rupture of H-bonds in detergent-isolated LH1 complexes are listed in Table 6. Also included in Table 6 are the data (line 5) for the membrane-bound β+9 mutant RC-LH1-PufX complexes. It can be seen that comparable H-bond energies were found for purified and membrane-embedded β+9 mutant complexes (lines 4 and 5, respectively), once again indicating that these integral membrane proteins largely retain their structural properties upon solubilization and purification in mild detergents.

The parameters for the LH1, RC-LH1, and WT core complexes with all the H-bonds intact at ambient pressure appear similar, whereas they are rather different from those obtained for the mutant complexes with half of these bonds removed. Most remarkably, the energy corresponding to the H-bond rupture in the WT complex (25 ± 2 kJ/mol) equals within the estimated uncertainty the sum of the rupture energies in the α+11 and β+9 mutants (10 ± 2 and 14 ± 2

kJ/mol, respectively). This greatly supports the earlier made conjecture in the context of LH2 complexes that the α- and β-types of H-bonds have quasi-independent and additive roles in reinforcement the dimeric building blocks of cyclic bacterial LH complexes. The data in Table 6 further suggest that there is practically no difference between the strength of H-bonds in open-ring (RC-LH1-PufX) and closed-ring (RC-LH1) core antennas. In every sense these complexes respond to high pressure remarkably similar. This is somewhat surprising, taken into account their rather different molecular structure, which is nearly planar in case of the monomeric RC-LH1 complex and significantly bent in case of the dimeric RC-LH1-PufX complex (see Figures 4 and 7, respectively).

Table 6. Thermodynamic parameters characterizing the breakage of H-bonds in core complexes.[a]

Sample	ΔG^0 kJ/mol	ΔV^0 ml/mol	$P_{1/2}$ MPa
iLH1	21 ± 3	–18 ± 2	1160 ± 30
iRC-LH1	25 ± 5	–25 ± 5	1000 ± 20
iRC-LH1-PufX (WT)	25 ± 2	–23 ± 2	1090 ± 20
iRC-LH1-PufX ($\beta Trp_{+9}Phe$)	14 ± 2	–20 ± 1	720 ± 20
mRC-LH1-PufX ($\beta Trp_{+9}Phe$)	14 ± 2	–15 ± 1	940 ± 20
iRC-LH1-PufX ($\alpha Trp_{+11}Phe$)	10 ± 2	–14 ± 1	700 ± 30

[a]Evaluated relative to the WT membrane.

The couplings existing between the RC and LH1 proteins are expected to re-inforce core complexes. This indeed appears to be the case (compare lines 1 and 2–3 in Table 6). Yet according to our estimates, the strengthening of H-bonds is so weak that it is nearly hidden by the present experimental uncertainty.

The smaller H-bond rupture energies in WT LH1 complexes (~25 kJ/mol for two bonds and 10–14 kJ/mol for single bond in the αβ-$BChl_2$ elementary unit) in comparison with WT LH2 complexes (~39 kJ/mol for two bonds and ~19 kJ/mol for single bond) are worth noticing. The volume effects in these complexes deviate even more, being up to 3 times smaller in LH1. These variances are most probably related to different structures of LH1 and LH2 complexes, already emphasized in Introduction. While in the LH1 complex the two H-bonds in each and every elementary αβ-$BChl_2$ dimer remain within this sub-unit, in the LH2 complex one H-bond reaches out a neighboring sub-unit, tying them strongly together. Breaking these inter-dimer H-bonds will almost certainly result in larger lattice reorganization (volume change) than breaking a

bond within the same protein sub-unit. According to this logic, it is plausible that the single H-bond that is broken in membrane bound LH2 complexes corresponds to the intra-dimer H-bond (i.e., the one involving αTyr45), because of a relatively small accompanying volume effect (see Table 4, first row).

4.3.3. Characterization the hidden high-energy conformational states revealed by high pressure

Throughout the present work we have maintained that (i) the spectral peculiarities induced by external high hydrostatic pressure are due to breakage of H-bonds, and that (ii) either all or half of the H-bonds in the B850 and B875 BChl rings of peripheral (LH2) and core (LH1) complexes, respectively, may be shattered by external pressure. The prime argument supporting these notions has been the quantitative similarity between the relative spectral blue shifts achieved upon removal of the specific H-bonds by genetic manipulations and the magnitude of the pressure-induced relative spectral blue shifts.

There is also another, perhaps, simpler and more direct possibility to prove this interpretation by comparing the spectral pressure dependence for the WT complex with the dependence for the mutant complex where all the H-bonds to antenna chromophores have been removed by genetic engineering. The latter spectra, as shown in Figures 14 and 15, are from the outset blue shifted with respect to the spectra of WT complexes. The notion is that in such H-bond mutants none of the irregularities related to rupture of H-bonds exist. The dependences obtained on such mutant complexes can then be used as reference with respect to the dependences measured on the complexes, where H-bonds are presumably intact at normal pressure. If at certain pressure total rupture of H-bonds occurs, for example, in WT samples, the pressure dependencies for WT samples and for mutants should coincide past that pressure. This is exactly what our experiment shows, see Figure 28.

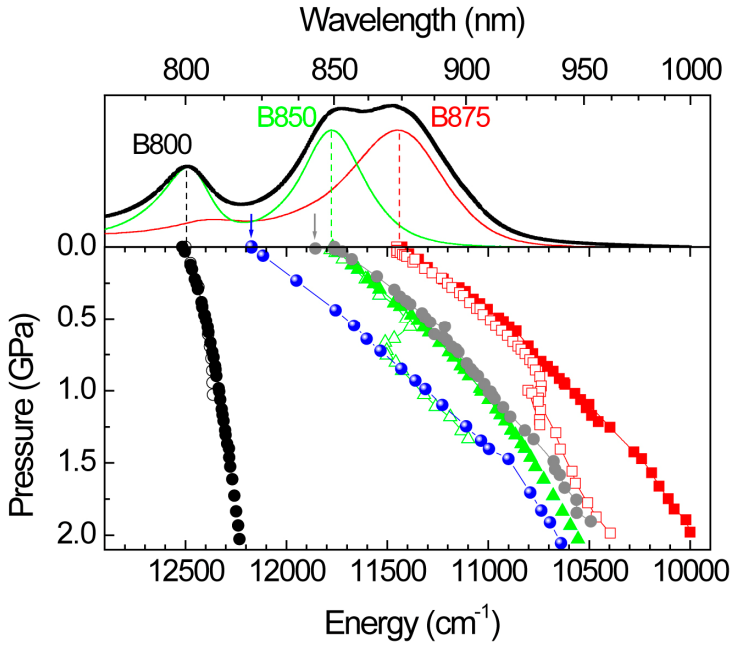

Figure 28. Pressure dependences of the B800 and B850 (shown in black and green), and B875 (red) absorption band maxima in WT LH2 and LH1 complexes, respectively. Open data points designate the detergent-isolated complexes, while filled ones, the membrane-bound complexes. Blue and grey points belong to the LH2 αβ-mutant membrane and the LH1 Trp+11-mutant membrane, respectively. Upper part of the figure shows absorption spectra of the complexes and the spectrum of full chromatophores. Blue and grey arrows, respectively, point to the absorbance maximum for the LH2 αβ-mutant membrane and the anticipated maximum for the RC-LH1-Puf X membrane with all the H-bonds to BChls broken.

As expected, the dependence for the αβ-mutant membrane (with no H-bonds to the B850 chromophores) is smooth; all the way from low to high pressures it goes fairly parallel with the dependence for the glycerol-enhanced WT LH2 membrane, albeit at higher energy. The dependence that designates isolated complexes and at low pressures follows the path of WT membrane complexes suddenly changes its course and starts trailing the αβ-mutant membranes. This unique experimental fact strongly favors our interpretation. We believe that in combination with other proof this notion is proved at least in the case of LH2 complexes. In the case of WT core complexes the evidence is less complete. This is because the double H-bond mutant core complexes have not been produced in stable form so far. Still, as demonstrated in Figure 28 for the LH1 single H-bond mutant membranes, similar outcome as with LH2 is plausible.

The data in this work imply that the high energy (blue shifted) states with broken H-bonds in LH complexes can be and in fact are stabilized by high

pressure. These states do not exist for WT complexes as stable thermodynamic entities at normal conditions, but are present in mutant complexes. To study the properties of these states, one thus has to rely on genetic engineering, which is frequently both costly and unpredictable. Given the great overlap between the data for WT and mutant complexes observed in Figure 28, one could get the most basic information about these states corresponding to normal conditions by simply extrapolating the high-pressure data to low pressures. Similar approach has earlier been used in the context of NMR studies [120]. In the optical energy range, this advance is original.

5. CONCLUSIONS AND THE MAIN RESULTS

According to the Le Chatelier principle, pressure shifts the thermodynamic equilibrium towards the states with lower volume. We have found using local-probe spectroscopic method that the lower-volume states stabilized by high hydrostatic pressure in the LH1 and LH2 light-harvesting chromoproteins are the states with shattered intramolecular H-bonds between the probe chromophore and the protein surroundings. Counter-intuitive as it might appear from the first sight that isotropic compression leads to breaking molecular bonds, this is not unusual. The best-known example is bulk solid water – ice , which melts under pressure. In the ice – water phase transition the multiple H-bonds formed in solid phase between the water molecules are broken simultaneously, resulting in the molar volume decrease. Cooperative rapture of H-bonds, followed by decrease in volume, is also observed in the present experiments. By analogy, one can introduce a pressure-induced phase transition in LH1 and LH2 protein complexes that, differently from the bulk ice, takes place on just a single molecule level. The single-molecule phase transition is a whole new concept that certainly awaits thorough future study.

In line with the objectives stated in chapter 2, the main results of this work are:

(i) A non-invasive high-pressure spectroscopy method to reversibly control tertiary and quaternary structures of membrane proteins and to investigate the energetics of H-bonds was developed. The technique that might be called “physical engineering” is complementary to genetic engineering, the latter being an invasive method, in contrast to noninvasive pressure technique.

(ii) By using this novel approach, remarkable stability against high hydrostatic pressures reaching 1.1 GPa was observed in case of the WT LH membrane chromoproteins from photosynthetic bacteria when they were protected by native membrane.

(iii) Detergent-isolation and genetic manipulations (leading to exchange of native carotenoids, partial loss of chromophores, and/or H-bonds that bind the chromophores to the surrounding protein scaffold) were found to significantly destabilize the membrane chromoproteins under high pressure. Co-solvents such as glycerol as well as high protein concentration, on the other hand, were able to stabilize not only detergent-isolated, which was known previously, but also the membrane-embedded chromoproteins.

(iv) Most notably, first evidence was obtained for reversible high-pressure-induced rupture of H-bonds in an integral membrane protein. The breakage of the H-bonds is most probably cooperative process, possibly triggered by significant weakening and final disruption of the so-called weak-link bonds. Based on the literature analyses, it is hypothesized that the principal reason of the pressure-induced denaturation of the proteins is penetration of the surrounding polar solvent molecules into the hydrophobic protein interior. Shear deformation of the chromophores binding pockets due to

mechanical anisotropy of the protein scaffold might also play role in this process.

(v) The energy required to break the H-bonds in WT LH1 and LH2 complexes are 10–20 times greater compared with the average thermal energy, RT, at ambient temperatures, which secures their great stability. A quasi-independent, additive role of H-bonds belonging to the α- and β-sublattices in reinforcement of the WT complexes was established, providing important insights into the design principles of natural photosynthetic complexes. The H-bond energies determined for the mutant complexes with just one set (α- or β-) of H-bonds intact appear only 4–6-fold greater than thermal energy at ambient temperature. This may not be enough for robust functioning of these proteins under harsh physiological conditions, explaining the evolutionary design of the LH complexes with double H-bonds in the basic unit. The reality that H-bonds are only one of the factors that play role in strengthening the proteins is further evidenced by the extra stabilizing effect of the RC when comparing the LH1-only complex with either RC-LH1 or RC-LH1-PufX complexes: the LH1-only sample requires, on average, less energy to break the H-bonds. Recalling finally the harvesting light role of the LH1 and LH2 complexes in photosynthesis, the H-bonds are not only essential for the structural stabilization of these complexes, bat are also important for tuning their light absorbing properties.

SUMMARY IN ESTONIAN

Kõrgrõhu-spektroskoopiline uurimus fotosünteetiliste bakterite valgust koguvate valkude kromofooride vesiniksidemetest

Käes olevas töös on uuritud fotosünteetilise bakteri, *Rhodobacter sphaeroides*, valgust püüdvate antennide käitumist kõrge hüdrostaatilise rõhu tingimustes, kus rõhutundliku nano-sondina kasutatakse valgus olevaid bakterklorofülle (BChl). Uuritud on nii membraansete kui detergent-isoleeritud valgust koguvate antennide (LH2 ja LH1) ja nende H-sideme, karotenoidi ja B800- mutantide käitumist rõhu all. Süsteemis toimuvad muutused rõhu all alluvad Le Chatelier printsiibile, kus rõhk toimib süsteemi termodünaamilisele tasakaalule ja rõhu kasvamine nihutab tasakaalu väiksema ruumalaga seisu suunas ja kahanemisel vastupidiselt. Mõõtmiste läbiviimiseks on rakendatud valdavalt kõrgrõhu absorptsioon-spektroskoopiat ning välja on töötatud meetodika andmete analüüsiks. Töö tulemused baseeruvad valgus olevate BChl-dele iseloomulike Q_y ja Q_x neelumisribade maksimumi asukoha nihkumisel ja laiuste muutustel, mis otseselt annavad informatsiooni BChl-de ja valgu vaheliste interaktsioonide muutuste kohta. Sininihke esinemine neelumisribade maksimumi tavapärases punanihkes ja samaaegse spektririba laienemine rõhu all on märk BChl-i ümbruses toimuvatest muutustest, mis viitavad BChl-ide ja valgu vahelise H-sidemete katkemisele. Saadud tulemus on kooskõlas kirjanduses esitatud vastavate H-sidemete mutantide neelumisribade maksimumi nihkumisega normaaltingimustel. Lisaks näitab spektririba laienemine BChl suurenenud liikumisvabadusest seostumistaskutes, mis samuti viitab H-sidemete katkemisele.

Olulisemateks tulemusteks on:

1. Kõrge rõhu spektroskoopia baasil on välja on töötatud metoodika, mis võimaldab uurida H-sidemete katkemist valgu tertsiaar- ja kvaternaar-struktuuride füüsilist terviklikkust säilitavates tingimustes. Seda tehnikat võiks nimetada ka valgu modifitseerimise "füüsikaliseks inseneeringu" meetodiks.
2. Tuvastatud on membraanis olevate valgust koguvate antennide erakordne stabiilsus (kuni 1.1 GPa).
3. Rõhu suhtes omavad uuritud valkudele destabiliseerivat mõju nende isoleerimine detergendi keskkonda ja geneetiline modifitseermine (natiivse karotenoidi asendamine neurosporeeniga, osaline kromofooride puudumine ning bakterklorofülle siduvate H-sidemete katkestamine). Kinnitust leidsid teadaolevad faktid, et ko-solvent (glütserool) ja kõrge valgu kontsentratsioon stabiliseerivad detergent-isoleeritud ja ka membraanis olevaid kromoproteiine.
4. Esimest korda on näidatud võimalik integraalse membraanse valgu H-sidemete katkemine, mis suure tõenäosusega on kooperatiivne. Kirjanduse andmetel võib H-sidemete katkemise põhjuseks olla kõrge rõhu tingimustes valgu sissemusse tunginud polaarse solvendi molekulidest või välistatud

pole ka võimalik H-sidemete katkemine valgus rõhu all toimuvate nihke-deformatsioonide tulemusena.

5. H-sidemete katkemiseks vaja minev energia valgust koguvates antennides on 10–20 korda suurem keskmisest termilisest energiast, RT, ümbritsevas keskkonnas, mis tagab nende valkude märkimisväärse stabiilsuse. Uuritud valkudes esineb üksteisega tugevalt assotsieerunud bakterklorofüllide stabiliseerimisel kahte tüüpi H-sidemeid, mille roll valgu stabiliseerimisel on individuaalne. H-sidemete mutantide H-sidemete energia on 4–6 korda suurem ümbritseva keskkonna termilisest energiast, mis tõenäoliselt ei ole piisav nende funktsioneerimiseks loomulikus looduslikus keskkonnas.

REFERENCES

[1] Xiong, J., Fischer, W.M., Inoue, K., Nakahara, M. and Bauer, C.E. (2000) Molecular evidence for the early evolution of photosynthesis. Science (New York, N.Y.) 289, 1724–1730.

[2] Blankenship, R.E., Olson, J.M. and Miller, M. (1995) Antenna complexes from green photosynthetic bacteria. In: Anoxygenic Photosynthetic Bacteria (Blankenship, R.E. et al., eds.), pp. 399-435, Kluwer Academic Publishers, Dordrecht.

[3] David, B., Ryan, Casey, Justin, Chris, Nate (2001) Bois Brule River Canoe Trip. In: http://www.google.ee/url?sa=i&rct=j&q=&source=images&cd=&cad=rja&docid=SsOYbka9ZcLw0M&tbnid=D9BJjJEDGx7NQM:&ved=&url=http%3A%2F%2Fd.umn.edu%2F~rhicks%2Frhicks1%2Fangler%2Fcanoetrip01.html&ei=R-y2UfbIFI_54QSL2oG4Cw&bvm=bv.47534661,d.bGE&psig=AFQjCNFExlv0UVnnBhpAWgN4EE-J0BntPQ&ust=1371028935816287.

[4] Imhoff, J. (2004) Taxonomy and Physiology of Phototrophic Purple Bacteria and Green Sulfur Bacteria. In: Anoxygenic Photosynthetic Bacteria SE – 1 (Blankenship, R. et al., eds.), pp. 1–15, Springer Nether–lands DA – 2004/01/01.

[5] Sener, M.K., Olsen, J.D., Hunter, C.N. and Schulten, K. (2007) Atomic-level structural and functional model of a bacterial photosynthetic membrane vesicle. Proceedings of the National Academy of Sciences of the United States of America 104, 15723–15728.

[6] Adams, P.G. and Hunter, C.N. (2012) Adaptation of intracytoplasmic membranes to altered light intensity in *Rhodobacter sphaeroides*. Biochimica et Biophysica Acta 1817, 1616–1627.

[7] Emerson, R. and Arnold, W.A. (1932) The photochemical reaction in photosynthesis. The Journal of General Physiology 16, 191–205.

[8] Sturgis, J.N. and Niederman, R.A. (2009) Organization and assembly of Light-Harvesting Complexes in the Purple Bacterial Membrane. In: The purple Phototropic Bacteria (Hunter, C.N., Daldal, F., Thurnauer, M.C., Beatty, J.T., ed.), pp. 253–273, Springer Science and Business Media B.V.

[9] Hu, X., Ritz, T., Damjanovic, A., Autenrieth, F. and Schulten, K. (2002) Photosynthetic apparatus of purple bacteria. Quarterly Reviews of Biophysics 35, 1–62.

[10] Freiberg, A. and Trinkunas, G. (2009) Unraveling the Hidden Nature of Antenna Excitations. In: Photosynthesis in silico SE – 4 (Laisk, A. et al., eds.), pp. 55–82, Springer Netherlands DA – 2009/01/01.

[11] Förster, T. (1965) Delocalized Excitation and Excitation Transfer, Florida State University.

[12] Shreve, A.P., Trautman, J.K., Frank, H.A., Owens, T.G. and Albrecht, A.C. (1991) Femtosecond energy-transfer processes in the B800-850 light-harvesting complex of *Rhodobacter sphaeroides 2.4.1*. Biochimica et Biophysica Acta 1058, 280–288.

[13] Macpherson, A.N., Arellano, J.B., Fraser, N.J., Cogdell, R.J. and Gillbro, T. (2001) Efficient Energy Transfer from the Carotenoid S 2 State in a Photosynthetic Light-Harvesting Complex. Biophysical Journal 80, 923–930.

[14] Cogdell, R.J., Isaacs, N.W., Howard, T.D., McLuskey, K., Fraser, N.J. and Prince, S.M. (1999) How photosynthetic bacteria harvest solar energy. Journal of bacteriology 181, 3869–3879.

[15] Trautman, J.K., Shreve, A.P., Violette, C.A., Frank, H.A., Owens, T.G. and Albrecht, A.C. (1990) Femtosecond dynamics of energy transfer in B800–850 light-harvesting complexes of *Rhodobacter sphaeroides*. Proceedings of the National Academy of Sciences of the United States of America 87, 215–19.

[16] Freiberg, A., Godik, V.I., Pullerits, T. and Timpman, K. (1989) Picosecond dynamics of directed excitation transfer in spectrally heterogeneous light-harvesting antenna of purple bacteria. Biochimica et Biophysica Acta 973, 93–104.

[17] Godik, V.I., Freiberg, A., Timpmann, K., Borisov, A.Y. and Rebane, K. (1987) Picosecond excitation energy transfer between different light-harvesting complexes and reaction centers in purple bacteria. In: Progress in Photosynthesis Research (Biggins, J., ed.), pp. 41–44, Nijhoff, Dordrecht, The Netherlands.

[18] Van Grondelle, R., Bergström, H., Sundström, V. and Gillbro, T. (1987) Energy transfer within the bacteriochlorophyll antenna of purple bacteria at 77 K, studied by picosecond absorption recovery. Biochimica et Biophysica Acta 894, 313–326.

[19] Sundström, V., Van Grondelle, R., Bergstroem, H., Aakesson, E. and Gillbro, T. (1986) Excitation-energy transport in the bacteriochlorophyll antenna systems of *Rhodospirillum rubrum* and *Rhodobacter sphaeroides*, studied by low-intensity picosecond absorption spectroscopy. Biochimica et Biophysica Acta 851, 431–446.

[20] Freiberg, A., Godik, V.I., Pullerits, T. and Timpmann, K.E. (1988) Directed picosecond excitation transport in purple photosynthetic bacteria. Chemical Physics 128, 227–235.

[21] Timpmann, K., Zhang, F.G., Freiberg, A. and Sundström, V. (1993) Detrapping of excitation energy from the reaction center in the photosynthetic purple bacterium *Rhodospirillum rubrum*. Biochimica et Biophysica Acta 1183, 185–193.

[22] Timpmann, K., Freiberg, A. and Sundström, V. (1995) Energy trapping and detrapping in the photosynthetic bacterium *Rhodopseudomonas viridis*: transfer-to-trap-limited dynamics. Chemical Physics 194, 275–283.

[23] Visscher, K.J., Bergstrom, H., Sundström, V., Hunter, C.N. and van Grondelle, R. (1989) Temperature dependence of energy transfer from the long wavelength antenna BChl-896 to the reaction center in *Rhodospirillum rubrum, Rhodobacter sphaeroides* (w.t. and M21 mutant) from 77 to 177 K, studied by picosecond absorption spectroscopy. Photosynthesis Research 22, 211–217.

[24] Ritz, T., Park, S. and Schulten, K. (2001) Kinetics of Excitation Migration and Trapping in the Photosynthetic Unit of Purple Bacteria. The Journal of Physical Chemistry B 105, 8259–8267.

[25] Papiz, M.Z., Prince, S.M., Howard, T., Cogdell, R.J. and Isaacs, N.W. (2003) The structure and thermal motion of the B800-850 LH2 complex from *Rps. acidophila* at 2.0 A resolution at 100 K: New structural features and functionally relevant motions. Journal of Molecular Biology 326, 1523–1538.

[26] Koepke, J., Hu, X., Muenke, C., Schulten, K. and Michel, H. (1996) The crystal structure of the light-harvesting complex II (B800-850) from *Rhodospirillum molischianum*. Structure 4, 581–597.

[27] Robert, B. and Lutz, M. (1985) Structures of antenna complexes of several *Rhodospirillales* from their resonance Raman spectra. Biochimica et Biophysica Acta 807, 10–23.

[28] Prince, S.M., Howard, T.D., Myles, D.A.A., Wilkinson, C., Papiz, M.Z., Freer, A.A., Cogdell, R.J. and Isaacs, N.W. (2003) Detergent structure in crystals of the

integral membrane light-harvesting complex LH2 from *Rhosopseudomonas acidophila* strain 10050. Journal of Molecular Biology 326, 307–315.

[29] McLuskey, K., Prince, S.M., Cogdell, R.J. and Isaacs, N.W. (2001) The crystallographic structure of the B800-820 LH3 light-harvesting complex from the purple bacteria *Rhodopseudomonas acidophila* stain 7050. Biochemistry 40, 8783–8789.

[30] Gudowska-Nowak, E., Newton, M.D. and Fajer, J. (1990) Conformational and Environmental Effects on Bacteriochlorophyll Optical Spectra: Correlatlons of Calculated Spectra with Structural Results. The Journal of Physical Chemistry 94, 5795.

[31] Freiberg, A., Timpmann, K. and Trinkunas, G. (2010) Spectral fine-tuning in excitonically coupled cyclic photosynthetic antennas. Chemical Physics Letters 500, 111–115.

[32] Karrasch, S., Bullough, P.A. and Ghosh, R. (1995) The 8.5 A projection map of the light-harvesting complex I from *Rhodospirillum rubrum* reveals a ring composed of 16 subunits. The EMBO Journal 14, 631–368.

[33] Roszak, A.W., Howard, T.D., Southall, J., Gardiner, A.T., Law, C.J., Isaacs, N.W. and Cogdell, R.J. (2003) Crystal structure of the RC-LH1 core complex from *Rhodopseudomonas palustris*. Science 302, 1969–1972.

[34] Qian, P., Hunter, C.N. and Bullough, P.A. (2005) The 8.5 Å Projection Structure of the Core RC-LH1-PufX Dimer of *Rhodobacter sphaeroides*. Journal of Molecular Biology 349, 948–960.

[35] Fotiadis, D., Qian, P., Philippsen, A., Bullough, P.A., Engel, A. and Hunter, C.N. (2004) Structural analysis of the reaction center light-harvesting complex I photosynthetic core complex of *Rhodospirillum rubrum* using atomic force microscopy. The Journal of Biological Chemistry 279, 2063–2068.

[36] Pugh, R.J., McGlynn, P., Jones, M.R. and Hunter, C.N. (1998) The LH1-RC core complex of *Rhodobacter sphaeroides*: interaction between components, time-dependent assembly, and topology of the PufX protein. Biochimica et Biophysica Acta 1366, 301–316.

[37] Jamieson, S.J., Wang, P., Qian, P., Kirkland, J.Y., Conroy, M.J., Hunter, C.N. and Bullough, P.A. (2002) Projection structure of the photosynthetic reaction centre-antenna complex of *Rhodospirillum rubrum* at 8.5 A resolution. The EMBO journal 21, 3927–3935.

[38] Sturgis, J.N., Olsen, J.D., Robert, B. and Hunter, C.N. (1997) Functions of conserved tryptophan residues of the core light-harvesting complex of *Rhodobacter sphaeroides*. Biochemistry 36, 2772–2778.

[39] Olsen, J.D., Sturgis, J.N., Westerhuis, W.H.J., Fowler, G.J.S., Hunter, C.N. and Robert, B. (1997) Site-directed modification of the ligands to the bacteriochlorophylls of the light-harvesting LH1 and LH2 complexes of *Rhodobacter sphaeroides*. Biochemistry 36, 12625–12632.

[40] Olsen, J.D., Sockalingum, G.D., Robert, B. and Hunter, C.N. (1994) Modification of a hydrogen bond to a bacteriochlorophyll a molecule in the light-harvesting 1 antenna of *Rhodobacter sphaeroides*. Proceedings of the National Academy of Sciences of the United States of America 91, 7124–8.

[41] Hsin, J., Gumbart, J., Trabuco, L.G., Villa, E., Qian, P., Hunter, C.N. and Schulten, K. (2009) Protein-Induced Membrane Curvature Investigated through Molecular Dynamics Flexible Fitting. Biophysical Journal 97, 321–329.

[42] Chandler, D.E., Hsin, J., Harrison, C.B., Gumbart, J. and Schulten, K. (2008) Intrinsic Curvature Properties of Photosynthetic Proteins in Chromatophores. Biophysical Journal 95, 2822–2836.

[43] Sener, M., Hsin, J., Trabuco, L.G., Villa, E., Qian, P., Hunter, C.N. and Schulten, K. (2009) Structural model and excitonic properties of the dimeric RC-LH1-PufX complex from *Rhodobacter sphaeroides*. Chemical Physics 357, 188–197.

[44] Hsin, J., Strümpfer, J., Sener, M., Qian, P., Hunter, C.N. and Schulten, K. (2010) Energy transfer dynamics in an RC-LH1-PufX tubular photosynthetic membrane. New Journal of Physics 12, 085005.

[45] Ermler, U., Michel, H. and Schiffer, M. (1994) Structure and function of the photosynthetic reaction center from *Rhodobacter sphaeroides*. Journal of Bioenergetics and Biomembranes 26, 5–15.

[46] Remy, A. and Gerwert, K. (2003) Coupling of light-induced electron transfer to proton uptake in photosynthesis. Nature Structural Biology 10, 637–644.

[47] Van Amerongen, H., Valkunas, L. and Van Grondelle, R. (2000) Photosynthetic Excitons, pp. 590, World Scientific, Singapore.

[48] Cogdell, R.J., Gall, A. and Köhler, J. (2006) The architecture and function of the light-harvesting apparatus of purple bacteria: from single molecules to in vivo membranes. Quarterly Reviews of Biophysics 39, 227–324.

[49] Van Dorssen, R.J., Hunter, C.N., Van Grondelle, R., Korenhof, A.H. and Amesz, J. (1988) Spectroscopic properties of antenna complexes of *Rhodobacter sphaeroides* in vivo. Biochimica et Biophysica Acta 932, 179–88.

[50] Grimm, B. (2006) Chlorophylls and Bacteriochlorophylls: Biochemistry, Biophysics, Functions and Applications, Springer.

[51] Rätsep, M., Cai, Z.-L., Reimers, J.R. and Freiberg, A. (2011) Demonstration and interpretation of significant asymmetry in the low-resolution and high-resolution Q(y) fluorescence and absorption spectra of bacteriochlorophyll a. The Journal of Chemical Physics 134, 024506.

[52] Loach, P.A. and Parkes-Loach, P.S. (2008) Structure-function relationships in bacterial light.harvesting complexes investigated by reconstitution techniques. In: The Purple Photosynthetic bacteria. (Hunter, C.N. et al., eds.), pp. 181–198, Springer, Dordrecht.

[53] Sundström, V., Pullerits, T. and van Grondelle, R. (1999) Photosynthetic light-harvesting: Reconciling dynamics and structure of purple bacterial LH2 reveals function of photosynthetic unit. The Journal of Physical Chemistry B 103, 2327–2346.

[54] Sener, M., Strümpfer, J., Timney, J.A., Freiberg, A., Hunter, C.N. and Schulten, K. (2010) Photosynthetic Vesicle Architecture and Constraints on Efficient Energy Harvesting. Biophysical Journal 99, 67–75.

[55] Pullerits, T., Chachisvilis, M. and Sundström, V. (1995) Exciton dynamics and delocalization length in B850 molecules of LH2 of *Rhodobacter sphaeroides*. In: Photosynthesis: from Light to Biosphere (Mathis, P., ed.), pp. 107–110, Kluwer Academic Publishers, Dordrecht.

[56] Koolhaas, M.H.C., Frese, R.N., Fowler, G.J.S., Bibby, T.A., Georgakopoulou, S., Zwan, G.v.d., Hunter, C.N. and van Grondelle, R. (1998) Identification of the Upper Exciton Component of the B850 Bacteriochlorophylls of the LH2 Antenna Complex, Using a B800-Free Mutant of *Rhodobacter sphaeroides*. Biochemistry 37, 4693–4698.

[57] Freiberg, A., Rätsep, M. and Timpmann, K. (2012) A comparative spectroscopic and kinetic study of photoexcitations in detergent-isolated and membrane-embedded LH2 light-harvesting complexes. Biochimica et Biophysica Acta 1817, 1471–1482.
[58] Gall, A., Fowler, G.J., Hunter, C.N. and Robert, B. (1997) Influence of the protein binding site on the absorption properties of the monomeric bacteriochlorophyll in *Rhodobacter sphaeroides* LH2 complex. Biochemistry 36, 16282–16287.
[59] Robert, B. and Frank, H.A. (1988) A resonance Raman investigation of the effect of lithium dodecyl sulfate on the B800-850 light-harvesting protein of *Rhodopseudomonas acidophila* 7750. Biochimica et Biophysica Acta 934, 401–5.
[60] Senge, M.O. (1992) New trends in photobiology: The conformational flexibility of tetrapyrroles - current model studies and photobiological relevance. Journal of Photochemistry and Photobiology B 16, 3–36.
[61] Bridgman, P.W. (1914) The coagulation of albumen by pressure. The Journal of Biological Chemistry 19, 511–512.
[62] Meersman, F., Smeller, L. and Heremans, K. (2006) Protein stability and dynamics in the pressure-temperature plane. Biochimica et Biophysica Acta 1764 , 346–354.
[63] Silva, J.L. and Weber, G. (1993) Pressure stability of proteins. Annual Review of Physical Chemistry 44, 89–113.
[64] Scharnagl, C., Reif, M. and Friedrich, J. (2005) Stability of proteins: Temperature, pressure and the role of the solvent. Biochimica et Biophysica Acta 1749, 187–213.
[65] Meersman, F., Daniel, I., Bartlett, D.H., Winter, R., Hazael, R. and McMillan, P.F. (2013) High-Pressure Biochemistry and Biophysics. Reviews in Mineralogy and Geochemistry 75, 607–648.
[66] Kadam, P.S., Jadhav, B.A., Salve, R.V. and Machewad, G.M. (2012) Review on the High Pressure Technology (HPT) for Food Preservation. Journal of Food Processing & Technology 3, 135.
[67] Roche, J., Caro, J.A., Norberto, D.R., Barthe, P., Roumestand, C., Schlessman, J.L., Garcia, A.E., García-Moreno, B.E. and Royer, C.A. (2012) Cavities determine the pressure unfolding of proteins. Proceedings of the National Academy of Sciences of the United States of America 109, 6945–6950.
[68] Nagae, T., Kawamura, T., Chavas, L.M.G., Niwa, K., Hasegawa, M., Kato, C. and Watanabe, N. (2012) High-pressure-induced water penetration into 3-isopropylmalate dehydrogenase. Acta Crystallographica Section D 68, 300–309.
[69] Collins, M.D., Hummer, G., Quillin, M.L., Matthews, B.W. and Gruner, S.M. (2005) Cooperative water filling of a nonpolar protein cavity observed by high-pressure crystallography and simulations. Proceedings of the National Academy of Sciences of the United States of America 102, 16668–16671.
[70] Grigera, J.R. and McCarthy, A.N. (2010) The Behavior of the Hydrophobic Effect under Pressure and Protein Denaturation. Biophysical Journal 98, 1626–1631.
[71] Sheu, S.-Y., Yang, D.-Y., Selzle, H.L. and Schlag, E.W. (2003) Energetics of hydrogen bonds in peptides. Proceedings of the National Academy of Sciences of the United States of America 100, 12683–12687.
[72] Wendler, K., Thar, J., Zahn, S. and Kirchner, B. (2010) Estimating the hydrogen bond energy. The Journal of Physical Chemistry. A 114, 9529–9536.

[73] Bondar, A.-N. and White, S.H. (2012) Hydrogen bond dynamics in membrane protein function. Biochimica et Biophysica Acta 1818, 942–950.
[74] Bowie, J.U. (2011) Membrane protein folding: how important are hydrogen bonds? Current Opinion in Structural Biology 21, 42–49.
[75] Li, H., Yamada, H. and Akasaka, K. (1998) Effect of pressure on individual hydrogen bonds in proteins. Basic pancreatic trypsin inhibitor. Biochemistry 37, 1167–1173.
[76] Nisius, L. and Grzesiek, S. (2012) Key stabilizing elements of protein structure identified through pressure and temperature perturbation of its hydrogen bond network. Nature Chemistry 4, 711–717.
[77] Nielsen, G. and Schwalbe, H. (2012) Protein NMR spectroscopy: Hydrogen bonds under pressure. Nature Chemistry 4, 693–695.
[78] Phelps, D.J. and Hesterberg, L.K. (2007) Protein disaggregation and refolding using high hydrostatic pressure. Journal of Chemical Technology and Biotechnology 82, 610–613.
[79] Jaenicke, R. (1981) Enzymes under extremes of physical conditions. Annual Review of Biophysics and Bioengineering 10, 1–67.
[80] Michels, P.C., Hei, D. and Clark, D.S. (1996) Pressure Effects on Enzyme Activity and Stability at High Temperatures. Advances in Protein Chemistry 48, 341–376.
[81] Boonyaratanakornkit, B.B., Park, C.B. and Clark, D.S. (2002) Pressure effects on intra- and intermolecular interactions within proteins. Biochimica et Biophysica Acta 1595, 235–249.
[82] McDermott, G., Prince, S.M., Freer, A.A., Hawthornthwaite-Lawless, A.M., Papiz, M.Z., Cogdell, R.J. and Isaacs, N.W. (1995) Crystal structure of an integral membrane light-harvesting complex from photosynthetic bacteria. Nature 374, 517–521.
[83] Prince, S.M., Papiz, M., . Z., Freer, A.A., McDermott, G., Hawthornthwaite-Lawless, A.M., Cogdell, R.J. and Isaacs, N.W. (1997) Apoprotein structure in the LH2 complex from *Rhodopseudomonas acidophila* strain 10050: modular assembly and protein pigment interactions. Journal of Molecular Biology 268, 412–423.
[84] Walz, T., Jamieson, S.J., Bowers, C.M., Bullough, P.A. and Hunter, C.N. (1998) Projection structures of three photosynthetic complexes from *Rhodobacter sphaeroides*: LH2 at 6 A, LH1 and RC-LH1 at 25 A. Journal of Molecular Biology 282, 833–845.
[85] Lesch, H., Schlichter, J., Friedrich, J. and Vanderkooi, J.M. (2004) Molecular probes: what is the range of their interaction with the environment? Biophysical Journal 86, 467–472.
[86] Jones, M.R., Fowler, G.J.S., Gibson, L.C.D., Grief, G.G., Olsen, J.D., Crielaard, W. and Hunter, C.N. (1992) Mutants of Rhodobacter sphaeroides lacking one or more pigment-protein complexes and complementation with reaction-center, LH1, and LH2 genes. Molecular Microbiology 6, 1173–84.
[87] Fowler, G.J.S., Visschers, R.W., Grief, G.G., Van Grondelle, R. and Hunter, C.N. (1992) Genetically modified photosynthetic antenna complexes with blue-shifted absorbance bands. Nature 355, 848–50.
[88] Fowler, G.J.S., Sockalingum, G.D., Robert, B. and Hunter, C.N. (1994) Blue shifts in bacteriochlorophyll absorbance correlate with changed hydrogen bonding patterns in light-harvesting 2 mutants of *Rhodobacter sphaeroides* with

alterations at alpha-Tyr-44 and alpha-Tyr-45. Biochemical Journal 299, 695–700.
[89] Kitamura, Y. and Itoh, T. (1987) Reaction volume of protonic ionization for buffering agents. Prediction of pressure dependence of pH and pOH. Journal of Solution Chemistry 16, 715–725.
[90] Neuman, R.C., Kauzmann, W. and Zipp, A. (1973) Pressure dependence of weak acid ionization in aqueous buffers. The Journal of Physical Chemistry 77, 2687–2691.
[91] Prive, G.G. (2007) Detergents for the stabilization and crystallization of membrane proteins. Structural Biology of Membrane Proteins 41, 388–397.
[92] Kaufmann, T.C., Engel, A. and Remigy, H.-W. (2006) A Novel Method for Detergent Concentration Determination. Biophysical Journal 90, 310–317.
[93] Mizoguchi, K., Fukui, K., Yanagishita, H., Nakane, T. and Nakata, T. (2002) Ultrafiltration behavior of a new type of non-ionic surfactant around the CMC. Journal of Membrane Science 208, 285–288.
[94] Hauser, H. (2000) Short-chain phospholipids as detergents. Biochimica et Biophysica Acta 1508, 164–181.
[95] de Haas, G.H., Bonsen, P.P., Pieterson, W.A. and van Deenen, L.L. (1971) Studies on phospholipase A and its zymogen from porcine pancreas. 3. Action of the enzyme on short-chain lecithins. Biochimica et Biophysica Acta 239, 252–266.
[96] Sturgis, J.N., Hunter, C.N. and Niederman, R.A. (1988) Spectra and extinction coefficients of near-infrared absorption bands in membranes of Rhodobacter sphaeroides mutants lacking light-harvesting and reaction center complexes. Photochemistry and Photobiology 48, 243–7.
[97] Lorenz, B., Shen, Y.R. and Holzapfel, W.B. (1994) Characterization of the new luminescence pressure sensor SrFCl:Sm2+. High Pressure Research 12, 91–99.
[98] Grasset, O. (2001) Calibration of the R ruby fluorescence lines in the pressure range [0-1 GPa] and the temperature range [250–300 K]. High Pressure Research 21, 139–157.
[99] Syassen, K. (2008) Ruby under pressure. High Pressure Research 28, 75–126.
[100] Shneour, E.A. (1962) Carotenoid pigment conversion in rhodopseudomonas spheroides. Biochimica et Biophysica Acta 62, 534–540.
[101] Freiberg, A., Timpmann, K., Ruus, R. and Woodbury, N.W. (1999) Disordered exciton analysis of linear and nonlinear absorption spectra of antenna bacteriochlorophyll aggregates: LH2-only mutant chromatophores of *Rhodobacter sphaeroides* at 8 K under spectrally selective excitation. The Journal of Physical Chemistry B 103, 10032–10041.
[102] Timpmann, K., Trinkunas, G., Olsen, J.D., Hunter, C.N. and Freiberg, A. (2004) Bandwidth of excitons in LH2 bacterial antenna chromoproteins. Chemical Physics Letters 398, 384–388.
[103] Rätsep, M., Hunter, C.N., Olsen, J.D. and Freiberg, A. (2005) Band structure and local dynamics of excitons in bacterial light-harvesting complexes revealed by spectrally selective spectroscopy. Photosynthesis Research 86, 37–48.
[104] Uyeda, G., Williams, J.C., Roman, M., Mattioli, T.A. and Allen, J.P. (2010) The influence of hydrogen bonds on the electronic structure of light-harvesting complexes from photosynthetic bacteria. Biochemistry 49, 1146–1159.
[105] Ellervee, A. and Freiberg, A. (2008) Formation of bacteriochlorophyll a coordination states under external high-pressure. Chemical Physics Letters 450, 386–390.

[106] Timpmann, K., Ellervee, A., Pullerits, T., Ruus, R., Sundström, V. and Freiberg, A. (2001) Short-range exciton couplings in LH2 photosynthetic antenna proteins studied by high hydrostatic pressure absorption spectroscopy. The Journal of Physical Chemistry B 105, 8436–8444.
[107] Wu, H.-M., Rätsep, M., Jankowiak, R., Cogdell, R.J. and Small, G.J. (1997) Comparison of the LH2 antenna complexes of *Rhodopseudomonas acidophila* (strain 10050) and *Rhodobacter sphaeroides* by high-pressure absorption, high-pressure hole burning, and temperature-dependent absorption spectroscopies. The Journal of Physical Chemistry B 101, 7641–7653.
[108] Wu, H.-M., Rätsep, M., Jankowiak, R., Cogdell, R.J. and Small, G.J. (1998) Hole-burning and absorption studies of the LH1 antenna complex of purple bacteria: Effects of pressure and temperature. The Journal of Physical Chemistry B 102, 4023–4034.
[109] Timpmann, K., Trinkunas, G., Qian, P., Hunter, C.N. and Freiberg, A. (2005) Excitons in core LH1 antenna complexes of photosynthetic bacteria: Evidence for strong resonant coupling and off-diagonal disorder. Chemical Physics Letters 414, 359–363.
[110] Pajusalu, M., Rätsep, M., Trinkunas, G. and Freiberg, A. (2011) Davydov splitting of excitons in cyclic bacteriochlorophyll a nanoaggregates of bacterial light-harvesting complexes between 4.5 and 263 K. A European Journal of Chemical Physics and Physical Chemistry 12, 634–644.
[111] Winter, R. and Dzwolak, W. (2004) Temperature-pressure configurational landscape of lipid bilayers and proteins. Cellular and Molecular Biology (Noisy-le-Grand, France) 50, 397–417.
[112] Kangur, L., Olsen, J.D., Hunter, C.N. and Freiberg, A. (2012) Estimating Hydrogen Bond Energy in Integral Membrane Chromoproteins by High Hydrostatic Pressure Optical Spectroscopy. In: Protein Structure (Dr Faraggi, E., ed.), InTech.
[113] Chryssomallis, G.S., Torgerson, P.M., Drickamer, H.G. and Weber, G. (1981) Effect of hydrostatic pressure on lysozyme and chymotrypsinogen detected by fluorescence polarization. Biochemistry 20, 3955–3959.
[114] Harano, Y., Yoshidome, T. and Kinoshita, M. (2008) Molecular mechanism of pressure denaturation of proteins. The Journal of Chemical Physics 129, 145103.
[115] Kangur, L., Timpmann, K. and Freiberg, A. (2008) Stability of integral membrane proteins against high hydrostatic pressure: The LH2 and LH3 antenna pigment-protein complexes from photosynthetic bacteria. The Journal of Physical Chemistry B 112, 7948–7955.
[116] Buche, A., Ellis, G. and Ramirez, J.M. (2001) Probing the binding site of 800-nm bacteriochlorophyll in the membrane-linked LH2 protein of Rhodobacter capsulatus by local unfolding and chemical modification. European Journal of Biochemistry 268, 2792–2800.
[117] Otzen, D. (2011) Protein-surfactant interactions: A tale of many states. Biochimica et Biophysica Acta 1814, 562–591.
[118] Schubert, A., Stenstam, A., Beenken, W.J.D., Herek, J.L., Cogdell, R.J., Pullerits, T. and V., S. (2004) In vitro self-assembly of the light harvesting pigment-protein LH2 revealed by ultrafast spectroscopy and electron microscopy. Biophysical Journal 86, 2363–2373.
[119] Hong, X., Weng, Y.-X. and Li, M. (2004) Determination of the topological shape of integral membrane protein light-harvesting complex LH2 from photo-

synthetic bacteria in the detergent solution by small-angle X-ray scattering. Biophysical Journal 86, 1082–1088.
[120] Akasaka, K., Kitahara, R. and Kamatari, Y.O. (2013) Exploring the folding energy landscape with pressure. Archives of Biochemistry and Biophysics 531, 110–115.
[121] Katrusiak, A. and Dauter, Z. (1996) Compressibility of lysozyme protein crystals by X-ray diffraction. Acta Crystallographica Section D: Biological Crystallography 52(Pt 3), 607–8.
[122] Fourme, R., Kahn, R., Mezouar, M., Girard, E., Hoerentrup, C., Prange, T. and Ascone, I. (2001) High-pressure protein crystallography (HPPX): instrumentation, methodology and results on lysozyme crystals. Journal of Synchrotron Radiation 8, 1149–1156.
[123] Sturgis, J.N., Gall, A., Ellervee, A., Freiberg, A. and Robert, B. (1998) The effect of pressure on the bacteriochlorophyll *a* binding sites of the core antenna complex from *Rhodospirillum rubrum*. Biochemistry 37, 14875–14880.
[124] Gall, A., Ellervee, A., Bellissent-Funel, M.-C., Robert, B. and Freiberg, A. (2001) Effect of High Pressure on the Photochemical Reaction Center from Rhodobacter sphaeroides R26.1. Biophysical Journal 80, 1487–1497.

ACKNOWLEDGEMENTS

First of all I wish to express my sincere gratitude to my supervisor Professor **Arvi Freiberg** for introducing me to the field of purple bacterial light harvesting system and the high-pressure experiments and for his professional guidance. I would like to thank him for help with thesis writing and writing articles, skilled, inspiring and creative discussions in experimental approach and result interpreting. It has been a great pleasure to work under your guidance.

Secondly, I would like to thank our previous group member **Aleksander Ellervee** for introducing me Diamond Anvil High-Pressure Cell handling. And I would like to thank our group members **Kõu Timpmann**, **Margus Rätsep**, **Kristjan Leiger**, **Hain Salujärv**, **Jörg Pieper**, **Mihkel Pajusalu**, **Manoop Chenchilian**, **Liis Reisberg** for help, guidance, advices, assistance, discussions and support.

I would like to thank Professor **Neil Hunter** and **John Olsen** from University of Sheffield, who kindly allowed experimental samples and assisted in writing articles.

I would like to thank **Robert Tiismus** for introduction me to Professor Arvi Freiberg.

I would like to express my sincere gratitude to all people who have supported in preparing this work.

APPENDIX: DIRECTIONS OF THE FUTURE RESEARCH

Directions of the future research

Although many useful experimental data to understand the H-bonds in membrane proteins, specifically in LH complexes of photosynthetic bacteria, have been obtained, the present work has also left several interesting question unanswered and/or raised new problems that await solutions in future research. As follows we give a brief outlook of some of these issues.

Additional proof for the high pressure-induced H-bond rupture. The experimental evidence gathered in this work in support the breakage of H-bonds is based on the analogy of optical spectral responses of physically (by external hydrostatic pressure) or genetically modified LH complexes. In certain sense this evidence is devious; it thus would be desirable to obtain additional experimental proof for the high pressure-induced H-bond rupture. There are in principle several experimental techniques able to provide this kind of structural information, incuding vibrational (Raman), NMR spectroscopy, and X-ray scattering. Unfortunately, applicability of most of these methods for the present purpose is questionable. For example, the high-pressure X-ray scattering [69,121,122] is not practical because it requires high-quality crystals, which most probably are not enough compressible to observed the H-bond breakage. The two other techniques require rather high density of the protein in the sample. Yet it was observed by us [115] that the WT LH proteins are stabilized against high pressure by high concentrations. This explains why the earlier attempts from this laboratory ([123,124]) with Raman spectroscopy did not succeed in demonstrating the rupture of H-bonds under high pressure. One of the interesting byproducts of the present work is that the CrtC- mutant LH2 complexes show rupture of H-bonds even at high local concentrations present in native membrane. Therefore, it will be one of our future priorities to study this sample by Raman spectroscopy.

Slow dissociation of LH chromoproteins under high pressure and estimation of the inter-subunit binding energy. The LH samples studied in this work demonstrated high resistivity to high-pressure denaturation, even when isolated out from the protective environment of the native membrane, using relatively low-concentrated detergents. However, under increased detergent concentration, the sample degradation becomes more and more evident when observed over a long period of time. For example, the data in Figure 29 show slow dissociation of isolated LH1 complexes at the elevated pressure of 0.3 GPa. To boost the dissociation process the detergent (DHPC) concentration was enhanced to 13 mM, instead of standard 3 mM. The dissociation is obvious from the decreasing of the B875 absorption band and from the simultaneous increasing of the B820 band, the known dimeric building block of the B875 antenna array. The dissociation is very slow, achieving the equilibrium state only in about 40 hours.

As can be seen from Figure 29A, the transition is characterized by isobestic point, meaning that under the chosen conditions there is only one dissociation product with a spectral maximum at 820 nm. The change of the absorbance at different spectral ranges corresponding to the reactant (B875) and product (B820) states can be used to monitor the kinetics and the equilibrium of the dissociation reaction. As can be concluded from the linear dependence in the half-logarithmic scale of the insert of Figure 29B, the decay of the B875 complex follows a pseudo-first order kinetics with a half lifetime of $t_{1/2}$= 9 h (dissociation constant K_d= 10^{-37} M). Further studies are under way to measure the time constants and dissociation equilibriums at different pressures, as well as to obtain the activation energy and volume of the dissociation reaction.

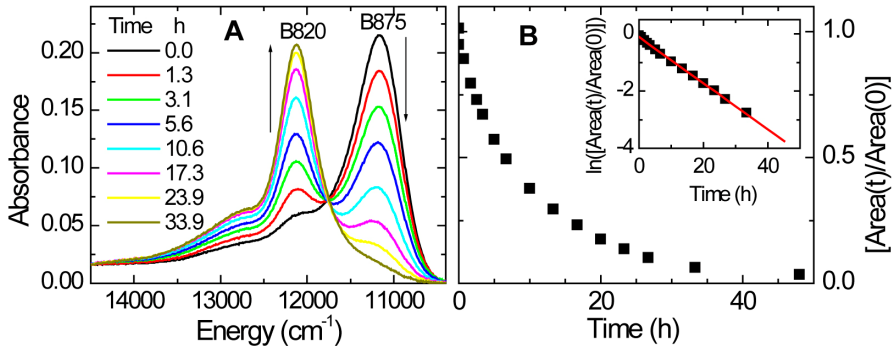

Figure 29. (A) Time dependence of the area-normalized absorption spectrum of isolated LH1 complexes from *Rba. sphaeroides* at 13 mM detergent (DHPC) concentration and at constant 0.3 GPa pressure. Arrows indicate the direction of the changing band intensity. (B) Decay kinetics of the relative (integral) intensity of the B875 band, corresponding to dissociation of the LH1 complexes. Insert demonstrates the respective pseudo first order reaction kinetics.

Systematic study of carotenoids in reinforcement the stability of light harvesting complexes by high-pressure spectroscopy. We have shown that replacement of native contents of carotenoids in *Rba. sphaeroides* (a mixture of spheroidene and spheroidenone with neurosporene), leads to destabilization of the structure of LH2 complexes. As a result, as demonstrated in Figure 23, the chromophores-binding H-bonds break under pressure, even when the protein complexes are protected by the native membrane. In the subsequent phase of the high-pressure studies, we are going to systematically study the role of carotenoids in reinforcement the stability of LH complexes.

CURRICULUM VITAE

Name: Liina Kangur
Date of birth: 01.03.1971
Citizenship: Estonian
Phone: +372 737 4738
E-mail: liina.kangur@ut.ee

Education:

1989–1996	B.Sc. in Chemistry, Faculty of Physics and Chemistry, University of Tartu
1997–2000	M.Sc. in Biochemistry, Faculty of Biology and Geography, University of Tartu

Professional employment:

01.01.2001–30.04.2003	University of Tartu, Institute of Molecular and Cell Biology, Researcher
01.05.2003–31.09.2005	Tallinn University of Technology, Department of Gene Technology, Chair of Genomics and Proteomics, Researcher
01.10.2008–…	University of Tartu, Institute of Physics, Laboratory of Biophysics, Researcher

Professional development:

1998	TEMPUS scholarship, University of Kiel, Faculty of Mathematics and Natural Sciences (Germany) visiting student
2008	ECONET scholarship, CEA-Saclay, Institute of Biology and Technology (France) guest scientist
2008	Protein expertise tour, GE Healthcare Bio-Sciences AB, GE (Pharmacia), Tartu 7–8th October

Organizational membership:

2003–	active member of the Estonian Naturalists' Society

ELULOOKIRJELDUS

Nimi: Liina Kangur
Sünniaeg: 01.03.1971
Kodakondsus: Eesti
Telefon: +372 737 4738
E-post: liina.kangur@ut.ee

Hariduskäik:

1989–1997	Tartu Ülikool Füüsika-keemia teaduskond, BSc keemia erialal
1997–2000	Tartu Ülikool, MSc (teaduskraad) bikeemias 2000

Erialane teenistuskäik:

01.01.2001–30.04.2003	Tartu Ülikool, Molekulaar- ja rakubioloogia instituut, teadur
01.05.2003–31.09.2005	Tallinna Tehnikaülikool, Geenitehnoloogia instituut, genoomika ja proteoomika õppetool, teadur
01.10.2005–	Tartu Ülikool, Füüsika instituut, biofüüsika labor, teadur

Erialane enesetäiendus:

1998	TEMPUS programmiraames vahetustudeng, Kieli Ülikool, Matemaatika ja loodusteaduste instituut, Saksamaa
2008	ECONET stipendium, CEA-Saclay, Biologia ja tehnoloogia instituut, Prantsusmaa
2008	Protein expertise tour – GE Healthcare Bio-Sciences AB, GE (Pharmacia), Biomeditsiini ja biotehnoloogia doktorikooli projekti (nr: 1.0101-0167) raames, Tartu 7 – 8th October

Organisatsiooniline kuuluvus:

2003-	Eesti Loodusuurijate Seltsi (Assotsieerunud Eesti Teaduste Akadeemiaga 23.01.1998) tegevliige

DISSERTATIONES BIOLOGICAE UNIVERSITATIS TARTUENSIS

1. **Toivo Maimets**. Studies of human oncoprotein p53. Tartu, 1991, 96 p.
2. **Enn K. Seppet**. Thyroid state control over energy metabolism, ion transport and contractile functions in rat heart. Tartu, 1991, 135 p.
3. **Kristjan Zobel**. Epifüütsete makrosamblike väärtus õhu saastuse indikaatoritena Hamar-Dobani boreaalsetes mägimetsades. Tartu, 1992, 131 lk.
4. **Andres Mäe**. Conjugal mobilization of catabolic plasmids by transposable elements in helper plasmids. Tartu, 1992, 91 p.
5. **Maia Kivisaar**. Studies on phenol degradation genes of *Pseudomonas* sp. strain EST 1001. Tartu, 1992, 61 p.
6. **Allan Nurk**. Nucleotide sequences of phenol degradative genes from *Pseudomonas sp.* strain EST 1001 and their transcriptional activation in *Pseudomonas putida.* Tartu, 1992, 72 p.
7. **Ülo Tamm**. The genus *Populus* L. in Estonia: variation of the species biology and introduction. Tartu, 1993, 91 p.
8. **Jaanus Remme**. Studies on the peptidyltransferase centre of the *E.coli* ribosome. Tartu, 1993, 68 p.
9. **Ülo Langel**. Galanin and galanin antagonists. Tartu, 1993, 97 p.
10. **Arvo Käärd**. The development of an automatic online dynamic fluorescense-based pH-dependent fiber optic penicillin flowthrought biosensor for the control of the benzylpenicillin hydrolysis. Tartu, 1993, 117 p.
11. **Lilian Järvekülg**. Antigenic analysis and development of sensitive immunoassay for potato viruses. Tartu, 1993, 147 p.
12. **Jaak Palumets**. Analysis of phytomass partition in Norway spruce. Tartu, 1993, 47 p.
13. **Arne Sellin**. Variation in hydraulic architecture of *Picea abies* (L.) Karst. trees grown under different enviromental conditions. Tartu, 1994, 119 p.
13. **Mati Reeben**. Regulation of light neurofilament gene expression. Tartu, 1994, 108 p.
14. **Urmas Tartes**. Respiration rhytms in insects. Tartu, 1995, 109 p.
15. **Ülo Puurand.** The complete nucleotide sequence and infections *in vitro* transcripts from cloned cDNA of a potato A potyvirus. Tartu, 1995, 96 p.
16. **Peeter Hõrak**. Pathways of selection in avian reproduction: a functional framework and its application in the population study of the great tit (*Parus major*). Tartu, 1995, 118 p.
17. **Erkki Truve**. Studies on specific and broad spectrum virus resistance in transgenic plants. Tartu, 1996, 158 p.
18. **Illar Pata**. Cloning and characterization of human and mouse ribosomal protein S6-encoding genes. Tartu, 1996, 60 p.
19. **Ülo Niinemets**. Importance of structural features of leaves and canopy in determining species shade-tolerance in temperature deciduous woody taxa. Tartu, 1996, 150 p.

20. **Ants Kurg**. Bovine leukemia virus: molecular studies on the packaging region and DNA diagnostics in cattle. Tartu, 1996, 104 p.
21. **Ene Ustav**. E2 as the modulator of the BPV1 DNA replication. Tartu, 1996, 100 p.
22. **Aksel Soosaar**. Role of helix-loop-helix and nuclear hormone receptor transcription factors in neurogenesis. Tartu, 1996, 109 p.
23. **Maido Remm**. Human papillomavirus type 18: replication, transformation and gene expression. Tartu, 1997, 117 p.
24. **Tiiu Kull**. Population dynamics in *Cypripedium calceolus* L. Tartu, 1997, 124 p.
25. **Kalle Olli**. Evolutionary life-strategies of autotrophic planktonic microorganisms in the Baltic Sea. Tartu, 1997, 180 p.
26. **Meelis Pärtel**. Species diversity and community dynamics in calcareous grassland communities in Western Estonia. Tartu, 1997, 124 p.
27. **Malle Leht**. The Genus *Potentilla* L. in Estonia, Latvia and Lithuania: distribution, morphology and taxonomy. Tartu, 1997, 186 p.
28. **Tanel Tenson**. Ribosomes, peptides and antibiotic resistance. Tartu, 1997, 80 p.
29. **Arvo Tuvikene**. Assessment of inland water pollution using biomarker responses in fish *in vivo* and *in vitro.* Tartu, 1997, 160 p.
30. **Urmas Saarma**. Tuning ribosomal elongation cycle by mutagenesis of 23S rRNA. Tartu, 1997, 134 p.
31. **Henn Ojaveer**. Composition and dynamics of fish stocks in the gulf of Riga ecosystem. Tartu, 1997, 138 p.
32. **Lembi Lõugas**. Post-glacial development of vertebrate fauna in Estonian water bodies. Tartu, 1997, 138 p.
33. **Margus Pooga**. Cell penetrating peptide, transportan, and its predecessors, galanin-based chimeric peptides. Tartu, 1998, 110 p.
34. **Andres Saag**. Evolutionary relationships in some cetrarioid genera (Lichenized Ascomycota). Tartu, 1998, 196 p.
35. **Aivar Liiv**. Ribosomal large subunit assembly *in vivo*. Tartu, 1998, 158 p.
36. **Tatjana Oja**. Isoenzyme diversity and phylogenetic affinities among the eurasian annual bromes (*Bromus* L., Poaceae). Tartu, 1998, 92 p.
37. **Mari Moora**. The influence of arbuscular mycorrhizal (AM) symbiosis on the competition and coexistence of calcareous grassland plant species. Tartu, 1998, 78 p.
38. **Olavi Kurina**. Fungus gnats in Estonia (*Diptera: Bolitophilidae, Keroplatidae, Macroceridae, Ditomyiidae, Diadocidiidae, Mycetophilidae*). Tartu, 1998, 200 p.
39. **Andrus Tasa**. Biological leaching of shales: black shale and oil shale. Tartu, 1998, 98 p.
40. **Arnold Kristjuhan.** Studies on transcriptional activator properties of tumor suppressor protein p53. Tartu, 1998, 86 p.

41. **Sulev Ingerpuu.** Characterization of some human myeloid cell surface and nuclear differentiation antigens. Tartu, 1998, 163 p.
42. **Veljo Kisand.** Responses of planktonic bacteria to the abiotic and biotic factors in the shallow lake Võrtsjärv. Tartu, 1998, 118 p.
43. **Kadri Põldmaa.** Studies in the systematics of hypomyces and allied genera (Hypocreales, Ascomycota). Tartu, 1998, 178 p.
44. **Markus Vetemaa.** Reproduction parameters of fish as indicators in environmental monitoring. Tartu, 1998, 117 p.
45. **Heli Talvik.** Prepatent periods and species composition of different *Oesophagostomum* spp. populations in Estonia and Denmark. Tartu, 1998, 104 p.
46. **Katrin Heinsoo.** Cuticular and stomatal antechamber conductance to water vapour diffusion in *Picea abies* (L.) karst. Tartu, 1999, 133 p.
47. **Tarmo Annilo.** Studies on mammalian ribosomal protein S7. Tartu, 1998, 77 p.
48. **Indrek Ots.** Health state indicies of reproducing great tits (*Parus major*): sources of variation and connections with life-history traits. Tartu, 1999, 117 p.
49. **Juan Jose Cantero.** Plant community diversity and habitat relationships in central Argentina grasslands. Tartu, 1999, 161 p.
50. **Rein Kalamees.** Seed bank, seed rain and community regeneration in Estonian calcareous grasslands. Tartu, 1999, 107 p.
51. **Sulev Kõks.** Cholecystokinin (CCK) — induced anxiety in rats: influence of environmental stimuli and involvement of endopioid mechanisms and erotonin. Tartu, 1999, 123 p.
52. **Ebe Sild.** Impact of increasing concentrations of O_3 and CO_2 on wheat, clover and pasture. Tartu, 1999, 123 p.
53. **Ljudmilla Timofejeva.** Electron microscopical analysis of the synaptonemal complex formation in cereals. Tartu, 1999, 99 p.
54. **Andres Valkna.** Interactions of galanin receptor with ligands and G-proteins: studies with synthetic peptides. Tartu, 1999, 103 p.
55. **Taavi Virro.** Life cycles of planktonic rotifers in lake Peipsi. Tartu, 1999, 101 p.
56. **Ana Rebane.** Mammalian ribosomal protein S3a genes and intron-encoded small nucleolar RNAs U73 and U82. Tartu, 1999, 85 p.
57. **Tiina Tamm.** Cocksfoot mottle virus: the genome organisation and translational strategies. Tartu, 2000, 101 p.
58. **Reet Kurg.** Structure-function relationship of the bovine papilloma virus E2 protein. Tartu, 2000, 89 p.
59. **Toomas Kivisild.** The origins of Southern and Western Eurasian populations: an mtDNA study. Tartu, 2000, 121 p.
60. **Niilo Kaldalu.** Studies of the TOL plasmid transcription factor XylS. Tartu 2000. 88 p.

61. **Dina Lepik.** Modulation of viral DNA replication by tumor suppressor protein p53. Tartu 2000. 106 p.
62. **Kai Vellak.** Influence of different factors on the diversity of the bryophyte vegetation in forest and wooded meadow communities. Tartu 2000. 122 p.
63. **Jonne Kotta.** Impact of eutrophication and biological invasionas on the structure and functions of benthic macrofauna. Tartu 2000. 160 p.
64. **Georg Martin.** Phytobenthic communities of the Gulf of Riga and the inner sea the West-Estonian archipelago. Tartu, 2000. 139 p.
65. **Silvia Sepp.** Morphological and genetical variation of *Alchemilla L.* in Estonia. Tartu, 2000. 124 p.
66. **Jaan Liira.** On the determinants of structure and diversity in herbaceous plant communities. Tartu, 2000. 96 p.
67. **Priit Zingel.** The role of planktonic ciliates in lake ecosystems. Tartu 2001. 111 p.
68. **Tiit Teder.** Direct and indirect effects in Host-parasitoid interactions: ecological and evolutionary consequences. Tartu 2001. 122 p.
69. **Hannes Kollist.** Leaf apoplastic ascorbate as ozone scavenger and its transport across the plasma membrane. Tartu 2001. 80 p.
70. **Reet Marits.** Role of two-component regulator system PehR-PehS and extracellular protease PrtW in virulence of *Erwinia Carotovora* subsp. *Carotovora*. Tartu 2001. 112 p.
71. **Vallo Tilgar.** Effect of calcium supplementation on reproductive performance of the pied flycatcher *Ficedula hypoleuca* and the great tit *Parus major,* breeding in Nothern temperate forests. Tartu, 2002. 126 p.
72. **Rita Hõrak.** Regulation of transposition of transposon Tn*4652* in *Pseudomonas putida*. Tartu, 2002. 108 p.
73. **Liina Eek-Piirsoo.** The effect of fertilization, mowing and additional illumination on the structure of a species-rich grassland community. Tartu, 2002. 74 p.
74. **Krõõt Aasamaa.** Shoot hydraulic conductance and stomatal conductance of six temperate deciduous tree species. Tartu, 2002. 110 p.
75. **Nele Ingerpuu.** Bryophyte diversity and vascular plants. Tartu, 2002. 112 p.
76. **Neeme Tõnisson.** Mutation detection by primer extension on oligonucleotide microarrays. Tartu, 2002. 124 p.
77. **Margus Pensa.** Variation in needle retention of Scots pine in relation to leaf morphology, nitrogen conservation and tree age. Tartu, 2003. 110 p.
78. **Asko Lõhmus.** Habitat preferences and quality for birds of prey: from principles to applications. Tartu, 2003. 168 p.
79. **Viljar Jaks.** p53 — a switch in cellular circuit. Tartu, 2003. 160 p.
80. **Jaana Männik.** Characterization and genetic studies of four ATP-binding cassette (ABC) transporters. Tartu, 2003. 140 p.
81. **Marek Sammul.** Competition and coexistence of clonal plants in relation to productivity. Tartu, 2003. 159 p

82. **Ivar Ilves.** Virus-cell interactions in the replication cycle of bovine papillomavirus type 1. Tartu, 2003. 89 p.
83. **Andres Männik.** Design and characterization of a novel vector system based on the stable replicator of bovine papillomavirus type 1. Tartu, 2003. 109 p.
84. **Ivika Ostonen.** Fine root structure, dynamics and proportion in net primary production of Norway spruce forest ecosystem in relation to site conditions. Tartu, 2003. 158 p.
85. **Gudrun Veldre.** Somatic status of 12–15-year-old Tartu schoolchildren. Tartu, 2003. 199 p.
86. **Ülo Väli.** The greater spotted eagle *Aquila clanga* and the lesser spotted eagle *A. pomarina*: taxonomy, phylogeography and ecology. Tartu, 2004. 159 p.
87. **Aare Abroi.** The determinants for the native activities of the bovine papillomavirus type 1 E2 protein are separable. Tartu, 2004. 135 p.
88. **Tiina Kahre.** Cystic fibrosis in Estonia. Tartu, 2004. 116 p.
89. **Helen Orav-Kotta.** Habitat choice and feeding activity of benthic suspension feeders and mesograzers in the northern Baltic Sea. Tartu, 2004. 117 p.
90. **Maarja Öpik.** Diversity of arbuscular mycorrhizal fungi in the roots of perennial plants and their effect on plant performance. Tartu, 2004. 175 p.
91. **Kadri Tali.** Species structure of *Neotinea ustulata*. Tartu, 2004. 109 p.
92. **Kristiina Tambets.** Towards the understanding of post-glacial spread of human mitochondrial DNA haplogroups in Europe and beyond: a phylogeographic approach. Tartu, 2004. 163 p.
93. **Arvi Jõers.** Regulation of p53-dependent transcription. Tartu, 2004. 103 p.
94. **Lilian Kadaja.** Studies on modulation of the activity of tumor suppressor protein p53. Tartu, 2004. 103 p.
95. **Jaak Truu.** Oil shale industry wastewater: impact on river microbial community and possibilities for bioremediation. Tartu, 2004. 128 p.
96. **Maire Peters.** Natural horizontal transfer of the *pheBA* operon. Tartu, 2004. 105 p.
97. **Ülo Maiväli.** Studies on the structure-function relationship of the bacterial ribosome. Tartu, 2004. 130 p.
98. **Merit Otsus.** Plant community regeneration and species diversity in dry calcareous grasslands. Tartu, 2004. 103 p.
99. **Mikk Heidemaa.** Systematic studies on sawflies of the genera *Dolerus, Empria,* and *Caliroa* (Hymenoptera: Tenthredinidae). Tartu, 2004. 167 p.
100. **Ilmar Tõnno.** The impact of nitrogen and phosphorus concentration and N/P ratio on cyanobacterial dominance and N_2 fixation in some Estonian lakes. Tartu, 2004. 111 p.
101. **Lauri Saks.** Immune function, parasites, and carotenoid-based ornaments in greenfinches. Tartu, 2004. 144 p.
102. **Siiri Rootsi.** Human Y-chromosomal variation in European populations. Tartu, 2004. 142 p.

103. **Eve Vedler.** Structure of the 2,4-dichloro-phenoxyacetic acid-degradative plasmid pEST4011. Tartu, 2005. 106 p.
104. **Andres Tover.** Regulation of transcription of the phenol degradation *pheBA* operon in *Pseudomonas putida*. Tartu, 2005. 126 p.
105. **Helen Udras.** Hexose kinases and glucose transport in the yeast *Hansenula polymorpha*. Tartu, 2005. 100 p.
106. **Ave Suija.** Lichens and lichenicolous fungi in Estonia: diversity, distribution patterns, taxonomy. Tartu, 2005. 162 p.
107. **Piret Lõhmus.** Forest lichens and their substrata in Estonia. Tartu, 2005. 162 p.
108. **Inga Lips.** Abiotic factors controlling the cyanobacterial bloom occurrence in the Gulf of Finland. Tartu, 2005. 156 p.
109. **Kaasik, Krista.** Circadian clock genes in mammalian clockwork, metabolism and behaviour. Tartu, 2005. 121 p.
110. **Juhan Javoiš.** The effects of experience on host acceptance in ovipositing moths. Tartu, 2005. 112 p.
111. **Tiina Sedman.** Characterization of the yeast *Saccharomyces cerevisiae* mitochondrial DNA helicase Hmi1. Tartu, 2005. 103 p.
112. **Ruth Aguraiuja.** Hawaiian endemic fern lineage *Diellia* (Aspleniaceae): distribution, population structure and ecology. Tartu, 2005. 112 p.
113. **Riho Teras.** Regulation of transcription from the fusion promoters generated by transposition of Tn*4652* into the upstream region of *pheBA* operon in *Pseudomonas putida*. Tartu, 2005. 106 p.
114. **Mait Metspalu.** Through the course of prehistory in india: tracing the mtDNA trail. Tartu, 2005. 138 p.
115. **Elin Lõhmussaar.** The comparative patterns of linkage disequilibrium in European populations and its implication for genetic association studies. Tartu, 2006. 124 p.
116. **Priit Kupper.** Hydraulic and environmental limitations to leaf water relations in trees with respect to canopy position. Tartu, 2006. 126 p.
117. **Heili Ilves.** Stress-induced transposition of Tn*4652* in *Pseudomonas Putida.* Tartu, 2006. 120 p.
118. **Silja Kuusk.** Biochemical properties of Hmi1p, a DNA helicase from *Saccharomyces cerevisiae* mitochondria. Tartu, 2006. 126 p.
119. **Kersti Püssa.** Forest edges on medium resolution landsat thematic mapper satellite images. Tartu, 2006. 90 p.
120. **Lea Tummeleht.** Physiological condition and immune function in great tits (*Parus major* l.): Sources of variation and trade-offs in relation to growth. Tartu, 2006. 94 p.
121. **Toomas Esperk.** Larval instar as a key element of insect growth schedules. Tartu, 2006. 186 p.
122. **Harri Valdmann.** Lynx (*Lynx lynx*) and wolf (*Canis lupus*) in the Baltic region: Diets, helminth parasites and genetic variation. Tartu, 2006. 102 p.

123. **Priit Jõers.** Studies of the mitochondrial helicase Hmi1p in *Candida albicans* and *Saccharomyces cerevisia*. Tartu, 2006. 113 p.
124. **Kersti Lilleväli.** Gata3 and Gata2 in inner ear development. Tartu, 2007. 123 p.
125. **Kai Rünk.** Comparative ecology of three fern species: *Dryopteris carthusiana* (Vill.) H.P. Fuchs, *D. expansa* (C. Presl) Fraser-Jenkins & Jermy and *D. dilatata* (Hoffm.) A. Gray (Dryopteridaceae). Tartu, 2007. 143 p.
126. **Aveliina Helm.** Formation and persistence of dry grassland diversity: role of human history and landscape structure. Tartu, 2007. 89 p.
127. **Leho Tedersoo.** Ectomycorrhizal fungi: diversity and community structure in Estonia, Seychelles and Australia. Tartu, 2007. 233 p.
128. **Marko Mägi.** The habitat-related variation of reproductive performance of great tits in a deciduous-coniferous forest mosaic: looking for causes and consequences. Tartu, 2007. 135 p.
129. **Valeria Lulla.** Replication strategies and applications of Semliki Forest virus. Tartu, 2007. 109 p.
130. **Ülle Reier**. Estonian threatened vascular plant species: causes of rarity and conservation. Tartu, 2007. 79 p.
131. **Inga Jüriado**. Diversity of lichen species in Estonia: influence of regional and local factors. Tartu, 2007. 171 p.
132. **Tatjana Krama.** Mobbing behaviour in birds: costs and reciprocity based cooperation. Tartu, 2007. 112 p.
133. **Signe Saumaa.** The role of DNA mismatch repair and oxidative DNA damage defense systems in avoidance of stationary phase mutations in *Pseudomonas putida.* Tartu, 2007. 172 p.
134. **Reedik Mägi**. The linkage disequilibrium and the selection of genetic markers for association studies in european populations. Tartu, 2007. 96 p.
135. **Priit Kilgas.** Blood parameters as indicators of physiological condition and skeletal development in great tits (*Parus major*): natural variation and application in the reproductive ecology of birds. Tartu, 2007. 129 p.
136. **Anu Albert**. The role of water salinity in structuring eastern Baltic coastal fish communities. Tartu, 2007. 95 p.
137. **Kärt Padari.** Protein transduction mechanisms of transportans. Tartu, 2008. 128 p.
138. **Siiri-Lii Sandre.** Selective forces on larval colouration in a moth. Tartu, 2008. 125 p.
139. **Ülle Jõgar.** Conservation and restoration of semi-natural floodplain meadows and their rare plant species. Tartu, 2008. 99 p.
140. **Lauri Laanisto.** Macroecological approach in vegetation science: generality of ecological relationships at the global scale. Tartu, 2008. 133 p.
141. **Reidar Andreson**. Methods and software for predicting PCR failure rate in large genomes. Tartu, 2008. 105 p.
142. **Birgot Paavel.** Bio-optical properties of turbid lakes. Tartu, 2008. 175 p.

143. **Kaire Torn.** Distribution and ecology of charophytes in the Baltic Sea. Tartu, 2008, 98 p.
144. **Vladimir Vimberg.** Peptide mediated macrolide resistance. Tartu, 2008, 190 p.
145. **Daima Örd.** Studies on the stress-inducible pseudokinase TRB3, a novel inhibitor of transcription factor ATF4. Tartu, 2008, 108 p.
146. **Lauri Saag.** Taxonomic and ecologic problems in the genus *Lepraria* (*Stereocaulaceae*, lichenised *Ascomycota*). Tartu, 2008, 175 p.
147. **Ulvi Karu.** Antioxidant protection, carotenoids and coccidians in greenfinches – assessment of the costs of immune activation and mechanisms of parasite resistance in a passerine with carotenoid-based ornaments. Tartu, 2008, 124 p.
148. **Jaanus Remm.** Tree-cavities in forests: density, characteristics and occupancy by animals. Tartu, 2008, 128 p.
149. **Epp Moks.** Tapeworm parasites *Echinococcus multilocularis* and *E. granulosus* in Estonia: phylogenetic relationships and occurrence in wild carnivores and ungulates. Tartu, 2008, 82 p.
150. **Eve Eensalu.** Acclimation of stomatal structure and function in tree canopy: effect of light and CO_2 concentration. Tartu, 2008, 108 p.
151. **Janne Pullat**. Design, functionlization and application of an *in situ* synthesized oligonucleotide microarray. Tartu, 2008, 108 p.
152. **Marta Putrinš.** Responses of *Pseudomonas putida* to phenol-induced metabolic and stress signals. Tartu, 2008, 142 p.
153. **Marina Semtšenko.** Plant root behaviour: responses to neighbours and physical obstructions. Tartu, 2008, 106 p.
154. **Marge Starast.** Influence of cultivation techniques on productivity and fruit quality of some *Vaccinium* and *Rubus* taxa. Tartu, 2008, 154 p.
155. **Age Tats.** Sequence motifs influencing the efficiency of translation. Tartu, 2009, 104 p.
156. **Radi Tegova.** The role of specialized DNA polymerases in mutagenesis in *Pseudomonas putida.* Tartu, 2009, 124 p.
157. **Tsipe Aavik.** Plant species richness, composition and functional trait pattern in agricultural landscapes – the role of land use intensity and landscape structure. Tartu, 2009, 112 p.
158. **Kaja Kiiver.** Semliki forest virus based vectors and cell lines for studying the replication and interactions of alphaviruses and hepaciviruses. Tartu, 2009, 104 p.
159. **Meelis Kadaja.** Papillomavirus Replication Machinery Induces Genomic Instability in its Host Cell. Tartu, 2009, 126 p.
160. **Pille Hallast.** Human and chimpanzee Luteinizing hormone/Chorionic Gonadotropin beta (*LHB/CGB*) gene clusters: diversity and divergence of young duplicated genes. Tartu, 2009, 168 p.
161. **Ain Vellak.** Spatial and temporal aspects of plant species conservation. Tartu, 2009, 86 p.

162. **Triinu Remmel.** Body size evolution in insects with different colouration strategies: the role of predation risk. Tartu, 2009, 168 p.
163. **Jaana Salujõe.** Zooplankton as the indicator of ecological quality and fish predation in lake ecosystems. Tartu, 2009, 129 p.
164. **Ele Vahtmäe.** Mapping benthic habitat with remote sensing in optically complex coastal environments. Tartu, 2009, 109 p.
165. **Liisa Metsamaa.** Model-based assessment to improve the use of remote sensing in recognition and quantitative mapping of cyanobacteria. Tartu, 2009, 114 p.
166. **Pille Säälik.** The role of endocytosis in the protein transduction by cell-penetrating peptides. Tartu, 2009, 155 p.
167. **Lauri Peil.** Ribosome assembly factors in *Escherichia coli.* Tartu, 2009, 147 p.
168. **Lea Hallik.** Generality and specificity in light harvesting, carbon gain capacity and shade tolerance among plant functional groups. Tartu, 2009, 99 p.
169. **Mariliis Tark.** Mutagenic potential of DNA damage repair and tolerance mechanisms under starvation stress. Tartu, 2009, 191 p.
170. **Riinu Rannap.** Impacts of habitat loss and restoration on amphibian populations. Tartu, 2009, 117 p.
171. **Maarja Adojaan.** Molecular variation of HIV-1 and the use of this knowledge in vaccine development. Tartu, 2009, 95 p.
172. **Signe Altmäe.** Genomics and transcriptomics of human induced ovarian folliculogenesis. Tartu, 2010, 179 p.
173. **Triin Suvi.** Mycorrhizal fungi of native and introduced trees in the Seychelles Islands. Tartu, 2010, 107 p.
174. **Velda Lauringson.** Role of suspension feeding in a brackish-water coastal sea. Tartu, 2010, 123 p.
175. **Eero Talts.** Photosynthetic cyclic electron transport – measurement and variably proton-coupled mechanism. Tartu, 2010, 121 p.
176. **Mari Nelis.** Genetic structure of the Estonian population and genetic distance from other populations of European descent. Tartu, 2010, 97 p.
177. **Kaarel Krjutškov.** Arrayed Primer Extension-2 as a multiplex PCR-based method for nucleic acid variation analysis: method and applications. Tartu, 2010, 129 p.
178. **Egle Köster.** Morphological and genetical variation within species complexes: *Anthyllis vulneraria* s. l. and *Alchemilla vulgaris* (coll.). Tartu, 2010, 101 p.
179. **Erki Õunap.** Systematic studies on the subfamily Sterrhinae (Lepidoptera: Geometridae). Tartu, 2010, 111 p.
180. **Merike Jõesaar.** Diversity of key catabolic genes at degradation of phenol and *p*-cresol in pseudomonads. Tartu, 2010, 125 p.
181. **Kristjan Herkül.** Effects of physical disturbance and habitat-modifying species on sediment properties and benthic communities in the northern Baltic Sea. Tartu, 2010, 123 p.

182. **Arto Pulk.** Studies on bacterial ribosomes by chemical modification approaches. Tartu, 2010, 161 p.
183. **Maria Põllupüü.** Ecological relations of cladocerans in a brackish-water ecosystem. Tartu, 2010, 126 p.
184. **Toomas Silla.** Study of the segregation mechanism of the Bovine Papillomavirus Type 1. Tartu, 2010, 188 p.
185. **Gyaneshwer Chaubey.** The demographic history of India: A perspective based on genetic evidence. Tartu, 2010, 184 p.
186. **Katrin Kepp.** Genes involved in cardiovascular traits: detection of genetic variation in Estonian and Czech populations. Tartu, 2010, 164 p.
187. **Virve Sõber.** The role of biotic interactions in plant reproductive performance. Tartu, 2010, 92 p.
188. **Kersti Kangro.** The response of phytoplankton community to the changes in nutrient loading. Tartu, 2010, 144 p.
189. **Joachim M. Gerhold.** Replication and Recombination of mitochondrial DNA in Yeast. Tartu, 2010, 120 p.
190. **Helen Tammert.** Ecological role of physiological and phylogenetic diversity in aquatic bacterial communities. Tartu, 2010, 140 p.
191. **Elle Rajandu.** Factors determining plant and lichen species diversity and composition in Estonian *Calamagrostis* and *Hepatica* site type forests. Tartu, 2010, 123 p.
192. **Paula Ann Kivistik.** ColR-ColS signalling system and transposition of Tn*4652* in the adaptation of *Pseudomonas putida.* Tartu, 2010, 118 p.
193. **Siim Sõber.** Blood pressure genetics: from candidate genes to genome-wide association studies. Tartu, 2011, 120 p.
194. **Kalle Kipper.** Studies on the role of helix 69 of 23S rRNA in the factor-dependent stages of translation initiation, elongation, and termination. Tartu, 2011, 178 p.
195. **Triinu Siibak.** Effect of antibiotics on ribosome assembly is indirect. Tartu, 2011, 134 p.
196. **Tambet Tõnissoo.** Identification and molecular analysis of the role of guanine nucleotide exchange factor RIC-8 in mouse development and neural function. Tartu, 2011, 110 p.
197. **Helin Räägel.** Multiple faces of cell-penetrating peptides – their intracellular trafficking, stability and endosomal escape during protein transduction. Tartu, 2011, 161 p.
198. **Andres Jaanus.** Phytoplankton in Estonian coastal waters – variability, trends and response to environmental pressures. Tartu, 2011, 157 p.
199. **Tiit Nikopensius.** Genetic predisposition to nonsyndromic orofacial clefts. Tartu, 2011, 152 p.
200. **Signe Värv.** Studies on the mechanisms of RNA polymerase II-dependent transcription elongation. Tartu, 2011, 108 p.
201. **Kristjan Välk.** Gene expression profiling and genome-wide association studies of non-small cell lung cancer. Tartu, 2011, 98 p.

202. **Arno Põllumäe.** Spatio-temporal patterns of native and invasive zooplankton species under changing climate and eutrophication conditions. Tartu, 2011, 153 p.
203. **Egle Tammeleht.** Brown bear (*Ursus arctos*) population structure, demographic processes and variations in diet in northern Eurasia. Tartu, 2011, 143 p.
205. **Teele Jairus.** Species composition and host preference among ectomycorrhizal fungi in Australian and African ecosystems. Tartu, 2011, 106 p.
206. **Kessy Abarenkov.** PlutoF – cloud database and computing services supporting biological research. Tartu, 2011, 125 p.
207. **Marina Grigorova.** Fine-scale genetic variation of follicle-stimulating hormone beta-subunit coding gene (*FSHB*) and its association with reproductive health. Tartu, 2011, 184 p.
208. **Anu Tiitsaar.** The effects of predation risk and habitat history on butterfly communities. Tartu, 2011, 97 p.
209. **Elin Sild.** Oxidative defences in immunoecological context: validation and application of assays for nitric oxide production and oxidative burst in a wild passerine. Tartu, 2011, 105 p.
210. **Irja Saar**. The taxonomy and phylogeny of the genera *Cystoderma* and *Cystodermella* (Agaricales, Fungi). Tartu, 2012, 167 p.
211. **Pauli Saag.** Natural variation in plumage bacterial assemblages in two wild breeding passerines. Tartu, 2012, 113 p.
212. **Aleksei Lulla.** Alphaviral nonstructural protease and its polyprotein substrate: arrangements for the perfect marriage. Tartu, 2012, 143 p.
213. **Mari Järve.** Different genetic perspectives on human history in Europe and the Caucasus: the stories told by uniparental and autosomal markers. Tartu, 2012, 119 p.
214. **Ott Scheler**. The application of tmRNA as a marker molecule in bacterial diagnostics using microarray and biosensor technology. Tartu, 2012, 93 p.
215. **Anna Balikova**. Studies on the functions of tumor-associated mucin-like leukosialin (CD43) in human cancer cells. Tartu, 2012, 129 p.
216. **Triinu Kõressaar.** Improvement of PCR primer design for detection of prokaryotic species. Tartu, 2012, 83 p.
217. **Tuul Sepp.** Hematological health state indices of greenfinches: sources of individual variation and responses to immune system manipulation. Tartu, 2012, 117 p.
218. **Rya Ero.** Modifier view of the bacterial ribosome. Tartu, 2012, 146 p.
219. **Mohammad Bahram.** Biogeography of ectomycorrhizal fungi across different spatial scales. Tartu, 2012, 165 p.
220. **Annely Lorents.** Overcoming the plasma membrane barrier: uptake of amphipathic cell-penetrating peptides induces influx of calcium ions and downstream responses. Tartu, 2012, 113 p.

221. **Katrin Männik.** Exploring the genomics of cognitive impairment: whole-genome SNP genotyping experience in Estonian patients and general population. Tartu, 2012, 171 p.
222. **Marko Prous.** Taxonomy and phylogeny of the sawfly genus *Empria* (Hymenoptera, Tenthredinidae). Tartu, 2012, 192 p.
223. **Triinu Visnapuu.** Levansucrases encoded in the genome of *Pseudomonas syringae* pv. tomato DC3000: heterologous expression, biochemical characterization, mutational analysis and spectrum of polymerization products. Tartu, 2012, 160 p.
224. **Nele Tamberg.** Studies on Semliki Forest virus replication and pathogenesis. Tartu, 2012, 109 p.
225. **Tõnu Esko.** Novel applications of SNP array data in the analysis of the genetic structure of Europeans and in genetic association studies. Tartu, 2012, 149 p.
226. **Timo Arula.** Ecology of early life-history stages of herring *Clupea harengus membras* in the northeastern Baltic Sea. Tartu, 2012, 143 p.
227. **Inga Hiiesalu.** Belowground plant diversity and coexistence patterns in grassland ecosystems. Tartu, 2012, 130 p.
228. **Kadri Koorem.** The influence of abiotic and biotic factors on small-scale plant community patterns and regeneration in boreonemoral forest. Tartu, 2012, 114 p.
229. **Liis Andresen.** Regulation of virulence in plant-pathogenic pectobacteria. Tartu, 2012, 122 p.
230. **Kaupo Kohv.** The direct and indirect effects of management on boreal forest structure and field layer vegetation. Tartu, 2012, 124 p.
231. **Mart Jüssi.** Living on an edge: landlocked seals in changing climate. Tartu, 2012, 114 p.
232. **Riina Klais.** Phytoplankton trends in the Baltic Sea. Tartu, 2012, 136 p.
233. **Rauno Veeroja.** Effects of winter weather, population density and timing of reproduction on life-history traits and population dynamics of moose (*Alces alces*) in Estonia. Tartu, 2012, 92 p.
234. **Marju Keis.** Brown bear (*Ursus arctos*) phylogeography in northern Eurasia. Tartu, 2013, 142 p.
235. **Sergei Põlme.** Biogeography and ecology of *alnus*- associated ectomycorrhizal fungi – from regional to global scale. Tartu, 2013, 90 p.
236. **Liis Uusküla.**. Tartu, 2013, 173 p.
237. **Marko Lõoke.** Studies on DNA replication initiation in *Saccharomyces cerevisiae.* Tartu, 2013, 112 p.
238. **Anne Aan.** Light- and nitrogen-use and biomass allocation along productivity gradients in multilayer plant communities. Tartu, 2013, 127 p.
239. **Heidi Tamm.** Comprehending phylogenetic diversity – case studies in three groups of ascomycetes. Tartu, 2013, 136 p.